UNIVERSIDADE FEDERAL DE SÃO CARLOS

CENTRO DE CIÊNCIAS BIOLÓGICAS E DA SAÚDE

PROGRAMA DE PÓS-GRADUAÇÃO EM ECOLOGIA E RECURSOS NATURAIS

CÍNTHIA BRUNO DE ABREU

EFEITOS DE MICROPARTÍCULAS DE PRATA, EM DIFERENTES MORFOLOGIAS, ISOLADAS E EM MISTURAS, SOBRE ORGANISMOS PLANCTÔNICOS DULCÍCOLAS DE DOIS DIFERENTES NÍVEIS TRÓFICOS

SÃO CARLOS – SP

2022

UNIVERSIDADE FEDERAL DE SÃO CARLOS

CENTRO DE CIÊNCIAS BIOLÓGICAS E DA SAÚDE

PROGRAMA DE PÓS-GRADUAÇÃO EM ECOLOGIA E RECURSOS NATURAIS

CÍNTHIA BRUNO DE ABREU

EFEITOS DE MICROPARTÍCULAS DE PRATA, EM DIFERENTES MORFOLOGIAS, ISOLADAS E EM MISTURAS, SOBRE ORGANISMOS PLANCTÔNICOS DULCÍCOLAS DE DOIS DIFERENTES NÍVEIS TRÓFICOS

Tese de Doutorado apresentada ao Programa de Pós-Graduação em Ecologia e Recursos Naturais do Centro de Ciências Biológicas e da Saúde da Universidade Federal de São Carlos, como parte dos requisitos para obtenção do título de Doutora em Ciências, área de concentração em Ecologia e Recursos Naturais.

Orientadora: Profa. Dra. Maria da Graça Gama Melão

Co-orientadora: Dra. Adrislaine da Silva Mansano Dornfeld

SÃO CARLOS – SP

2022

UNIVERSIDADE FEDERAL DE SÃO CARLOS

Centro de Ciências Biológicas e da Saúde
Programa de Pós-Graduação em Ecologia e Recursos Naturais

Folha de Aprovação

Defesa de Tese de Doutorado da candidata Cinthia Bruno de Abreu, realizada em 27/04/2022.

Comissão Julgadora:

Profa. Dra. Maria da Graça Gama Melão (UFSCar)

Profa. Dra. Odete Rocha (UFSCar)

Profa. Dra. Raquel Aparecida Moreira (USP)

Profa. Dra. Renata Fracácio Francisco (UNESP)

Profa. Dra. Fernanda Cristina Massaro (BIOTOX)

O Relatório de Defesa assinado pelos membros da Comissão Julgadora encontra-se arquivado junto ao Programa de Pós-Graduação em Ecologia e Recursos Naturais.

Dedico aos meus pais, Irineu e Iracedis, pelo apoio, ensinamentos, dedicação e amor.

AGRADECIMENTOS

À Profa. Dra. Maria da Graça Gama Melão pela orientação, confiança e ensinamentos.

À Dra. Adrislaine da Silva Mansano Dornfeld pela co-orientação, amizade, paciência, dedicação, carinho e ensinamentos.

Ao Prof. Dr. Elson Longo da Silva pela oportunidade e parceria estabelecida entre o Centro de Desenvolvimento de Materias Funcionais (CDMF) e o Laboratório de Plâncton (Departamento de Hidrobiologia – UFSCar).

Ao Prof. Dr. Hugo Sarmento e à Profa. Dra. Ana Teresa Lombardi por disponibilizarem equipamentos essenciais para obtenção dos dados desta tese. Aos docentes, secretaria e coordenação de curso do Programa de Pós-Graduação em Ecologia e Recursos Naturais (PPGERN/ UFSCar – São Carlos).

À Universidade Federal de São Carlos (*campus* sede) e ao Departamento de Hidrobiologia pela estrutura oferecida para realização desta pesquisa. Aos funcionários da instituição.

Aos amigos de laboratório, pelo acolhimento e ensinamentos, pela convivência e amizade, companheirismo, pelos cafés e ajuda nas atividades práticas.

Aos co-autores dos artigos, fundamentais no planejamento e execução dos experimentos, bem como análises dos dados e correção dos artigos, também por me apoiar em cada desafio.

Às professoras e pesquisadoras Odete Rocha, Renata Fracácio, Raquel Moreira e Fernanda Massaro por aceitarem fazer parte da banca de defesa e pelas valiosas correções e contribuições para a conclusão desta tese.

À minha família e aos meus amigos por todo o incentivo, amor e apoio. Em especial meus pais Irineu e Iracedis, e meu companheiro de vida, Lucas.

Por fim, ao CNPq pela bolsa concedida (141255/2018-8) e à FAPESP pelo suporte financeiro.

O importante é não parar de questionar. A curiosidade tem sua própria razão de existir.

Albert Einstein

Resumo

Atualmente, partículas com prata em sua composição têm chamado atenção, pela ampla aplicabilidade. Em especial, o tungstato de prata (α-Ag_2WO_4), possui ação microbicida, fungicida e antitumoral, é utilizado em processos de fotocatálise, sensores, entre outros. Ainda, o material pode ser uma fonte de liberação de íons prata, cuja toxicidade para organismos aquáticos é amplamente conhecida. Desse modo, o objetivo dessa pesquisa foi avaliar os efeitos e mecanismos tóxicos do α-Ag_2WO_4, em diferentes morfologias (cúbica – C e *rod* – R), via múltiplos parâmetros (*endpoints*), sobre duas espécies planctônicas de água doce, a microalga *Raphidocelis subcapitata* e o cladócero *Ceriodaphnia silvestrii*. Para isso, foram realizados testes de toxicidade aguda e crônica com os compósitos isolados para ambas as espécies e ensaios de toxicidade aguda de misturas com o cladócero. Os resultados dos testes de toxicidade com a microalga indicaram que α-Ag_2WO_4 afetou parâmetros populacionais, como crescimento celular; morfológicos, como complexidade celular; bioquímicos, tais como composição de carboidratos totais e conteúdo de clorofila *a* e fisiológicos, como a produção de espécies reativas de oxigênio (EROs) e alterações nos parâmetros aferidos pelo Phyto-PAM, tais como rendimento máximo e complexo de evolução do oxigênio (CEO). Para o cladócero *C. silvestrii* foram observados efeitos negativos significantes somente nos testes de toxicidade aguda (48h), em que ambas as morfologias de α-Ag_2WO_4 causaram imobilidade nos organismos quando expostos aos compósitos isolados e em mistura. Com relação à exposição combinada de α-Ag_2WO_4 – C e α-Ag_2WO_4 – R o modelo de referência de Ação Independente (IA) com desvio dependente do nível de dose (DL) foi o que melhor se ajustou aos dados, indicando sinergismo em baixas concentrações e antagonismo em doses elevadas. Os efeitos negativos sobre os organismos provavelmente foram causados pela liberação de íons prata do α-Ag_2WO_4. Diferentemente da exposição aguda, a exposição crônica de α-Ag_2WO_4 – C e α-Ag_2WO_4 – R isolados não causaram danos significativos na reprodução e crescimento dos cladóceros. Comparando a toxicidade dos microcristais sobre as duas espécies testadas, foi possível identificar que o cladócero possui maior sensibilidade às diferentes morfologias de α-Ag_2WO_4 (CE_{50}-48h = 0,64 μg L^{-1} para α-Ag_2WO_4 – C e CE_{50}-48h = 0,81 μg L^{-1} para α-Ag_2WO_4 –R) em comparação com a microalga (CI_{50}–96h= 23,47 μg L^{-1} para α-Ag_2WO_4 – C e CI_{50}-96h= 13,72 μg L^{-1} para α-Ag_2WO_4 – R), o que ressalta a importância de se avaliar mais de um nível trófico em estudos ecotoxicológicos.

Palavras-chave: *Ceriodaphnia silvestrii*. Microcristais. Múltiplos *endpoints*. *Raphidocelis subcapitata*. Tungstato de prata. Morfologias (cúbica – C e rod – R).

Abstract

Currently, particles with silver in their composition have drawn attention for their wide applicability. In particular, the silver tungstate (α-Ag_2WO_4), which has microbicidal, fungicidal and antitumor activities, is used in photocatalysis processes, sensors, among others. Furthermore, the material can be a source of release of silver ions, whose toxicity to aquatic organisms is widely known. Thus, the objective of this research was to evaluate the effects and toxic mechanisms, via multiple endpoints, of α-Ag_2WO_4, in different morphologies (cubic - C - and rod - R) on two freshwater planktonic species, the microalgae *Raphidocelis subcapitata* and the cladoceran *Ceriodaphnia silvestrii*. For this, acute and chronic toxicity tests were performed with the isolated composites for both species and toxicity tests of mixtures with the cladoceran. The results of ecotoxicity tests with the microalgae indicated that α-Ag_2WO_4 affected population parameters, such as cell growth; morphological, such as cell complexity; biochemical, such as total carbohydrate composition and chlorophyll *a* content; and physiological, such as the production of reactive oxygen species (ROS) and changes in parameters measured by Phyto-PAM, such as maximum yield and oxygen evolution complex (OEC). For the species *C. silvestrii* significant negative effects were observed only in the acute toxicity tests, where both morphologies caused immobility in the organisms when exposed to the composites isolated and in mixture. Regarding the combined exposure of α-Ag_2WO_4 - C and α-Ag_2WO_4 - R the reference model of Independent Action (IA) with dose-level dependent (DL) deviation was the best fit to the data, indicating synergism at low concentrations and antagonism at high doses. The negative effects on organisms were probably caused by the availability of silver ions, which are highly toxic. Unlike acute exposure, chronic exposure of α-Ag_2WO_4 - C and α-Ag_2WO_4 - R alone did not cause significant reproductive damage to cladocerans. Comparing the toxicity of microcrystals on the two species of organisms tested, it was possible to identify that the cladoceran has a higher sensitivity, to the different morphologies of α-Ag_2WO_4 (EC_{50}-48h= 0.64 μg L^{-1} para α-Ag_2WO_4 – C e EC_{50}-48h= 0.81 μg L^{-1} para α-Ag_2WO_4 –R) compared to the microalgae (IC_{50}-96h= 23.47 μg L^{-1} para α-Ag_2WO_4 – C e IC_{50}-96h= 13.72 μg L^{-1} para α-Ag_2WO_4 – R), which highlights the importance in evaluating more than one trophic level in ecotoxicological studies.

Keywords: *Ceriodaphnia silvestrii*. Microcrystals. Multiple endpoints. *Raphidocelis subcapitata*. Silver tungstate. Morphologies (cube – C and rod – R).

Lista de Figuras

Introdução geral

CAPÍTULO 1

Toxicity of α-Ag_2WO_4 microcrystals to freshwater microalga *Raphidocelis subcapitata* at cellular and population levels

Supplementary material:

CAPÍTULO 2

Effects of α-Ag_2WO_4 crystals on photosynthetic efficiency and biomolecule composition of the algae *Raphidocelis subcapitata*

Supplementary material:

CAPÍTULO 3

Effects of different α-Ag_2WO_4 morphologies isolated and mixture for a Neotropical cladoceran

Supplementary material:

Lista de Tabelas

CAPÍTULO 1

Toxicity of α-Ag_2WO_4 microcrystals to freshwater microalga *Raphidocelis subcapitata* at cellular and population levels

Supplementary material:

CAPÍTULO 2

Effects of α-Ag_2WO_4 crystals on photosynthetic efficiency and biomolecule composition of the algae *Raphidocelis subcapitata*

Supplementary material:

CAPÍTULO 3

Effects of different α-Ag_2WO_4 morphologies isolated and mixture for a Neotropical cladoceran

Supplementary material:

Sumário

Estrutura da Tese

Esta tese foi redigida e estruturada em três capítulos, compostos pelos artigos científicos, os quais possuem Resumo, Introdução, Materiais e Métodos, Resultados, Discussão, Conclusões e Referências Bibliográficas de acordo com as normas das revistas científicas nas quais foram publicados ou foram submetidos. Anteriormente aos capítulos com artigos, há uma revisão do tema abordado, com uma introdução geral.

Capítulo 1- Artigo intitulado: Toxicity of α-Ag_2WO_4 microcrystals to freshwater microalga *Raphidocelis subcapitata* at cellular and population levels – artigo publicado na revista Chemosphere – Neste trabalho, avaliaram-se os efeitos de α-Ag_2WO_4 em diferentes morfologias (cúbica e rod, α-Ag_2WO_4 – C e α-Ag_2WO_4 – R) sobre *Raphidocelis subcapitata* a partir da exposição crônica (96 h). Os parâmetros avaliados foram taxa de crescimento, fluorescência da clorofila *a*, complexidade e tamanho celular, e produção intracelular de espécies reativas de oxigênio (EROs). Todos esses parâmetros foram analisados via citometria de fluxo. Ainda, foi feita análise e quantificação de íons liberados pelos microcristais em cada concentração testada.

Capítulo 2 - Artigo intitulado: Effects of α-Ag_2WO_4 crystals on photosynthetic efficiency and biomolecule composition of the algae *Raphidocelis subcapitata* – artigo publicado na revista Water, Air, & Soil Pollution- Neste estudo, foi avaliada a toxicidade do α-Ag_2WO_4 – R (*rod*) para *Raphidocelis subcapitata*. Foram investigados a densidade celular ao longo do experimento (96 h), o conteúdo de clorofila *a* e carboidratos totais, ambos em 96 horas ao final da exposição, atividade fotossintética, a partir dos parâmetros de rendimento máximo e complexo de evolução do oxigênio, durante o experimento.

Capítulo 3 - Artigo intitulado: Effects of different α-Ag_2WO_4 morphologies isolated and mixture for a Neotropical cladoceran – Submetido à revista Chemosphere – Neste capítulo o objetivo foi avaliar a toxicidade do α-Ag_2WO_4 em diferentes morfologias (cúbica e *rod*, α-Ag_2WO_4 – C e α-Ag_2WO_4 – R) sobre o clacócero *Ceriodaphnia silvestrii*. Foram realizados testes de toxicidade aguda, com os compósitos isolados e em mistura, e toxicidade crônica dos microcristais isolados. A partir disso, foram determinados os valores de CE_{50}-48h e os parâmetros analisados foram: imobilidade, taxa de filtração e ingestão, fertilidade e comprimento maternal.

A partir dos três capítulos, foram feitas as conclusões gerais e as considerações finais da tese.

Contextualização teórica e justificativa

1. Introdução

1.1 Histórico e ecotoxicologia

O histórico de exploração de recursos ambientais está voltado para suprir a demanda crescente da população humana tanto para a produção, quanto para o consumo de produtos. A partir da Revolução Industrial e com o crescimento e distribuição da população mundial, a quantidade de produtos disponíveis no mercado é cada vez maior e isso está diretamente relacionado com a degradação ambiental (Singh, 2016). Diante disso, considerando a geração crescente de resíduos, é de extrema importância avaliar os impactos, para tentar reduzi-los e contê-los.

A teoria de Paracelsus (1493-1541) estabelece que uma dada substância é classificada como um veneno ou não dependendo da dose e não do composto em si. Essa afirmativa constitui a primeira lei, dentre as Leis Básicas que regem a toxicologia. A segunda lei, postulada por Ambroise Pare, afirma que as "reações biológicas a produtos químicos são específicas para cada produto químico", ou seja, cada composto possui uma especificidade em relação ao efeito causado (Singh, 2016). O perigo que a substância apresenta aos seres vivos e ao meio ambiente, depende das características dos compostos e do tempo de exposição, já que os organismos têm sensibilidades diferentes (Van den Brink et al., 2006). A toxicidade, por sua vez, é caracterizada pela exposição e avaliação, as quais são medidas pelas relações e transformadas em índices (Azevedo e Chasin, 2004). Ou seja, a toxicologia objetiva prever os riscos provenientes da exposição de diversas substâncias tóxicas e para isso é necessário adotar formas e métodos adequados para manipular os compostos tóxicos. Portanto, é essencial conhecer os limites máximos, nas diferentes áreas de abrangência da toxicologia, para então ser possível gerir os riscos causados pelas exposições aos compostos químicos (Costa et al., 2008; Zagatto e Bertoletti, 2006).

A Ecotoxicologia é definida como "ciência preocupada em estudar como os ecossistemas metabolizam, transformam, degradam, eliminam, acumulam e sofrem ação da toxicidade dos produtos químicos que neles penetram." (Azevedo e Chasin, 2004). O conceito de Ecotoxicologia surgiu com o aumento da poluição e degradação ambiental e foi originalmente definida por Truhaut (1977) como a ciência que tem a finalidade de impedir e prevenir os efeitos tóxicos causados por substâncias ou até mesmo saber como bloquear,

reverter e remediar os efeitos de substâncias químicas em organismos vivos (populações, comunidades e ecossistemas). Para isto, são desenvolvidos estudos para verificar os efeitos tóxicos de substâncias químicas sobre a biota (Fernicola et al., 2004).

A avaliação da toxicidade para uma dada espécie é feita por meio de bioensaios em condições controladas (testes ecotoxicológicos). Tais testes de toxicidade são utilizados, por exemplo, para verificar a qualidade da água e a poluição por contaminantes, já que a avaliação de variáveis biológicas e respostas biológicas (*endpoints*) evidenciam o quanto uma substância pode ser danosa aos organismos (Costa et al., 2008). Portanto, a Ecotoxicologia fornece o conhecimento que subsidia a elaboração de leis, políticas públicas, programas e diretrizes para o gerenciamento de riscos (Azevedo e Chasin, 2004)

1.2 Misturas tóxicas

Como mencionado anteriormente, conhecer e entender os efeitos causados pela contaminação é crucial na avaliação de risco ambiental e para a saúde humana. No entanto, a maioria dos estudos ecotoxicológicos é realizada com substâncias isoladas (Cassee et al., 1998; Ferreira et al., 2008). As avaliações de riscos das misturas tóxicas ganharam a atenção de cientistas (Silva et al., 2022; Reis et al., 2022; Gebara et al., 2021; Gebara et al., 2020; Moreira et al., 2020; Mansano et al., 2017) e de políticas reguladoras, já que no ambiente raramente os compostos ocorrerão de forma isolada. Diante disso, os organismos aquáticos não estarão expostos aos contaminantes isolados (Faust et al., 2003). De acordo com Feron et al. (1995), o estudo de toxicidade de misturas engloba a identificação do componente da mistura que possui mais risco, através da avaliação de risco e perigo. Estes mesmos autores ressaltam que a abordagem estatística com planejamento fatorial utilizando pelo menos dois níveis tróficos é usada para identificar as interações entre compostos isolados.

Segundo Faust et al. (2003), para uma análise preditiva da toxicidade de misturas em ambientes aquáticos há dois modelos importantes: o modelo de Adição de Concentração (CA) (Loewe e Muischnek, 1926) e o de Ação Independente (IA) (Bliss, 1939). O modelo de Adição de Concentração (CA) estabelece que os compostos individuais com o mesmo modo de ação agem sobre o mesmo alvo molecular e contribuem para uma resposta comum em proporção a suas toxicidades relativas. Este modelo conceitual é definido como a soma das toxicidades relativas dos componentes individuais em uma mistura (Ferreira et al., 2008; Groten, 2000; Loureiro et al., 2010) e é matematicamente descrito pela seguinte fórmula

(Berenbaum, 1985), em que C_i corresponde à concentração do químico *i* na mistura e EC_{Xi} corresponde à concentração de efeito do químico *i* que produz o mesmo efeito (x%) como a mistura toda.

$$\sum_{i=1}^{n} \frac{Ci}{ECxi} = 1$$

Já o modelo de Ação Independente (IA) (Bliss, 1939) preconiza que os compostos individuais afetam os organismos através de modos de ação diferentes, sendo assim seus efeitos são independentes um do outro durante a exposição, absorção e ação tóxica. Sua fórmula é baseada na probabilidade das repostas, em que Y corresponde à resposta biológica, C*i* corresponde à concentração dos químicos na mistura, q_i (C_i) é a probabilidade de não-resposta, u_{max} é a resposta do controle para *endpoints* e Π é a função de multiplicação.

$$Y = \mu \max \prod_{i=1}^{n} qi\ (Ci)$$

No meio ambiente, os compostos podem interagir dentro dos organismos, então podem ocorrer desvios de ambos os modelos de referência, como sinergismo, que é um efeito tóxico mais severo ou antagonismo, um efeito de menor severidade; e ainda desvios dependentes de nível da dose ou relação de dose (Jonker et al., 2005; Loureiro et al., 2010). Diante disso, a ferramenta MIXTOX propicia a avaliação desses desvios (Jonker et al., 2005), que podem ser sinergismo ou antagonismo (S/A), dependentes do nível da dose (*Dose Level* – DL) ou da proporção da dose (*Dose Ratio* – DR). No desvio DL, os efeitos da toxicidade são diferentes em doses baixas e elevadas dos compostos. Diferentemente disso, em DR a toxicidade é dependente da composição da mistura (Jonker et al., 2005).

Para representar graficamente as interações oriundas das misturas tóxicas, com doses isoladas e combinadas, que provocam X% de efeito de dois compostos, é usado o isobolograma. Essa representação gráfica é composta por isoboles de aditividade, sinergismo e antagonismo (Figura 1). Nos eixos X e Y, são representadas as respectivas doses do composto 1 e do composto 2, em que cada ponto corresponde a um par de doses que atingem o CE_{50} quando estão associados. Nos isobologramas, as CE_{50} oriundos da aplicação isolada de cada produto são unidas, formando a isobole de aditividade. Os outros valores de CE_{50} obtidos da associação em diferentes proporções dos produtos podem ser avaliados em relação à sua posição diante da isobole de aditividade. Então, a ação é de aditividade se esses pontos

estiverem posicionados na região de entorno da isobole de aditividade; a ação é de sinergismo se esses pontos ficarem posicionados abaixo e a ação é de antagonismo se estiverem localizados acima. Sendo assim, isoboles representadas de forma linear correspondem a não interação, isoboles representadas de forma côncava representam sinergismo e finalmente, isoboles convexas representam antagonismo (Kruse et al., 2006; Ryall e Tan, 2015). Uma isobole enviesada com ambas formas representam alterações no tipo de interação sinergística ou antagônica dependendo da faixa de concentrações.

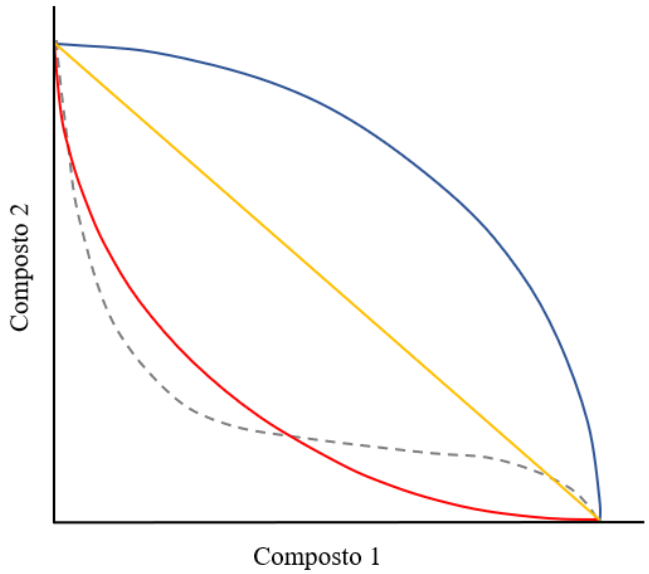

Figura 1. Interações entre os compostos 1 e 2 são representadas pelo isobolograma. A aditividade (sem interação) é apresentada pela linha amarela, sinergismo pela curva vermelha e antagonismo pela curva azul. Uma isobole enviesada é representada pela linha pontilhada. Fonte: Modificado de Bell (2005).

1.3 Substância teste (tungstato de prata (α-Ag_2WO_4)), toxicidade e múltiplos *endpoints*

Os tungstatos são óxidos mistos com aplicações inovadoras e, por isso, têm chamado a atenção de cientistas (Santana et al., 2014). São semicondutores que compõem um grupo de materiais funcionais com propriedades interessantes (Santana et al., 2014; Assis et al., 2018).

Em especial, o tungstato de prata (α-Ag_2WO_4) é um componente dessa classe de materiais e pode ter diferentes estruturas cristalográficas: β-hexagonal, γ -cúbica e α-ortorrômbica (Silva et al., 2014). As estruturas β e γ-Ag_2WO_4 são consideradas metaestáveis e quando aquecidas a 187 ºC e 257 ºC podem ser transformadas em α-Ag_2WO_4. Diferentemente, a estrutura α-Ag_2WO_4 é mais estável, quando aquecida até aproximadamente 347 ºC (Jacomaci et al., 2019).

O α-Ag_2WO_4 possui propriedades físicas e química notáveis, que o tornam um material multifuncional (Laier et al., 2020), que possui, por exemplo, atividade antitumoral (Lin et al., 2012; Assis et al., 2019) e microbicida (Nobre et al., 2019; Macedo et al., 2019; Laier et al., 2020; Alvarez-Roca et al., 2021), e é usado em sensores (Silva et al., 2014; Muthamizh et al., 2015, Silva et al., 2016), em materiais magnéticos (Assis et al., 2020) e como fotocatalisador na degradação de corantes orgânicos (Macedo et al., 2018; Arumugam et al., 2020; Ayappan et al., 2020; Cruz et al., 2020; Dai et al., 2010; Macedo et al., 2019). Todas essas propriedades são definidas de acordo com o tamanho, a morfologia e a estrutura do cristal (Cruz et al., 2020; Laier et al., 2020; Assis et al., 2021). Considerando esses fatores intrínsecos dos microcristais, a morfologia pode ser destacada como um dos mais relevantes (Cruz et al., 2020), já que é justamente a superfície a responsável na determinação dos sítios ativos (Macedo et al., 2018).

As diferenças na energia superficial das facetas que integram as morfologias de α-Ag_2WO_4 cúbico (α-Ag_2WO_4 – C) e α-Ag_2WO_4 *rod* (α-Ag_2WO_4 – R) estão descritas de forma detalhada em Macedo et al. (2018). Nesse estudo, os autores mostram que a morfologia cúbica tem um arranjo de superfícies de (010), (100) e (001) e é obtida pelo uso de dodecil sulfato de sódio (SDS), um surfactante aniônico, em sua síntese. De acordo com Macedo et al. (2018), o SDS estabiliza as superfícies (100) e (001) e impede o surgimento da superfície predominante da morfologia rod- hexagonal (010), (001) e (101), sendo que as diferenças existentes entre cada morfologia são (101) para α-Ag_2WO_4 - R e (100) para α-Ag_2WO_4-C. A superfície (101) tem 4 *clusters* vagos na sua superfície ([AgO_3.3Vo], [AgO_5.2Vo] e dois [WO_5. Vo]) enquanto que a superfície (100) tem 3 *clusters* vazios na sua superfície ([AgO_3.3Vo], [AgO_5.2Vo] e um [WO_5. Vo]). Estes aglomerados representam os centros de atividade superficial destas superfícies e são apontados como os locais de atividade. Por sua vez, esses locais são responsáveis pela propriedade dos materiais de interagir, por exemplo, com organismos, além de liberar íons prata (Ag).

Lopes et al. (2014) destacam que a liberação dos íons das partículas possui relação com a área de superfície, tamanho, forma e estrutura da partícula e é dependente de como a mesma é sintetizada, além de sofrer variações de acordo com o meio em que são dispersas. A liberação de íons nos ecossistemas aquáticos pelas partículas é uma preocupação e pode ser uma ameaça aos organismos, especialmente os íons de prata, por terem interações conhecidas com proteínas e enzimas (Navarro et al., 2008) e serem altamente tóxicos para a biota aquática (Stoiber et al., 2015).

De modo geral, compósitos que possuem prata em sua composição causam toxicidade a diferentes grupos taxonômicos (Navarro et al., 2008; Oukarroum et al., 2012; He et al., 2012; Angel et al., 2013; Ribeiro et al., 2014; Sohn et al., 2015; Koser et al., 2017, Martins et al., 2007), tais como plantas aquáticas (Varga et al., 2018), peixes (Griffitt et al., 2012), bactérias (Fabrega et al., 2009), microalgas (Kleiven et al., 2019; Ribeiro et al., 2015; Sendra et al., 2017) e microcrustáceos, especialmente os da ordem Cladocera (Hook and Fisher, 2001; Kim et al., 2011; Gaiser et al., 2011; Wang et al., 2012; Angel et al., 2013; Sakamoto et al., 2014; Seitz et al., 2015; Sohn et al., 2015; Shen et al., 2015; Becaro et al., 2015). No que se refere à toxicidade de α-Ag_2WO_4, sabe-se que esse microcristal afeta a sobrevivência de bactérias resistentes a antibióticos e fungos (Foggi et al., 2017a; Foggi et al., 2017b).

A intensidade dos efeitos tóxicos para os organismos planctônicos depende de alguns fatores, como a quantidade de matéria orgânica dissolvida e presença ou ausência de alimento, no caso dos cladóceros, o pH da água, tamanho, revestimento e funcionalização das partículas e tempo de exposição dos organismos (Farré et al., 2009; Liu e Hurt, 2010; Zhao e Wang 2012; Newton et al., 2013; Conine e Frost, 2016). Segundo Jung et al. (2017), o destino e impacto ecotoxicológico das partículas são determinados pela interação de vários fatores: liberação de íons tóxicos, especiação de íons liberados, bem como a carga superficial.

Os principais danos aos organismos aquáticos, causados por íons prata e por materiais que possuem prata em sua composição, incluem danos em nível populacional, como inibição ao crescimento e em nível intracelular, como danos ao DNA e estresse oxidativo (Rogers et al., 2018; He et al., 2012; Huang et al., 2016; Sorensen et al., 2016; Lekamge et al., 2020) para microalgas. Em cladóceros, os íons prata e materiais a base de prata podem gerar comprometimento nas taxas de ingestão (Ribeiro et al., 2014), estresse oxidativo com produção de espécies reativas de oxigênio - EROs (Poynton et al., 2012, Levard et al., 2012; Newton et al., 2013; Fu et al., 2014), inibição do crescimento e alteração na reprodução (Bielmyer et al., 2002).

Por outro lado, com relação à toxicidade do tungstato, alguns estudos prévios, descrevem que o tungstato de sódio, utilizado na síntese de α-Ag_2WO_4, inibe o crescimento de *Selenastrum capricornutum* (*Raphidocelis subcapitata*) em torno de 75% em uma concentração de aproximadamente 2,42 g L^{-1} e apresenta uma CL_{50} de 0,344 g L^{-1} para *D. magna* (Strigul et al., 2009). Ainda, Khangarot e Ray (1989) obtiveram uma CE_{50} 48 h de 89,39 mg L^{-1} para tungstato de sódio (Na_2WO_4). Isso mostra, portanto, que o tungstato de sódio é pouco tóxico levando em consideração essas espécies citadas.

Neste estudo, foram escolhidas duas espécies de organismos planctônicos, pertencentes a dois diferentes níveis tróficos: um produtor primário e um consumidor primário (herbívoro). A espécie de microalga utilizada como organismo teste foi a *Raphidocelis subcapitata* (Korshikov) Hindák, 1990 (anteriormente denominada de *Selenastrum capricornutum* e *Pseudokirchneriella subcapitata*), uma alga verde unicelular integrante do grupo das clorofíceas. Ocorre em ambientes oligotróficos a eutróficos (Blaise e Vasseur, 2005), é cosmopolita e internacionalmente recomendada como organismo teste (OECD, 2011) em estudos ecotoxicológicos, por apresentar rápido ciclo de vida e crescimento, além de ser facilmente mantida e cultivada em condições controladas de laboratório. De modo geral, os efeitos deletérios sobre a espécie de microalga clorofícea *Raphidocelis subcapitata* compreendem os níveis populacional, como a inibição do crescimento (Kleiven et al., 2019), morfológico, alterando a complexidade e o tamanho celular, a composição bioquímica (Alho et al., 2020) e processos fisiológicos (Kleiven et al., 2019; Alho et al., 2020).

Considerando que as microalgas são organismos autótrofos responsáveis por processos essenciais à manutenção da vida na Terra, como a produção de oxigênio e a fixação de carbono (Ribeiro et al., 2015), e contribuem com cerca de 40% da produtividade global de biomassa (Dash et al., 2012), as alterações nos processos fotossintéticos da produção primária podem causar sérios problemas aos ecossistemas e também à espécie humana, com comprometimento do abastecimento de alimentos e mudanças climáticas (Rai et al., 1996).

As avaliações de parâmetros fisiológicos e bioquímicos em estudos ecotoxicológicos com algas ainda são escassas, mesmo quando tais parâmetros são estudados separadamente. A avaliação ecotoxicológica a partir de múltiplos parâmetros (*endpoints*) propicia uma abordagem integrada, que confere melhor compreensão dos resultados nos diferentes níveis de toxicidade (Domingues et al., 2016). Nos testes de toxicidade com células algais, o uso da citometria de fluxo permite avaliar precisamente como o ciclo celular é afetado, a partir do

crescimento, tamanho e complexidade celular, além de identificar a produção intracelular de EROs (Alho et al., 2020).

Além disso, sabe-se que diversos fatores ambientais afetam o estado fisiológico dos produtores primários, por comprometerem a fotossíntese ou os processos bioquímicos. Por isso, a aferição dos parâmetros fotossintéticos é fundamental e representa uma forma confiável para identificar o estresse ambiental (Juneau e Popovic, 2000). Portanto, a avaliação de parâmetros fotossintéticos via fluorímetro de amplitude modulada (Phytoplankton Analyzer, Phyto-PAM, Heinz Walz GmbH, Germany) e a determinação do teor de clorofila *a* indicam a saúde fisiológica de organismos autótrofos (Juneau et al., 2005). Ainda, a determinação da quantidade de moléculas biológicas, como carboidratos totais, é essencial para entender a resposta das microalgas após a exposição aos contaminantes, porque mudanças nas condições ambientais podem afetar significativamente a composição qualitativa da biomassa (Markou et al., 2012). Os carboidratos compõem a parede celular e atuam no armazenamento dentro da célula algal, provendo a energia utilizada nos processos metabólicos (Geider e La Roche, 2002; Raven e Beardall, 2004). Esses compostos de armazenamento permitem que as microalgas possam ajustar seu crescimento face às mudanças nas condições ambientais (Kromkamp, 1987).

Por outro lado, os efeitos negativos sobre os consumidores primários (herbívoros), como os microcrustáceos da Ordem Cladocera, geralmente englobam imobilidade (Becaro et al., 2015; Gebara et al., 2019) e mortalidade (Sohn et al., 2015), produção de EROs (Mansano et al., 2018) e alterações metabólicas, como modificações nas taxas de ingestão e reprodução (Mansano et al., 2018). Esses efeitos deletérios sobre os cladóceros podem comprometer a produtividade secundária e o fluxo de energia, com sérios danos a diferentes níveis tróficos do ecossistema aquático.

O consumidor primário nativo da região Neotropical, utilizado no presente estudo foi a espécie *Ceriodaphnia silvestrii* (Família Daphniidae, Super Ordem Cladocera), a qual possui ocorrência em corpos d'água dos estados de São Paulo, Rio Grande do Sul, Goiás e Distrito Federal (ElMoor-Loureiro, 1997; Rocha e Güntzel, 2000). Essa espécie de cladócero é comumente utilizada em estudos ecotoxicológicos, por ser facilmente cultivada em condições controladas em laboratório e já ter suas condições de cultivo bem estabelecidas (Fonseca e Rocha, 2004). Além de possuir um ciclo de vida curto, com reprodução por partenogênese e alta taxa de fecundidade (Fonseca e Rocha, 2004), também possui grande sensibilidade a diversos contaminantes (Moreira et al., 2014; Mansano et al., 2018; de Lucca et al., 2018; Gebara et al., 2021). Quando comparada às espécies exóticas, a espécie nativa *C. silvestrii*

apresenta respostas distintas aos contaminantes (Moreira et al., 2014), o que reforça a importância do seu uso em estudos de regiões tropicais. Essa espécie é considerada um organismo padrão em testes de toxicidade, de acordo com a Associação Brasileira de Normas Técnicas – NBR 13373 (ABNT, 2017).

1.4 Justificativa

Avanços na síntese e na fabricação de materiais funcionais como α-Ag_2WO_4 podem gerar benefícios sociais e econômicos em virtude de suas potenciais aplicações, tais como em: sensores (Silva et al., 2014; Muthamizh et al., 2015, Silva et al., 2016), remoção de poluentes da água (Macedo et al., 2018; Arumugam et al., 2020; Ayappan et al., 2020; Cruz et al., 2020; Dai et al., 2010; Macedo et al., 2019), materiais magnéticos (Assis et al., 2020), uso como microbicida (Nobre et al., 2019; Macedo et al., 2019; Laier et al., 2020; Alvarez-Roca et al., 2021) e até ação antitumoral (Lin et al., 2012; Assis et al., 2019).

Apesar de haver muitos trabalhos que avaliam a ecotoxicidade de compósitos a base de prata, não existem, até o momento, trabalhos que avaliem os efeitos da toxicidade do α-Ag_2WO_4 para espécies planctônicas, especialmente para a espécie de cladócero neotropical *Ceriodaphnia silvestrii* e para a microalga clorofícea *Raphidocelis subcapitata*. Considerando a sensibilidade desses organismos aquáticos a diversos tipos de contaminantes (Mansano et al., 2018; De Lucca et al.,2018; Gebara et al., 2021), e a inexistência de informações sobre os efeitos tóxicos causados pelo α-Ag_2WO_4, com morfologias diferentes, faz-se necessário um estudo que avalie estes compósitos isolados e em mistura, com diferentes tipos de exposição, considerando testes de toxicidade aguda e crônica e que especialmente avaliem múltiplos parâmetros do ciclo de vida dos organismos. Os resultados obtidos neste estudo podem subsidiar as agências reguladoras, no estabelecimento de limiares seguros de microcristais de prata para o ambiente aquático e auxiliar no desenvolvimento de materiais funcionais mais seguros para a biota.

Referências

ABNT, Associação Brasileira de Normas Técnicas. Ecotoxicologia aquática – Toxicidade crônica – Método de ensaio com *Ceriodaphnia* spp (Crustacea, Cladocera) ABNT NBR 13373. 15p, 2017.

ALHO, L.O. G., et al. Photosynthetic, morphological and biochemical biomarkers as tools to investigate copper oxide nanoparticle toxicity to a freshwater chlorophyceae. **Environmental Pollution**, v. 265, p. 114856, 2020.

ALVAREZ-ROCA, R. et al. Selective Synthesis of α-, β-, and γ-Ag_2WO_4 Polymorphs: Promising Platforms for Photocatalytic and Antibacterial Materials. **Inorganic Chemistry**, v. 60, n. 2, p. 1062–1079, 2021.

ANGEL, B. M. et al. The impact of size on the fate and toxicity of nanoparticulate silver in aquatic systems. **Chemosphere**, v. 93, n. 2, p. 359–365, 2013.

ARUMUGAM, R. et al. One-pot preparation of AgBr / α-Ag_2WO_4 composite with superior photocatalytic activity under visible-light irradiation. **Colloids and Surfaces A**, v. 586, n. October 2019, p. 124079, 2020.

ASSIS, M. et al. Towards the scale-up of the formation of nanoparticles on α-Ag_2WO_4 with bactericidal properties by femtosecond laser irradiation. **Scientific Reports**, v. 8, n. 1, p. 1–11, 2018.

ASSIS, Marcelo de et al. Ag nanoparticles/α-Ag_2WO_4 composite formed by electron beam and femtosecond irradiation as potent antifungal and antitumor agents. **Scientific reports**, v. 9, n. 1, p. 1-15, 2019.

ASSIS, M. et al. Unconventional Magnetization Generated from Electron Beam and Femtosecond Irradiation on α-Ag_2WO_4: A Quantum Chemical Investigation. **ACS Omega**, v. 5, n. 17, p. 10052–10067, 2020.

ASSIS, M. et al. Revealing the nature of defects in α-Ag_2WO_4 by positron annihilation lifetime spectroscopy: A joint experimental and theoretical study. **Crystal Growth and Design**, v. 21, n. 2, p. 1093–1102, 2021.

AYAPPAN, C. et al. Facile preparation of novel Sb_2S_3 nanoparticles / rod-like α -Ag_2WO_4 heterojunction photocatalysts : Continuous modulation of band structure towards the efficient removal of organic contaminants. **Separation and Purification Technology**, v. 236, n. November 2019, p. 116302, 2020.

AZEVEDO, FA de; CHASIN, AA da M. As bases toxicológicas da ecotoxicologia. **São Carlos, SP: RiMa**, v. 2004, p. 30-36, 2003.

BECARO, A. A. et al. Toxicity of PVA-stabilized silver nanoparticles to algae and microcrustaceans. **Environmental Nanotechnology, Monitoring and Management**, v. 3, p. 22–29, 2015.

BELL, A. Antimalarial drug synergism and antagonism: mechanistic and clinical significance. **FEMS Microbiology Letters, v.** 253, n. 2, p. 171-184, 2005.

BERENBAUM, M.C. The expected effect of a combination of agents: The general solution. **Journal of Theoretical Biology,** v. 114, n. 3, p. 413-431, 1985.

BIELMYER, G.K., Bell, R.A. and Klaine, S.J. Effects of ligand- bound silver on *Ceriodapnia dubia*. **Environmental Toxicology and Chemmistry**, v. 21, n. 10, p. 2204-2208, 2002.

BLAISE, C., VASSEUR, P. Algal microplate toxicity test. In: Blaise C, Férard J-F (eds). Small-scale freshwater toxicity investigations. Vol 1. Springer, p. 137-179, 2005.

BLISS, C.I.. The toxicity of poisons applied jointly. **Annals of applied Biology, v. 26**, n. 3, p. 585-615, 1939.

CASSEE, F. R. et al. Toxicological evaluation and risk assessment of chemical mixtures. **Critical Reviews in Toxicology**, v. 28, n. 1, p. 73–101, 1998.

CONINE, Andrea L.; FROST, Paul C. Variable toxicity of silver nanoparticles to *Daphnia magna*: effects of algal particles and animal nutrition. **Ecotoxicology**, v. 26, n. 1, p. 118-126, 2017.

COSTA, Carla Regina et al. A toxicidade em ambientes aquáticos: discussão e métodos de avaliação. **Química nova**, v. 31, p. 1820-1830, 2008.

CRUZ, L. et al. Multi-dimensional architecture of Ag/α-Ag_2WO_4 crystals: insights into microstructural, morphological, and photoluminescence properties. **CrystEngComm**, v. 22, n. 45, p. 7903–7917, 2020.

DAI, X. et al. Facile hydrothermal synthesis and photocatalytic activity of bismuth tungstate hierarchical hollow spheres with an ultrahigh surface area **Dalton Transactions**, v. 39, n. 14,. p. 3426–3432, 2010.

DASH, A. et al. Effect of Silver Nanoparticles on Growth of eukaryotic green algae. **Nano-micro letters**, v. 4, n. 3, p. 158–165, 2012.

DOMINGUES, I. et al. Effects of ivermectin on *Danio rerio*: a multiple endpoint approach: behaviour, weight and subcellular markers. **Ecotoxicology**, v. 25, n. 3, p. 491–499, 2016.

FABREGA, J. et al. Silver nanoparticle impact on bacterial growth: Effect of pH, concentration, and organic matter. **Environmental Science & Technology**, v. 43, n. 19, p. 7285–7290, 2009.

FARRÉ, M. et al. Ecotoxicity and analysis of nanomaterials in the aquatic environment. **Analytical and Bioanalytical Chemistry**, v. 393, n. 1, p. 81–95, 2009.

FAUST, M. et al. Joint algal toxicity of 16 dissimilarly acting chemicals is predictable by the concept of independent action. **Aquatic toxicology**, v. 63, n. 1, p. 43-63, 2003.

FERNÍCOLA, N. A. G. G.; BOHRER-MOREL, M. B. C.; BAINY, A. C. D. Ecotoxicologia. **As bases toxicológicas da ecotoxicologia. São Carlos: RiMa**, 2003.

FERON, V. J. et al. Toxicology of chemical mixtures: challenges for today and the future. **Toxicology**, v. 105, n. 2–3, p. 415–427, 1995.

FERREIRA, A. L. G.; LOUREIRO, S.; SOARES, A. M. V. M. Toxicity prediction of binary combinations of cadmium, carbendazim and low dissolved oxygen on *Daphnia magna*. **Aquatic Toxicology**, v. 89, n. 1, p. 28–39, 2008.

FOGGI, C. C. et al. Tuning the Morphological, Optical, and Antimicrobial Properties of α-Ag_2WO_4 Microcrystals Using Different Solvents. **Crystal Growth & Design**, v. 17, n. 12, p. 6239–6246, 2017.

FONSECA; ROCHA, A. L. The life-cycle of *Ceriodaphnia silvestrii* Daday, 1902, a Neotropical endemic species (Crustacea, Cladocera, Daphnidae). **Acta Limnol. Bras**, v. 16, n. 4, p. 319–328, 2004.

FU, Peter P., Xia, Q., Hwang, H. M., Ray, P. C., & Yu, H. Mechanisms of nanotoxicity: generation of reactive oxygen species. **Journal of food and drug analysis**, v. 22, n. 1, p. 64-75, 2014.

GAISER, B. K. et al. Effects of silver and cerium dioxide micro- and nano-sized particles on *Daphnia magna*. **Journal of Environmental Monitoring**, v. 13, n. 5, p. 1227-1235, 2011.

GEBARA, R. C. et al. Effects of iron oxide nanoparticles (Fe_3O_4) on life history and metabolism of the Neotropical cladoceran *Ceriodaphnia silvestrii*. **Ecotoxicology and environmental safety**, v. 186, p. 109743, 2019.

GEBARA, Renan Castelhano et al. Zinc and aluminum mixtures have synergic effects to the algae *Raphidocelis subcapitata* at environmental concentrations. **Chemosphere**, v. 242, p. 125231, 2020.

GEBARA, R. C. et al. Toxicity and Risk Assessment of Zinc and Aluminum Mixtures to *Ceriodaphnia silvestrii* (Crustacea: Cladocera). **Environmental Toxicology and Chemistry**, v. 40, n. 10, p. 2912–2922, 2021.

GEIDER, R.; ROCHE, J. LA; GEIDER, R. J. Redfield revisited: variability of C:N:P in marine microalgae and its biochemical basis. **European Journal of Phycology Society**, v. 371, n. 37, p. 1–17, 2002.

GRIFFITT, R. J. et al. Effects of chronic nanoparticulate silver exposure to adult and juvenile sheepshead minnows (*Cyprinodon variegatus*). **Environmental Toxicology and Chemistry**, v. 31, n. 1, p. 160–167, 2012.

GROTEN, J.P. Mixtures and interactions. **Food Chem. Toxicol**. v.38, p. 65-71, 2000.

HE, D.; DORANTES-ARANDA, J. J.; WAITE, T. D. Silver nanoparticle-algae interactions: Oxidative dissolution, reactive oxygen species generation and synergistic toxic effects. **Environmental Science and Technology**, v. 46, n. 16, p. 8731–8738, 2012.

HOOK, S. E.; FISHER, N. S. Sublethal effects of silver in zooplankton: Importance of exposure pathways and implications for toxicity testing. **Environmental Toxicology and Chemistry**, v. 20, n. 3, p. 568–574, 2001.

HU, J. et al. Quantifying the effect of nanoparticles on As(V) ecotoxicity exemplified by nano-Fe_2O_3 (magnetic) and nano-Al_2O_3. **Environmental Toxicology and Chemistry**, v. 31, n. 12, p. 2870–2876, 2012.

HUANG, J.; CHENG, J.; YI, J. Impact of silver nanoparticles on marine diatom *Skeletonema costatum*. **Journal of Applied Toxicology**, v. 36, n. 10, p. 1343-1354, 2016.

JACOMACI, N. et al. Dielectric Behavior of α-Ag_2WO_4 and its Huge Dielectric Loss Tangent. **Materials Research**, v. 22, n. 4, p. 2–11, 2019.

JONKER, M. J. et al. Significance testing of synergistic/antagonistic, dose level-dependent, or dose ratio-dependent effects in mixture dose-response analysis. **Environmental Toxicology and Chemistry: An International Journal**, v. 24, n. 10, p. 2701–2713, 2005.

JUNEAU, P.; GREEN, B. R.; HARRISON, P. J. Simulation of Pulse-Amplitude-Modulated (

PAM) fluorescence : Limitations of some PAM-parameters in studying environmental stress effects. **Photosynthetica**, v. 43, n. 1, p. 75–83, 2005.

JUNEAU, P.; POPOVIC, R. Evidence for the Rapid Phytotoxicity and Environmental Stress Evaluation Using the PAM Fluorometric Method : Importance and Future Application. **Ecotoxicology**, v. 8, n. 6, p. 449-455, 2000.

JUNG, Y. et al. Implications of Pony Lake Fulvic Acid for the aggregation and dissolution of oppositely charged surface-coated silver nanoparticles and their ecotoxicological effects on *Daphnia magna.* **Environmental science & technology**, v. 52, n. 2, p. 436-445, 2017.

KHANGAROT, B. S.; RAY, P. K. Investigation of correlation between physicochemical properties of metals and their toxicity to the water flea *Daphnia magna* Straus. **Ecotoxicology and Environmental Safety**, v. 18, n. 2, p. 109–120, 1989.

KIM, J.; KIM, S.; LEE, S. Differentiation of the toxicities of silver nanoparticles and silver ions to the Japanese medaka (*Oryzias latipes*) and the cladoceran *Daphnia magna.* **Nanotoxicology**, v. 5, n. 2, p. 208–214, 2011.

KLEIVEN, M.; MACKEN, A.; OUGHTON, D. H. Growth inhibition in *Raphidocelis subcapita* e Evidence of nanospecific toxicity of silver nanoparticles. **Chemosphere**, v. 221, p. 785–792, 2019.

KROMKAMP, Jacco. Formation and functional significance of storage products in cyanobacteria. **New Zealand Journal of Marine and Freshwater Research**, v. 21, n. 3, p. 457-465, 1987.

KRUSE, N.D., VIDAL, R.A., TREZZI, M.M. Curvas de resposta e isobolograma como forma de descrever a associação de herbicidas inibidores do fotossistema II e da síntese de carotenóides. **Planta daninha, v.** 24, n. 3, p. 579-587, 2006.

LEKAMGE, S. et al. The toxicity of coated silver nanoparticles to the alga *Raphidocelis subcapitata*. **SN Applied Sciences**, v. 2, n. 4, p. 1-14, 2020.

LEVARD, C. et al. Environmental transformations of silver nanoparticles: Impact on stability and toxicity. **Environmental Science and Technology**, v. 46, n. 13, p. 6900–6914, 2012.

LIN, C. A. O. et al. Anti-tumor activity of self-charged (Eu, Ca): WO_3 and Eu: $CaWO_4$ nanoparticles. **Bulletin of Materials Science**, v. 35, n. 5, p. 767–772, 2012.

LIU, Jingyu; HURT, Robert H. Ion release kinetics and particle persistence in aqueous nano-silver colloids. **Environmental science & technology**, v. 44, n. 6, p. 2169-2175, 2010.

LOEWE, S., MUISCHNEK, H.. Combinated effects I announcement–implements to the problem. **Naunyn-Schmiedebergs Arch.. Exp. Pathol. Pharmakol,** v. 114, p. 313-326, 1926.

LOUREIRO, S. et al. Toxicity of three binary mixtures to *Daphnia magna*: comparing chemical modes of action and deviations from conceptual models. **Environ. Toxicol. Chem**, v. 29, n. 8, p. 1716-1726, 2010.

LOPES, S. et al. Zinc oxide nanoparticles toxicity to *Daphnia magna*: Size-dependent effects and dissolution. **Environmental Toxicology and Chemistry**, v. 33, n. 1, p. 190–198, 2014.

LUCCA, G. M. DE; FREITAS, E. C. Effects of TiO_2 Nanoparticles on the Neotropical Cladoceran *Ceriodaphnia silvestrii* by Waterborne and Dietary Routes. **Water, Air, & Soil**

Pollution, v. 229, n. 9, p. 1-16, 2018.

MACEDO, N. G. et al. Surfactant-Mediated Morphology and Photocatalytic Activity of α-Ag_2WO_4 material. **The Journal of Physical Chemistry C**, v. 122, n. 15, p. 8667-8679, 2018.

MACEDO, N. G. et al. Tailoring the Bactericidal Activity of Ag Nanoparticles / α -Ag_2 WO_4 Composite Induced by Electron Beam and Femtosecond Laser Irradiation : Integration of Experiment and Computational Modeling. **ACS Applied Bio Materials**, v. 2, n. 2, p. 824-837, 2019.

MANSANO, A. S. et al. Toxicity of copper oxide nanoparticles to Neotropical species *Ceriodaphnia silvestrii* and *Hyphessobrycon eques*. **Environmental Pollution**, v. 243, p. 723–733, 2018.

MANSANO, Adrislaine S. et al. Effects of diuron and carbofuran and their mixtures on the microalgae *Raphidocelis subcapitata*. **Ecotoxicology and environmental safety**, v. 142, p. 312-321, 2017.

MARKOU, G.; CHATZIPAVLIDIS, I.; GEORGAKAKIS, D. Carbohydrates Production and Bio-flocculation Characteristics in Cultures of *Arthrospira* (*Spirulina*) *platensis*: Improvements Through Phosphorus Limitation Process. **Bioenergy Research**, v. 5, n. 4, p. 915–925, 2012.

MARTINS, J.; OLIVA TELES, L.; VASCONCELOS, V. Assays with *Daphnia magna* and *Danio rerio* as alert systems in aquatic toxicology. **Environment international**, v. 33, n. 3, p. 414–25, 2007.

MOREIRA, R. A. et al. A comparative study of the acute toxicity of the herbicide atrazine to cladocerans *Daphnia magna*, *Ceriodaphnia silvestrii* and *Macrothrix flabelligera*. **Acta Limnologica Brasiliensia**, v. 26, n. 1, p. 1–8, 2014.

MOREIRA, Raquel Aparecida et al. Exposure to environmental concentrations of fipronil and 2, 4-D mixtures causes physiological, morphological and biochemical changes in *Raphidocelis subcapitata*. **Ecotoxicology and Environmental Safety**, v. 206, p. 111180, 2020.

MUTHAMIZH, S. et al. $MnWO_4$ nanocapsules: Synthesis, characterization and its electrochemical sensing property. **Journal of Alloys and Compounds**, v. 619, p. 601–609, 2015.

NAVARRO, E. et al. Toxicity of silver nanoparticles to *Chlamydomonas reinhardtii.* **Environmental science & technology**, v. 42, n. 23, p. 8959–64, 2008.

NEWTON, K. M. et al. Silver nanoparticle toxicity to *Daphnia magna* is a function of dissolved silver concentration. **Environmental Toxicology and Chemistry**, v. 32, n. 10, p. 2356–2364, 2013.

NOBRE, F. X. et al. Antimicrobial properties of α-Ag_2WO_4 rod-like microcrystals synthesized by sonochemistry and sonochemistry followed by hydrothermal conventional method. **Ultrasonics Sonochemistry**, v. 58, n. November 2018, p. 104620, 2019.

OECD - Organizations for Economic Cooperation and Development. Guidelines for the Testing Chemicals. Freshwater Alga and Cyanobacteria, Growth Inhibition test. OECD section 2 Test No. 201, Paris, 2011.

OUKARROUM, A. et al. Inhibitory effects of silver nanoparticles in two green algae,

Chlorella vulgaris and *Dunaliella tertiolecta*. **Ecotoxicology and Environmental Safety**, v. 78, p. 80–85, 2012.

POYNTON, H. C. et al. Toxicogenomic responses of nanotoxicity in *Daphnia magna* exposed to silver nitrate and coated silver nanoparticles. **Environmental Science and Technology**, v. 46, n. 11, p. 6288–6296, 2012.

RAI, L. C.; TYAGI, B.; MALLICK, N. Alternation in Photosynthetic Characteristics of Anabaena doliolum Following Exposure to UVB and Pb. **Photochemistry and photobiology**, v. 64, n. 4, p. 658–663, 1996.

RAVEN, J. A.; BEARDALL, J. Carbohydrate Metabolism and Respiration in Algae. In: **Photosynthesis in algae**. Springer, Dordrecht, 2003. p. 205-224.

REIS, Larissa Luiza et al. Effects of cadmium and cobalt mixtures on growth and photosynthesis of *Raphidocelis subcapitata* (Chlorophyceae). **Aquatic Toxicology**, p. 106077, 2022.

RIBEIRO, F. et al. Silver nanoparticles and silver nitrate induce high toxicity to *Pseudokirchneriella subcapitata*, *Daphnia magna* and *Danio rerio*. **Science of the Total Environment**, v. 466–467, p. 232–241, 2014.

RIBEIRO, F. et al. Uptake and elimination kinetics of silver nanoparticles and silver nitrate by *Raphidocelis subcapitata* : The influence of silver behaviour in solution. **Nanotoxicology**, v. 9, n. 6, p. 686-695, 2015.

ROCHA, O.; GÜNTZEL, AM. Crustáceos branquiópodos. In: ISMAEL, D., VALENTI, WC., MATSUMURA-TUNDISI, T. and ROCHA, O. Biodiversidade do estado de São Paulo, Brasil: invertebrados de água doce. vol. 4. São Paulo: FAPESP. p.110-144, 1999.

ROGERS, K.R. et al. Characterization of engineered nanoparticles in commercially available spray disinfectant products advertised to contain colloidal silver. **Science of the Total Environment**. v. 619–620, p. 1375–1384, 2018.

RYALL, K.A., TAN, A. Systems biology approaches for advancing the discovery of effective drug combinations. **J. Cheminform**. v. 7, n., p. 1-15, 2015.

SAKAMOTO, M. et al. Free Silver Ion as the Main Cause of Acute and Chronic Toxicity of Silver Nanoparticles to Cladocerans. **Archives of Environmental Contamination and Toxicology**, v. 68, n. 3, p. 500–509, 2014.

SANTANA, Y. V. B. DE et al. Silver Molybdate and Silver Tungstate Nanocomposites with Enhanced Photoluminescence. **Nanomaterials and Nanotechnology**, v. 4, p. 22, 2014.

SEITZ, F. et al. Effects of silver nanoparticle properties, media pH and dissolved organic matter on toxicity to *Daphnia magna*. **Ecotoxicology and Environmental Safety**, v. 111, p. 263–270, 2015.

SENDRA, M. et al. Direct and indirect effects of silver nanoparticles on freshwater and marine microalgae (*Chlamydomonas reinhardtii* and *Phaeodactylum tricornutum*). **Chemosphere**, v. 179, p. 279-289, 2017.

SHEN, M. H. et al. Exposure Medium: Key in Identifying Free Ag^{+} as the Exclusive Species of Silver Nanoparticles with Acute Toxicity to *Daphnia magna*. **Scientific Reports**, v. 5, p. 4–11, 2015.

SILVA, Ana Rita R. et al. Mixture toxicity prediction of substances from different origin sources in *Daphnia magna*. **Chemosphere**, v. 292, p. 133432, 2022.

SILVA, L. F. et al. A novel ozone gas sensor based on one-dimensional (1D) α-Ag_2WO_4 nanostructures. **Nanoscale**, v. 6, n. 8, p. 4058–4062, 2014.

SILVA, L.F., Catto, A.C., Avansi, W., Cavalcante, L.S., Mastelaro, V.R., Andrés, J., Aguir, K., Longo, E., Acetone gas sensor based on α-Ag_2WO_4 nanorods obtained via a microwave-assisted hydrothermal route. **Journal ofAlloys Compounds**, v. 683, p. 186–190, 2016.

SINGH, A. K. Chapter 5 - Principles of Nanotoxicology. In: SINGH, A. K. B. T.-E. N. (Ed.). . Boston: Academic Press, 2016. p. 171–227.

SOHN, E. K. et al. Aquatic Toxicity Comparison of Silver Nanoparticles and Silver Nanowires. **BioMed Research International** v. 2015, 2015.

SØRENSEN, S. N. et al. Acute and chronic effects from pulse exposure of *D. magna* to silver and copper oxide nanoparticles. **Aquatic Toxicology**, v. 180, p. 209-217, 2016.

STOIBER, Tasha et al. Influence of hardness on the bioavailability of silver to a freshwater snail after waterborne exposure to silver nitrate and silver nanoparticles. **Nanotoxicology**, v. 9, n. 7, p. 918-927, 2015.

STRIGUL, N. et al. Acute toxicity of boron, titanium dioxide, and aluminum nanoparticles to *Daphnia magna* and *Vibrio fischeri*. **Desalination**, v. 248, n. 1–3, p. 771–782, 2009.

TRUHAUT, René. Ecotoxicology: objectives, principles and perspectives. **Ecotoxicology and environmental safety**, v. 1, n. 2, p. 151-173, 1977.

VAN DEN BRINK, Paul J. et al. Predictive value of species sensitivity distributions for effects of herbicides in freshwater ecosystems. **Human and Ecological Risk Assessment**, v. 12, n. 4, p. 645-674, 2006.

VARGA, A. M.; HORVATI, J. Physiological and biochemical effect of silver on the aquatic plant *Lemna gibba* L.: evaluation of commercially available product containing colloidal silver. **Aquatic Toxicology**, 2018.

ZAGATTO, P.A., Bertoletti, E., Ecotoxicologia. In: Zagatto, P.A. Ecotoxicologia aquática. São Carlos: Rima. 1-12. 2006.

ZHAO, C.; WANG, W. Importance of surface coatings and soluble silver in silver nanoparticles toxicity to *Daphnia magna*. **Nanotoxicology**, v. 6, n. June, p. 361–370, 2012.

2. Objetivos e hipóteses

2.1 Objetivo geral

Avaliar os efeitos de microcristais de tungstato de prata (α-Ag_2WO_4), em duas morfologias, cúbica e *rod*, sobre organismos planctônicos em diferentes níveis tróficos, usando a microalga *Raphidocelis subcapitata* e o cladócero *Ceriodaphnia silvestrii*, como organismos teste, por meio de múltiplos *endpoints*.

2.2 Objetivos específicos

• Determinar os efeitos da toxicidade de α-Ag_2WO_4-C e α-Ag_2WO_4-R sobre *Raphidocelis subcapitata*, pela avaliação do seu crescimento, tamanho e complexidade celular; composição bioquímica e atividade fotossintética (eficiência fotossintética - Phyto PAM) e espécies reativas de oxigênio (EROs);

• Determinar a toxicidade aguda dos compostos isolados e em mistura sobre *Ceriodaphnia silvestrii*, via água, pela avaliação de parâmetros de imobilidade e taxas de alimentação;

• Determinar a toxicidade crônica dos compostos α-Ag_2WO_4-C e α-Ag_2WO_4-R sobre *Ceriodaphnia silvestrii*, pela avaliação de parâmetros reprodutivos, como a produção de neonatos e comprimento materno (ao final da exposição).

2.3 Hipóteses

• Os íons de prata liberados pelo tungstato de prata causam efeitos deletérios na microalga *Raphidocelis subcapitata* (produtor primário) e no cladócero *Ceriodaphnia silvestrii* (consumidor primário);

• Os efeitos das micropartículas isoladas são diferentes dos efeitos observados para os compostos em mistura, pois os efeitos podem ser possivelmente potencializados com as micropartículas em mistura;

• Diferentes morfologias causam toxicidade diferente para os organismos, com a maior toxicidade sendo causada pelo α-Ag_2WO_4 – R;

• A sensibilidade dos organismos em relação ao α-Ag_2WO_4 é diferente, sendo o cladócero *Ceriodaphnia. silvestrii* mais sensível ao α-Ag_2WO_4 do que a alga *Raphidocelis subcapitata*.

Capítulo 1. Toxicity of α-Ag_2WO_4 microcrystals to freshwater microalga *Raphidocelis subcapitata* at cellular and population levels

Publicado em: Chemosphere, v. 288 Part 2, p. 132536, 2022. DOI 10.1016/j.chemosphere.2021.132536

Highlights

- α-Ag_2WO_4–R (rod) was more toxic than α-Ag_2WO_4–C (cube) to *R. subcapitata*
- At 96 h, there was total population growth inhibition at the highest concentrations
- Both microcrystal shapes altered the cellular complexity of *R. subcapitata*
- α-Ag_2WO_4 exposure led to decreased chlorophyll *a* fluorescence at all concentrations
- α-Ag_2WO_4–R induced ROS production at the highest concentration (31.76 μg L^{-1})

ABSTRACT

Silver-based materials have microbicidal action, photocatalytic activity and electronic properties. The increase in manufacturing and consumption of these compounds, given their wide functionality and application, is a source of contamination to freshwater ecosystems and causes toxicity to aquatic biota. Therefore, for the first time, we evaluated the toxicity of the silver tungstate (α-Ag_2WO_4), in different morphologies (cube and rod), for the microalga *Raphidocelis subcapitata*. To investigate the toxicity, we evaluated the growth rate, cell complexity and size, reactive oxygen species (ROS) production and chlorophyll *a* (Chl a) fluorescence. The α-Ag_2WO_4 – R (rod) was 1.7 times more toxic than α-Ag_2WO_4 – C (cube), with IC_{10} and IC_{50} values of, respectively, 8.68 ± 0.91 μg L^{-1} and 13.72 ± 1.48 μg L^{-1} for α-Ag_2WO_4 – R and 18.60 ± 1.61 μg L^{-1} and 23.47 ± 1.16 μg L^{-1} for α-Ag_2WO_4 - C. The release of silver ions was quantified and indicated that the silver ions dissolution from the α-Ag_2WO_4 – R ranged from 34 to 71%, while the Ag ions from the α-Ag_2WO_4 – C varied from 35 to

97%. The α-Ag_2WO_4 – C induced, after 24 h exposure, the increase of ROS at the lowest concentrations (8.81 and 19.32 μg L^{-1}), whereas the α-Ag_2WO_4 – R significantly induced ROS production at 96 h at the highest concentration (31.76 μg L^{-1}). Both microcrystal shapes significantly altered the cellular complexity and decreased the Chl *a* fluorescence at all tested concentrations. We conclude that the different morphologies of α-Ag_2WO_4 negatively affect the microalga and are important sources of silver ions leading to harmful consequences to the aquatic ecosystem.

Keywords: ROS, Chlorophyceae, α-Ag_2WO_4, ecotoxicity, silver microparticles, growth inhibition.

1. Introduction

Recently, silver-based materials have drawn attention due to their excellent antimicrobial properties (Nobre et al., 2019; Penha et al., 2020). The high production of these materials increases the availability in the environment presenting a health risk to aquatic ecosystems leading to damage to different species of organisms, such as bacteria (Fabrega et al., 2009), microcrustaceans (Sorensen et al., 2016**)**, fish (Griffitt et al., 2011), aquatic plants (Varga et al., 2018) and microalgae (Ribeiro et al., 2015; Sendra et al., 2017; Kleiven et al., 2019). Among these materials**,** the silver tungstate (α-Ag_2WO_4) is a multifunctional material with physical and chemical properties relevant for different functions **(**Laier et al., 2020**)**. Silver tungstates are widely used in the microbial (Nobre et al., 2019; Macedo et al., 2019; Laier et al., 2020; Alvarez-Roca et al., 2021**)** and antitumor activity (Lin et al., 2012; Assis et al., 2019), sensors (Silva et al., 2014; Muthamizh et al., 2015, Silva et al., 2016), magnetic materials (Assis et al., 2020) and photocatalysts areas (Dai et al., 2010; Macedo et al., 2018).

This composite has been widely studied in fighting antibiotic resistant bacteria and fungi, such as *Staphylococcus aureus* (MRSA) and *Candida albicans* (Foggi et al., 2017). Besides that, this composite has the potential for gas detection and luminescence (Penha et al., 2020), and even to decontaminate organic dyes in polluted waters through photocatalysis (Macedo et al., 2018). Since α-Ag_2WO_4 becomes the focus of many studies, it is essential to know its impact on the environment, especially in aquatic environments.

The activity of α-Ag_2WO_4 is related to its size, morphology, composition and surface structure **(**Laier et al., 2020; Assis et al., 2021). Among these factors, the morphology of the compound is a major one because it is the surface that determines the number of active sites, which consequently significantly alters its properties (Macedo et al., 2018). Another crucial factor to be considered, regarding its toxicity, is the amount of ions released by the α-Ag_2WO_4. Zhao et al. (2012) emphasizes the importance of evaluating the Ag release as a result of particle surface changes in ecotoxicity studies, because the toxicity is often caused by the interaction of Ag ions with biological molecules, such as proteins and enzymes (Navarro et al., 2008). In relation to the environmental concentration threshold determined by the Environmental Agencies, it corresponds only to the ionic silver level. The ionic silver concentration limit in the United States is 3.2 µg L^{-1}, in Canada 0.1 µg L^{-1}, in Australia and New Zealand 0.05 µg L^{-1}, and in Scotland 0.1 µg L^{-1} (Kwak et al., 2015). The World Health Organization (2011) determined that the ionic silver limit up to 0.1 mg L^{-1} in drinking water poses no health risks (Lalau et al., 2020**)**. In Brazil, the National Council for the Environment - CONAMA 357/05 (Brasil, 2005) sets a limit of up to 0.01 mg L^{-1} of silver in freshwater.

Microalgae are essential in aquatic ecosystems as they are primary producers, producing oxygen for the maintenance of life of other organisms (Ribeiro et al., 2015; Wang et al., 2016). As they are at the base of aquatic food webs, damage to these organisms can impact higher trophic levels and the entire ecosystem (Munawar et al., 1989). Especially for

microalgae, it is widely known and discussed in the literature that silver-based materials can cause toxicity and adverse effects, such as oxidative stress, DNA damage and growth inhibition (Rogers et al., 2010; He et al., 2012; Huang et al., 2016; Sorensen et al., 2016; Lekamge et al., 2020). Furthermore, silver ions are extremely toxic to aquatic organisms, as they interact with biological molecules, compromising their functions (Odzak et al., 2017), in particular photosynthetic organisms.

In this study, we aimed to investigate the toxicity caused by two morphologies of α-Ag_2WO_4, cube (α-Ag_2WO_4 - C) and rod (α-Ag_2WO_4 - R) on the microalgae *Raphidocelis subcapitata*. This species is a cosmopolitan Chlorophyceae widely used in ecotoxicological studies due to its sensitivity to several contaminants (Mansano et al., 2017; Gebara et al., 2020; Reis et al., 2020). Moreover, it responds quickly to environmental changes (Almeida et al., 2019). We evaluated the toxicity of the isolated composites from multiple endpoints at the population (growth rate), morphological (cell complexity and size) and intracellular level (Chl *a* fluorescence and ROS production). This is the first study reporting the effects of α-Ag_2WO_4, in different morphologies for an aquatic organism. Understanding the toxicity mechanism of these compounds on a primary producer provides relevant information for the proper and cautious use of silver-based materials. In addition, our results are useful in guiding norms and resolutions with safe thresholds for freshwater ecosystems.

2. Material and methods

2.1 Synthesis and characterization of α-Ag_2WO_4

The samples of α-Ag_2WO_4 were synthesized by the coprecipitation (CP) method in aqueous medium, both to form rod and cube morphologies (Macedo et al., 2018). For α-Ag_2WO_4 - R, two solutions were prepared: (i) 1.10^{-3} mol of $Na_2WO_4.2H_2O$ (Sigma-Aldrich, 99.9% purity)

in 100 ml of distilled water and (ii) 2.10^{-3} mol of $AgNO_3$ (Cennabras, 99.8 % purity) in 100 ml of distilled water. Both were heated to 70 ° C and then solution (ii) was added to solution (i) under magnetic stirring. After that, the formation of a white precipitate was observed, which was left under stirring for 10 min. The precipitate was then separated by centrifugation (1 minute – 4400 rpm), washed five times with distilled water until pH ~ 7, and dried for 12 h at 60 °C. To obtain the α-Ag_2WO_4 - C, 1 g of sodium dodecyl sulfate (Sigma-Aldrich, 99% purity) was added to the solution (i) before adding solution (ii). The samples were characterized by X-ray diffraction (XRD) using a D/Max-2500PC diffractometer (Rigaku,) with Cu Kα radiation (λ = 1.5406 Å) and the morphologies of the samples were observed by field emission scanning electronic microscopy (FE-SEM) operated at 10 kV (Supra 35-VP, Carl Zeiss). The hydrodynamic size, polydispersity index (PdI) and zeta potential of the particles were measured in exposure medium and in ultrapure water at 0 h and 96 h by dynamic light scattering (DLS) using Zetasizer Nano ZS90, Malvern.

2.2 Silver concentrations and ion release

The silver concentrations in α-Ag_2WO_4 test solutions used in the toxicity tests (Tables S1 and S2, Supplementary material) were determined by inductively coupled plasma mass spectrometry (ICP-MS PerkinElmer NexION 2000), where the limits of quantification and detection were 0.0084 and 0.0028 μg L^{-1}, respectively. To detect the free silver ions, each sample was centrifuged (Eppendorf 5702 R, Germany) at 4400 rpm for 60 min using a 3 kDa Amicon centrifugal filter (Merck Millipore, Darmstadt, Germany) to remove α-Ag_2WO_4 particles or agglomerates. The filtered volumes were subsequently quantified using ICP-MS and therefore the fraction <3 kDa was considered dissolved Ag.

2.3 Algae culture and toxicity tests

The *R. subcapitata* inoculum was obtained from the Department of Ecology and Evolutionary Biology (DEBE, Federal University of São Carlos - UFSCar, São Carlos - SP, Brazil) and cultivated in culture medium CHU-12 (Chu, 1942) (Table S3, Supplementary material) at 25 ± 1 ºC, with light intensity (≅130 μmol photon m^{-2} s^{-1} LED light) and 12h/12h of light/ dark photoperiod. The room temperature was 24.5 - 25 °C and the pH values were around 7 – 8.5 and did not vary by more than 1.5 units. The particles were dispersed in ultrapure water using a bath sonicator (Ultra cleaner 1400 Unique) for 30 min and subsequently, were used to prepare test solutions. The algal cultures in the exponential growth phase were inoculated in a concentration of 1 x 10^5 cells ml^{-1} in 500 ml polycarbonate erlenmeyers containing 250 ml of test solutions. *R. subcapitata* was exposed for 96 h to concentrations of 0.00, 8.81, 19.32, 27.78, 32.87 and 36.25 μg L^{-1} for α-Ag_2WO_4-C and 0.00, 4.11, 5.84, 10.55, 10.67 and 31.76 μg L^{-1} for α-Ag_2WO_4-R. These concentrations were chosen based on preliminary tests. The toxicity tests followed the OECD (2006) guidelines, and 3 tests were performed, each one with triplicates for control and treatments.

2.4 Flow cytometric analysis

For algal cell counting, 1.8 ml samples were fixed with formaldehyde buffered with borax (1% final concentration) at room temperature. In the following step, the samples were frozen in liquid nitrogen and stored at -20°C until analysis. For ROS analysis, 495 μL of each sample and 5 μL of DCFH-DA (2′,7′-Dichlorofluorescein diacetate, Sigma Aldrich) diluted in dimethylsulfoxide (10^4 μM) were aliquoted, with a final concentration of 10 μM. After that, the samples were kept in the dark for 60 min and immediately analyzed by flow cytometry. Cell density and ROS measurements were performed in a FACSCalibur cytometer (Becton

Dickinson, San Jose, CA, USA) with a 15mW argon-ion laser (488 nm excitation), using 6 µm fluorescent beads as an internal standard (Fluoresbrite carboxylate microspheres; Polysciences, Warrington, Pennsylvania, USA). The cells of *R. subcapitata* were identified using the parameter side scatter (SSC–H) *versus* red fluorescence (FL3-H), according to Sarmento et al., (2008), and for relative ROS, the parameters FL3-H and FL1-H (green fluorescence) were used. The relative values of FL3-H (Chl *a* fluorescence), SSC-H (cell complexity), and FSC-H (cell size) of *R. subcapitata* were calculated using the measurements of the fluorescent beads, as described in Mansano et al. (2017). The data were analyzed in FlowJo V10 software. Equations 1 and 2 were used to calculate the relative ROS (Hong et al., 2009). The relative growth rates (RGR) were determined using equation 3 (Bao et al. 2011), where N_t is the cell density at time t; N_0 is the initial cell density and t is the exposure time. Thus, growth inhibition % was calculated by comparing the population growth rates of controls (considered 100%) with the treatments. The percent inhibition in yield (%Iy) was calculated for each treatment replicate according equation 4 (OECD, 2011, where Y_C is mean value for yield in the control group and Y_T is the value for yield for the treatment replicate.

$$FL1\text{-}H_{relative} = \log (FL1\text{-}H \text{ of samples}) / \log (FL1\text{-}H \text{ of beads}) \quad \text{(eq. 1)}$$

$$ROS_{relative}\ (\%) = (FL1\text{-}H_{relative\ [treatments]} / FL1\text{-}H_{\ relative\ [control\ group]}) \text{ X } 100 \quad \text{(eq. 2)}$$

$$RGR = (N_t – N_0)_{\ Treatment} / (N_t – N_0)_{\ Control} \quad \text{(eq. 3)}$$

$$\%I_y = (Y_C – Y_T) / Y_C \text{ X } 100 \quad \text{(eq. 4)}$$

2.5 Data analysis

The inhibitory concentrations (IC_{10} and IC_{50}) based on relative growth rates were calculated by non-linear regression logistic curves using Statistica 7.0 software (Statsoft, 2004). Statistical analyses were performed in the SigmaPlot software version 11.0 (Systat, 2008). To assess the differences between control and treatments, normal distributed data were analyzed

with one-way ANOVA, followed by Dunnett's post-hoc multiple comparison test. For non-normal data, Kruskal-Wallis test and multiple comparisons with Dunn's test were performed. Statistical significance level was defined as $p < 0.05$.

3. Results and discussion

3.1 Characterization of particles and ion release

The characterization of α-Ag_2WO_4 particles by XRD is shown in Fig S1 Supplementary Material. For both α-Ag_2WO_4 - R and α-Ag_2WO_4 - C samples, the phase of α-Ag_2WO_4 with an orthorhombic structure was obtained, according to the Inorganic Crystal Structure Database (ICSD) file no. 293487 (Cavalcante et al., 2012). This structure belongs to the spatial group *Pn2n*, and is formed by Ag ([AgO_x], x = 2, 4, 6 and 7) and W ([WO_6]) complexes clusters. (Assis et al., 2018; Assis et al., 2019). No additional phases were observed, showing that the material obtained has a high purity.

FE-SEM images of the samples are shown in Figure 1. For α-Ag_2WO_4-C, the homogeneous formation of microstructured cubes was observed, with an average length of 0.83 ± 0.21 μm and an average width of 0.75 ± 0.17 μm. For α-Ag_2WO_4-R, the homogeneous formation of rods with a hexagonal face were obtained, with an average length of 1.22 ± 0.10 μm and an average width of 0.23 ± 0.70 μm.

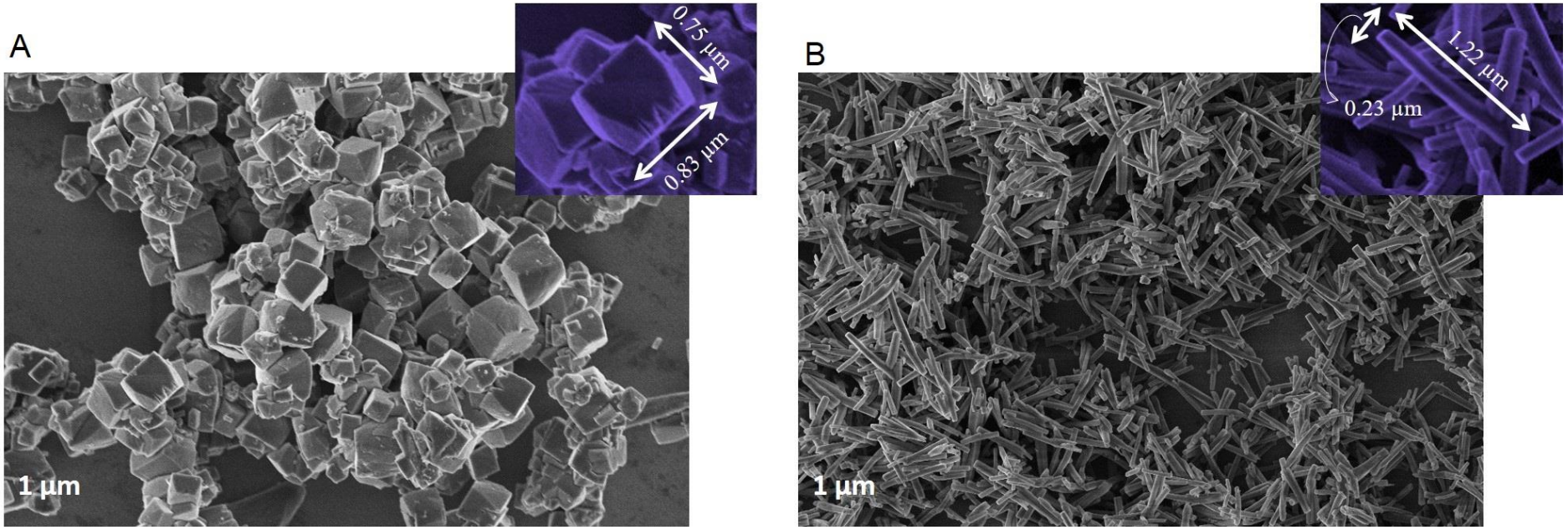

Fig. 1. FE-SEM images of α-Ag_2WO_4 – C (A) and α-Ag_2WO_4 – R (B).

The data of microparticle characterization in culture medium and in ultrapure water are summarized in Tables S4 and S5 (Supplementary material). The hydrodynamic diameter of particles dispersed in the culture medium ranged from 589 to 1475 nm for α-Ag_2WO_4 - C and from 202 to 735 nm for α-Ag_2WO_4 - R. The results of the zeta potential, at 0 h and 96 h for both microparticles, showed a tendency for rapid aggregation and incipient instability. On average, the values found did not exceed -10 mV. Suspensions considered stable in aqueous solutions have zeta potential values higher +30 mV and below −30 mV (Stensberg et al., 2011**)**. In our study, we found slightly negative values and close to zero which confirms the electrostatic instability (Lodeiro et al., 2017; Kleiven et al., 2018; Kleiven et al., 2019). The PdI values were higher than 0.510 ± 0.22 for α-Ag_2WO_4-C and higher than 0.421 ± 0.07 for α-Ag_2WO_4-R, which indicated that the microparticles formed aggregates/agglomerates.

We observed that the free silver ion release from the samples varied (Fig. 2). The dissolution of silver ions from increasing concentrations of α-Ag_2WO_4 – R followed a sigmoidal behavior (Fig. 2A), while the Ag ions from the α-Ag_2WO_4 – C had an increasing linear trend (Fig. 2B). For α-Ag_2WO_4 - C the fraction of dissolved silver ions in the suspension ranged from 34.24% (which corresponds to 5.24 μg Ag L^{-1}, at the concentration of 32.87 μg L^{-1}) to 71.22% (corresponds to 2.95 μg Ag L^{-1}, at the concentration of 8.81 μg L^{-1}) (Table S1, Supplementary material). For α-Ag_2WO_4 – R, the fraction of dissolved silver ions in the suspension ranged from 35.52 % (5.25 μg Ag L^{-1} at concentration 31.76 μg L^{-1}) to 96.66% (corresponding to 4.55 μg Ag L^{-1} at concentration 10.67 μg L^{-1}) (Table S2, Supplementary material).

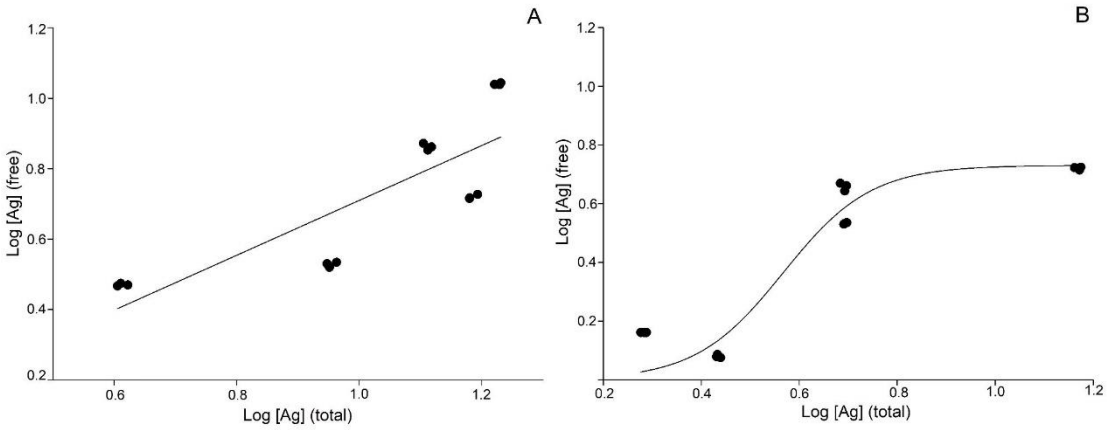

Fig. 2. Total silver concentration *versus* free silver ion concentration in α-Ag_2WO_4 - C (A) (Linear regression equation f = -0.0686+0.7786*x, with r^2 = 0.68) and α-Ag_2WO_4 - R (B) (Sigmoid regression equation f= 0.7307/(1+exp(-(x-0.5674)/0.0893, with r^2 = 0.91).

The ion dissolution of the particles is related to the surface area, size, shape, structure and it is dependent on the methodology used in the synthesis, functionalization, and medium in which they were dispersed (Lopes et al., 2014; Jung et al., 2017; Lekamge et al., 2020). There are discussions about the importance of particle size, in which very small particles have greater dissolution, due to the surface area, i.e., nano-sized particles compared to micro-sized particles have a greater surface area and greater ion dissolution (Beer et al., 2012; Dobias et al., 2013; Sendra et al., 2017). However, our data highlight that even though they are microcrystal, there was a large amount of silver ion released from the treatments and the α-Ag_2WO_4 particles were important sources of free silver ion, causing toxicity to the algal cells, as discussed in the following topics.

Toxicity of α-Ag_2WO_4 microparticles

3.1.1 Growth inhibition

The α-Ag_2WO_4 - R and α-Ag_2WO_4 - C caused negative effects on the relative growth rates of *R. subcapitata* (Fig. 3). After 96 h of exposure to α-Ag_2WO_4 – C, the population growth was

significantly decreased in concentrations of 27.78 μg L^{-1}, 32.87 μg L^{-1} and 36.25 μg L^{-1} (Dunnett's test, $p < 0.05$) (Fig. 3A). Regarding the α-Ag_2WO_4 – R, the algae growth was significantly reduced at the concentrations of 10.55 μg L^{-1}, 10.67 μg L^{-1} and 31.76 μg L^{-1} when compared to the control (Dunnett's test, $p < 0.05$) (Fig. 3B). We observed a relationship between availability of silver ions released from microcrystal and growth inhibition. Fig. 3C and 3D show the silver ion concentrations in each α-Ag_2WO_4 – C and α-Ag_2WO_4 – R treatment, respectively.

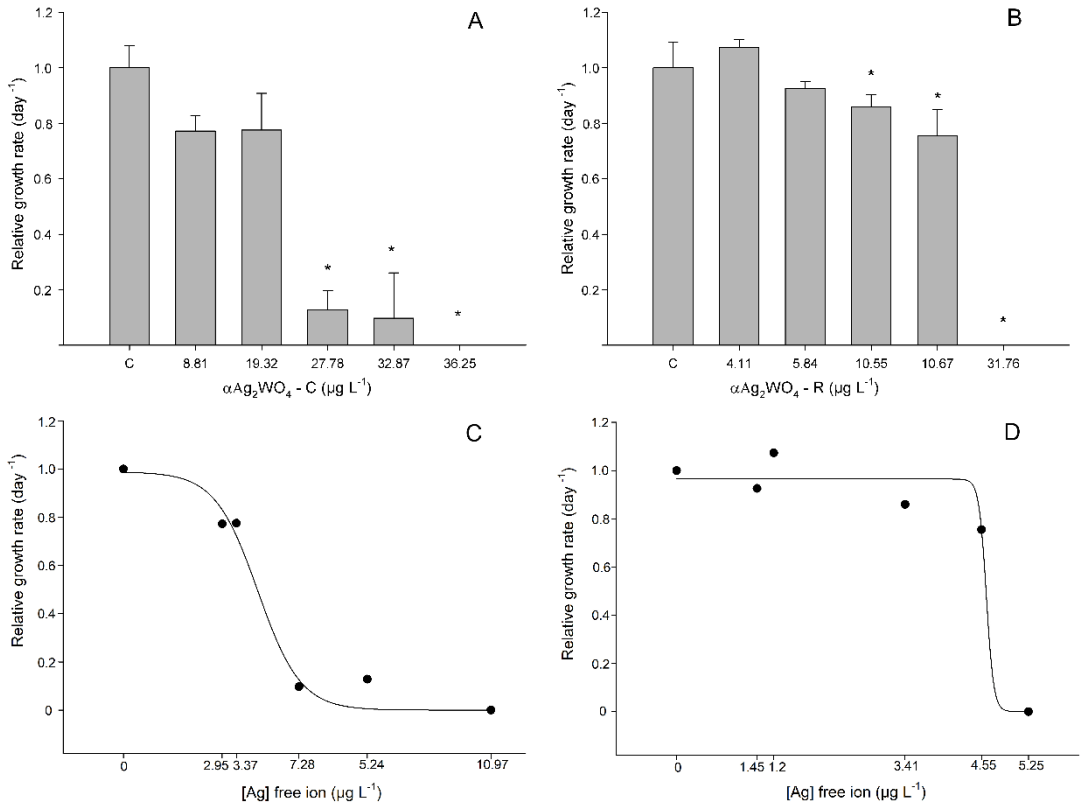

Fig. 3. Relative growth rates (mean ± standard deviation) of *Raphidocelis subcapitata* after 96 h exposure to different concentrations of α-Ag_2WO_4 - C (A) and α-Ag_2WO_4 - R (B). Relative growth rates (mean ± standard deviation) of *Raphidocelis subcapitata* versus concentration of free ions (in relation to silver) of α-Ag_2WO_4 – C (C) (Sigmoid regression equation f= 0.9883/(1+exp(-(x-4.0112)/-0.6389), with r^2 = 0.96) and α-Ag_2WO_4 – R (D) (Sigmoid regression equation f= 0.9648/(1+exp(-(x-4.6207)/-0.0552)), with r^2 = 0.94). Concentrations are expressed in μg L^{-1}, where: C = control group and asterisks represent a significant difference (Dunnett's test, $p < 0.05$) of treatments compared to the control group.

The percent of yield inhibition (%Iy) are summarized in Table S6 and S7 (Supplementary material). According to the OECD, this parameter is calculated based on biomass and is required by some countries to meet regulatory aspects, therefore considered as an additional variable. In this study, we observed the significant increase (Dunnett's test, $p < 0.05$) of percent inhibition in yield (%Iy) in the α-Ag_2WO_4 – C and α-Ag_2WO_4 – R treatments when compared to the control group, like the results found by Sohn et al., (2015).

The IC_{10} and IC_{50} values were, respectively, 18.60 ± 1.61 μg L^{-1} and 23.47 ± 1.16 μg L^{-1} for α-Ag_2WO_4 – C, and 8.68 ± 0.91 μg L^{-1} and 13.72 ± 1.48 μg L^{-1} for α-Ag_2WO_4 – R, showing a higher toxicity of the rod of 1.7 times in comparison to the α-Ag_2WO_4 – C morphology. The higher toxicity of α-Ag_2WO_4 – R can be explained by the existing differences in the shape and surfaces of each compound. These surfaces are closely related to the number of active sites and consequently to their properties (Laier et al., 2020).

In the theoretical study by Macedo et al. (2018), it is detailed that α-Ag_2WO_4 has differences in the surface energy of the facets that make up each microcrystal morphology. The cubic morphology has a combination of surfaces (010), (100) and (001) and is obtained by using sodium dodecyl sulfate (SDS), which is responsible for stabilizing the surfaces (100) and (001). In addition, the use of SDS prevents the emergence of the predominant surface of the hexagonal rod-like morphology (010), (001) and (101). The different surfaces between the samples are (101) for α-Ag_2WO_4 - R and (100) for α-Ag_2WO_4 - C. The surface (101) has 4 vacant clusters on its surface ([$AgO_3.3V_o$], [$AgO_5.2V_o$] and two [$WO_5.V_o$]) while the surface (100) has 3 vacant clusters on its surface ([$AgO_3.3V_o$], [$AgO_5.2V_o$] and one [$WO_5.V_o$]). These clusters represent the centers of surface activity of these surfaces, they are considered as their active sites, and influence the ability of materials to interact with the alga and the release of silver ions. The difference in these surfaces of sample explains the greater toxicity of α-Ag_2WO_4 - R in inhibiting the growth of *R. subcapitata* as the greater number of active sites of

this compound are closely related to the surface. Thereby, we highlight the importance of considering the surface properties and particle shapes in evaluating their toxicities. Regarding biological studies for growth inhibition effects, the α-Ag_2WO_4 was evaluated as a microbicidal agent, where the minimum inhibitory concentration (MIC) and the minimum fungicidal concentrations (MFC) were reported with values of 62.5 μg ml^{-1} for *C. albicans* (Foggi et al., 2017a). Another study evaluated the ability of α-Ag_2WO_4 to fight *C. albicans*, with a MIC/MFC value of 7.81 μg ml^{-1} (Foggi et al., 2017b). Comparing these growth data with our results, we found that α-Ag_2WO_4 was substantially more toxic to *R. subcapitata* than to the fungus. In addition, comparing the IC_{50} values of the microparticles with other studies, we found that α-Ag_2WO_4 (cubic and rod) affected *R. subcapitata* growth more than the smaller particle sizes. For example, Ribeiro et al. (2014), when evaluating the toxicity of silver nanoparticles (AgNPs), found IC_{50}-72h value for *R. subcapitata* of 32.40 μg L^{-1}. Sohn et al. (2015) observed that *R. subcapitata* exposed to silver nanowires (AgNWs) and AgNPs showed IC_{50}-72h values of 2.57 mg L^{-1} and 0.74 mg L^{-1}, respectively. All these values are higher than the IC_{50}-96h for α-Ag_2WO_4 – C and α-Ag_2WO_4 – R calculated in our study, which points out that the α-Ag_2WO_4, even as a microcrystal, has a higher toxicity to *R. subcapitata* than that found for nanoparticles in the above cited studies. This result can be explained because the α-Ag_2WO_4 semiconductor has a high capacity to produce ROS (OH* and O_2H*), which leads to a high oxidative stress for living organisms (Assis et al., 2019).

The IC_{50}-96h calculated based on the concentration of free Ag from α-Ag_2WO_4 - C and α-Ag_2WO_4 - R were 3.94 μg Ag L^{-1} and 4.76 μg Ag L^{-1}, respectively. These values are consistent with the EC_{50} values described in the literature for *R. subcapitata* exposed to dissolved Ag, for example, the EC_{50} of 3.6 μg L^{-1} reported by Sekine et al. (2015). Thus, the toxicity of both microparticles in our study can be explained by the release of Ag^+ ions. It is important to note that in Brazil the CONAMA determines 10 μg L^{-1} of ionic silver as an

adequate threshold to maintain freshwater quality (Brasil, 2005). Our results show that concentrations of ionic silver from microcrystals lower than those established by Brazilian legislation can impact freshwater microalgae. This reinforces the importance of investigating the toxicity of functional microparticle-based materials to aquatic organisms, especially organisms that make up the base of the trophic chain, because the aquatic ecosystem can be an important fate for the microcrystals and the ions released by them.

3.1.2 ROS measurements

After 24 h of exposure to α-Ag_2WO_4 - C, we observed a significant increase in the amount of relative ROS in algal cells exposed to concentrations of 8.81 and 19.32 μg L^{-1} (Dunnett's test, $p<0.05$). At 96 h, the relative ROS decreased significantly at concentrations of 8.81, 19.32, and 27.78 μg L^{-1} (Dunnett's test, $p<0.05$) (Fig. 4A). For α-Ag_2WO_4 - R, at 96 h there was a significant reduction in intracellular ROS content at concentrations 10.55 and 10.67 μg L^{-1} (Dunnett's test, $p<0.05$) and a significant increase at the highest concentration tested (Dunnett's test, $p<0.05$) when compared to the control. (Fig. 4B).

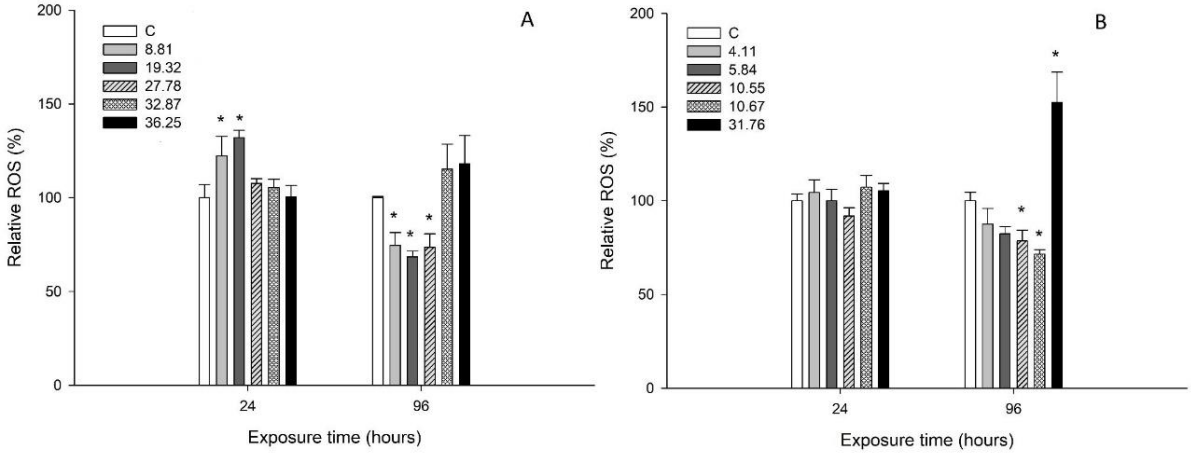

Fig. 4. Reactive oxygen species (ROS) produced by *Raphidocelis subcapitata* exposed to α-Ag_2WO_4 - C (A) and α-Ag_2WO_4 - R (B). Concentrations are expressed in μg L^{-1}, where: C =control group and asterisks represent a significant difference (Dunnett's test, $p<0.05$) of treatments compared to the control group.

The formation of intracellular ROS can be induced in the presence of light, that is, mediated by photocatalytic properties of the materials (Nadia von Moss and Slaveykova, 2013; Vale et al., 2016). Therefore, we can state that the ROS production by microalgae was induced by exposure to α-Ag_2WO_4. Foggi et al. (2017a) reported that ROS can influence the cell death of *C. albicans* exposed to α-Ag_2WO_4. Thus, the authors considered the ROS production an important route of toxicity.

We observed that significant relative ROS production was closely linked with growth inhibition at the highest concentration (31.76 μg L^{-1}) of α-Ag_2WO_4-R. ROS can act as signaling molecules and alter gene expression, besides causing modifications in nucleic acids, proteins and lipids, and cell damage (Okamoto et al., 2003), and, therefore, we suggest that ROS generation was responsible for the total growth inhibition after 96 h exposure. High levels of ROS, when the antioxidant limit of the cell is exceeded, can cause disorderly oxidation of biological and cellular molecules, leading to oxidative stress with changes in cell structure (Halliwell and Gutteridge, 1999), cell disruption, and death (Nadia von Moss and Slaveykova, 2013; Taylor et al., 2015; Vale et al. 2016). According to Okamoto et al. (2003), the formation of ROS in autotrophs is a serious risk, because a source of $O^{\cdot}{}_2^{-}$ is the reduction of a single electron of molecular oxygen by the electron transport chain. In addition, mitochondria and chloroplasts are vulnerable to oxidative damage.

However, microalgae have antioxidant mechanisms that are activated when excessive ROS production occurs, as reported by Lekamge et al. (2019). These researchers observed the activation of antioxidant enzymes when *R. subcapitata* was exposed to particles with silver.

Moreover, it was reported that *Chlorella vulgaris* could continue photosynthesis at high concentrations of silver nanoparticles, because it was able to activate antioxidant enzymes and detoxify the reactive oxygen species (Qian et al., 2016**)**. This may explain the reduction of relative ROS at some concentrations after 96 h of microcrystal exposure. The Chlorophyceae exposed to α-Ag_2WO_4 may have activated these antioxidant mechanisms and decreased ROS content at concentrations of 8.81, 19.32, and 27.78 μg L^{-1} for α-Ag_2WO_4-C and 10.55 and 10.67 μg L^{-1} for α-Ag_2WO_4-R (Fig. 4A and Fig. 4B). This significant reduction in ROS is corroborated by the growth data, where no complete inhibition at these same concentrations were observed. We emphasize that we did not evaluate and quantify these antioxidant enzymes, but they were possibly activated due to the stress state caused by the microcrystal.

3.1.3 Cell complexity, size and chlorophyll *a* fluorescence

For *R. subcapitata* exposed to α-Ag_2WO_4- C, we verified morphological changes when compared to the control (Fig. 5A**).** There was a significant reduction (Dunnett's test, $p<0.05$) in cell complexity (SSC-H) at concentrations of 8.81 and 19.32 μg L^{-1} and a significant increase (Dunnett's test, $p<0.05$) at concentrations of 27.78, 32.87, and 36.25 μg L^{-1}. For α-Ag_2WO_4- R, there was a significant increase (Dunnett's test, $p<0.05$) in cell complexity (SSC-H) at the highest concentration (31.76 μg L^{-1}) and a reduction in other concentrations, which were also statistically significant (Dunnett's test, $p<0.05$). There were no statistically significant differences for cell size (FSC-H) exposed to α-Ag_2WO_4- C and α-Ag_2WO_4- R.

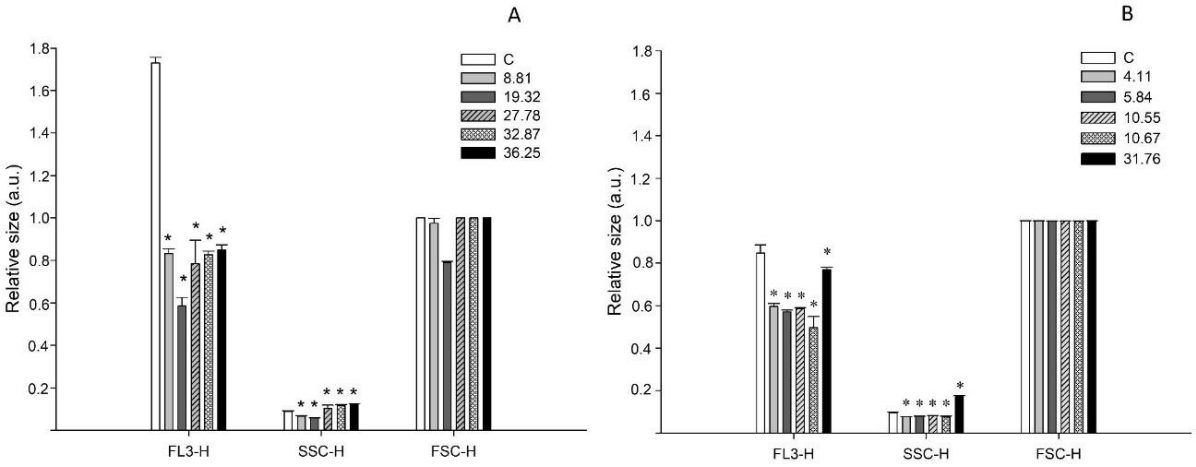

Fig. 5. Chlorophyll *a* fluorescence (FL3-H relative), cell complexity (SSC–H relative) and size (FSC–H relative) (mean ± standard deviation) of *Raphidocelis subcapitata* exposed to the different concentrations of α-Ag_2WO_4 – C (A) and α-Ag_2WO_4 – R (B). Concentrations are expressed in μg L^{-1}, where: C =control group and asterisks represent a significant difference (Dunnett's test, $p < 0.05$) of treatments compared to the control group. Values are expressed in arbitrary units (a.u.)

The increase in complexity observed in some concentrations of α-Ag_2WO_4- C (27.78, 32.87, and 36.25 μg L^{-1}) and at the highest concentration of α-Ag_2WO_4 - R is probably a result of the internalization of ionic silver, as already observed for other metals (Gebara et al., 2020). Almeida et al. (2019) reported that cell granularity changes may represent detoxification mechanisms through the immobilization of toxic elements inside the cell. Specifically, for the highest concentration of rod microparticle (31.76 μg L^{-1}), the cell complexity results corroborate the relative ROS and growth inhibition data for this treatment, indicating that ion internalization (observed by increased cell complexity) was directly related to the significant increase in ROS and complete inhibition of cell growth. On the other hand, reduced cell complexity was associated with significantly reduced ROS, for α-Ag_2WO_4 - C (at concentrations 8.81 and 19.32 μg L^{-1}) and α-Ag_2WO_4 - R. This is a strong indication that the cells exposed to the different microcrystal morphologies activated defense mechanisms, with reduced cell complexity, relative ROS reduction, and no complete inhibition of cell growth.

Regarding Chl *a* fluorescence (FL3-H) for both microparticle morphologies, there was a statistically significant reduction (Dunnett's test, $p < 0.05$) in FL3-H at all concentrations tested (Fig. 5A and Fig. 5B). This reduction possibly indicates that exposure to α-Ag_2WO_4 affected pigment synthesis. Sendra et al. (2017) highlighted that fluorescence measured with FL3 detector can be used as an indicator in assessing the physiological state of algal cells and also pointed out that the reduction in FL3 is related to impairment in pigment synthesis of cells exposed to contaminants. Thus, we assume that the decreased Chl *a* production may have caused consequences to the microalga photosynthetic performance, contributing to population growth inhibition.

Conclusion

Our results showed that both morphologies of α-Ag_2WO_4 caused population growth inhibition, changes in cell morphology (cell complexity) and, at the intracellular level, induced ROS production and reduced Chl *a* fluorescence. The α-Ag_2WO_4 – R showed greater toxicity to algal cells than α-Ag_2WO_4 – C, caused by differences in the surface energy of each crystal, which are closely related to the number of active sites. In addition, silver ions are important sources and seem to be responsible for the toxicity, deserving attention, because the limit set by legislation for ionic silver in aquatic ecosystems is higher than the concentration of silver that caused toxicity for freshwater alga. We emphasize that particle shape is an intrinsic and essential aspect in assessing the toxicity of microparticle-based functional materials, because its reactivity is also conditioned by morphology and surface area. Considering that the aquatic ecosystem is an important fate of contaminants, we highlight the importance of this investigation in providing subsidies for a better understanding of the toxicity of α-Ag_2WO_4 and the potential risks that compounds in different morphologies may

pose to microalgae, supporting regulatory actions to establish safe thresholds for these compounds and silver ions.

Acknowledgements

This work was funded in part São Paulo Research Foundation - FAPESP (FAPESP CEPID-finance code 2013/07296-2; finance code 2018/07988-5), Financier of Studies and Projects FINEP, National Council for Scientific and Technological Development - CNPq (finance code 166281/2017-4 and 141255/2018-8), and Coordination for the Improvement of Higher Education Personnel - CAPES (finance code 001 and 88887.364036/2019-00). We would also like to thank Dr. Ana Teresa Lombardi and Dr. Hugo Miguel Preto de Moraes Sarmento for the permission to use their laboratories, as well as the equipment.

References

Almeida, C., Gomes, T., Habuda-Stanic, M., Lomba, J.A.B., Romic, Zeljka, Turkalj, J.V., Lillicrap, A., 2019. Characterization of multiple biomarker responses using flow cytometry to improve environmental hazard assessment with the green microalgae *Raphidocelis subcapitata*. Science of the Total Environment journal 687, 827–838. https://doi.org/10.1016/j.scitotenv.2019.06.124

Alvarez-Roca, R., Gouveia, A.F., De Foggi, C.C., Lemos, P.S., Gracia, L., Da Silva, L.F., Vergani, C.E., San-Miguel, M., Longo, E., Andrés, J., 2021. Selective Synthesis of α-, β-, and γ-Ag_2WO_4 Polymorphs: Promising Platforms for Photocatalytic and Antibacterial Materials. Inorg. Chem. 60, 1062–1079. https://doi.org/10.1021/acs.inorgchem.0c03186

Arumugam, R., Osman, S., Pan, J., Khan, A., Yang, V., 2020. One-pot preparation of AgBr / α-Ag_2WO_4 composite with superior photocatalytic activity under visible-light irradiation. Colloids Surfaces A 586, 124079. https://doi.org/10.1016/j.colsurfa.2019.124079

Assis, M., Cordoncillo, E., Torres-Mendieta, R., Beltrán-Mir, H., Mínguez-Vega, G., Oliveira, R., Leite, E.R., Foggi, C.C., Vergani, C.E., Longo, E., Andrés, J., 2018. Towards the scale-up of the formation of nanoparticles on α-Ag_2WO_4 with bactericidal properties by femtosecond laser irradiation. Sci. Rep. 8, 1–11. https://doi.org/10.1038/s41598-018-19270-9

Assis, M., Robeldo, T., Foggi, C.C., Kubo, A.M., Condoncillo, E., 2019. Composite Formed by Electron Beam and Femtosecond Irradiation as Potent Antifungal and Antitumor

Agents 1–15. https://doi.org/10.1038/s41598-019-46159-y.

Assis, M., Pontes Ribeiro, R.A., Carvalho, M.H., Teixeira, M.M., Gobato, Y.G., Prando, G. A., Mendonça, C.R., De Boni, L., Aparecido De Oliveira, A.J., Bettini, J., Andrés, J., Longo, E., 2020. Unconventional magnetization generated from electron beam and femtosecond irradiation on α-Ag_2WO_4: a quantum chemical investigation. ACS Omega 5, 10052–10067. https://doi.org/10.1021/acsomega.0c00542.

Assis, M., Ponce, M.A., Gouveia, A.F., Souza, D., de Campos da Costa, J.P., Teodoro, V., Gobato, Y.G., Andres, J., Macchi, C., Somoza, A., Longo, E., 2021. Revealing the nature of defects in α-Ag_2WO_4 by positron annihilation lifetime spectroscopy: a joint experimental and theoretical study. Cryst. Growth Des. 21, 1093–1102. https://doi. org/10.1021/acs.cgd.0c01417.

Ayappan, C., Jayaraman, V., Palanivel, B., Pandikumar, A., 2020. Separation and Puri fi cation Technology Facile preparation of novel Sb_2S_3 nanoparticles / rod-like α -Ag_2WO_4 heterojunction photocatalysts : Continuous modulation of band structure towards the e ffi cient removal of organic contaminants. Sep. Purif. Technol. 236, 116302. https://doi.org/10.1016/j.seppur.2019.116302

Bao, V.W.W., Leung, K.M.Y., Qiu, J.W., Lam, M.H.W., 2011. Acute toxicities of five commonly used antifouling booster biocides to selected subtropical and cosmopolitan marine species. Mar. Pollut. Bull. 62, 1147–1151. https://doi.org/10.1016/j.marpolbul.2011.02.041

Beer, C., Foldbjerg, R., Hayashi, Y., Sutherland, D.S., Autrup, H., 2012. Toxicity of silver nanoparticles-Nanoparticle or silver ion? Toxicol. Lett. 208, 286–292. https://doi.org/10.1016/j.toxlet.2011.11.002

BRASIL, 2005. Ministério do Meio Ambiente. Conselho Nacional do Meio Ambiente CONAMA. Resolução n0 357, de 17 de março de 2005. Diário Oficial da União, Brasília

Cavalcante, L.S., Almeida, M.A.P., Avansi, W., Tranquilin, R.L., Longo, E., Batista, N.C., Paulista, U.E., Box, P.O., 2012. Cluster Coordination and Photoluminescence Properties of α-Ag_2WO_4 microcrystals. https://doi.org/10.1021/ic300948n

Chu, S.P., 1942. The Influence of the Mineral Composition of the Medium on the Growth of Planktonic Algae: Part I. Methods and Culture Media. J. Ecol. 30, 284. https://doi.org/10.2307/2256574

Cruz, L., Teixeira, M.M., Teodoro, V., Jacomaci, N., Laier, L.O., Assis, M., Macedo, N.G., Tello, A.C.M., Da Silva, L.F., Marques, G.E., Zaghete, M.A., Teodoro, M.D., Longo, E., 2020. Multi-dimensional architecture of Ag/α-Ag_2WO_4 crystals: insights into microstructural, morphological, and photoluminescence properties. CrystEngComm 22, 7903–7917. https://doi.org/10.1039/d0ce00876a

Dai, X., Luo, Y., Zhang, W., Fu, S., 2010. Facile hydrothermal synthesis and photocatalytic activity of bismuth tungstate hierarchical hollow spheres with an ultrahigh surface area † 3426–3432. https://doi.org/10.1039/b923443h

Dobias, J., Bernier-Latmani, R., 2013. Silver release from silver nanoparticles in natural waters. Environ. Sci. Technol. 47 (9), 4140–4146. https://doi.org/10.1021/ es304023p.

Fabrega, J., Fawcett, S.R., Renshaw, J.C., Lead, J.R., 2009. Silver nanoparticle impact on bacterial growth: Effect of pH, concentration, and organic matter. Environ. Sci. {&}

Technol. 43, 7285–7290. https://doi.org/10.1021/es803259g

Foggi, C.C., Fabbro, M.T., Santos, L.P.S., de Santana, Y.V.B., Vergani, C.E., Machado, A.L., Cordoncillo, E., Andrés, J., Longo, E., 2017a. Synthesis and evaluation of A-Ag_2WO_4 as novel antifungal agent. Chem. Phys. Lett. 674, 125–129. https://doi.org/10.1016/j.cplett.2017.02.067

Foggi, C.C., de Oliveira, R.C., Fabbro, M.T., Vergani, C.E., Andres, J., Longo, E., Machado, A.L., 2017b. Tuning the Morphological, Optical, and Antimicrobial Properties of α-Ag_2WO_4 Microcrystals Using Different Solvents. Cryst. Growth Des. 17, 6239–6246. https://doi.org/10.1021/acs.cgd.7b00786

Gebara, R.C., Alho, L.O.G., Rocha, G.S., Mansano, A.S., Melão, M.G.G., 2020. Zinc and aluminum mixtures have synergic effects to the algae *Raphidocelis subcapitata* at environmental concentrations. Chemosphere 242, 125231. https://doi.org/ 10.1016/j.chemosphere.2019.125231.

Griffitt, R.J., Brown-Peterson, N.J., Savin, D.A., Manning, C.S., Boube, I., Ryan, R.A., Brouwer, M., 2012. Effects of chronic nanoparticulate silver exposure to adult and juvenile sheepshead minnows (*Cyprinodon variegatus*). Environ. Toxicol. Chem. 31, 160–167. https://doi.org/10.1002/etc.709

Halliwell, B., Gutteridge, J.M.C., 1999. Free Radicals in Biology and Medicine., 3rd. Oxford University Press, New York, p. 936pp.

He, D., Dorantes-Aranda, J.J., Waite, T.D., 2012. Silver nanoparticle-algae interactions: Oxidative dissolution, reactive oxygen species generation and synergistic toxic effects. Environ. Sci. Technol. 46, 8731–8738. https://doi.org/10.1021/es300588a

Hong, Y., Hu, H., Xie, X., Sakoda, A., Sagehashi, M., Li, F., 2009. Gramine-induced growth inhibition , oxidative damage and antioxidant responses in freshwater cyanobacterium *Microcystis aeruginosa* 91, 262–269. https://doi.org/10.1016/j.aquatox.2008.11.014

Kleiven, M., Rossbach, L.M., Gallego-Urrea, J.A., Brede, D.A., Oughton, D.H., Coutris, C., 2018. Characterizing the behavior, uptake, and toxicity of NM300K silver nanoparticles in *Caenorhabditis elegans*. Environ. Toxicol. Chem. 37, 1799–1810. https://doi.org/10.1002/etc.4144.

Huang, J., Cheng, J., Yi, J., 2016. Impact of silver nanoparticles on marine diatom *Skeletonema costatum*. https://doi.org/10.1002/jat.3325

Kleiven, M., Macken, A., Oughton, D.H., 2019. Growth inhibition in *Raphidocelis subcapita* e Evidence of nanospecific toxicity of silver nanoparticles. Chemosphere 221, 785–792. https://doi.org/10.1016/j.chemosphere.2019.01.055

Kwak, J.II, Cui, R., Sun-Hwa, N., Kim, S.W., Chae, Y., An, Y.J., 2015. Multispecies toxicity test for silver nanoparticles to derive hazardous concentration based on species sensitivity distribution for the protection of aquatic ecosystems. Nanotoxicology 5390. https://doi.org/10.3109/17435390.2015.1090028.

Laier, L.O., Assis, M., Foggi, C.C., Gouveia, A.F., Vergani, C.E., Santana, L.C.L., Cavalcante, L.S., Andrés, J., Longo, E., 2020. Surface - dependent properties of α - Ag_2WO_4 : a joint experimental and theoretical investigation. Theor. Chem. Acc. 1–11. https://doi.org/10.1007/s00214-020-02613-z

Lalau, C.M., Simioni, C., Vicentini, D.S., Ouriques, L.C., Mohedano, R.A., Puerari, R.C., Matias, W.G., 2020. Science of the Total Environment Toxicological effects of AgNPs on duckweed (*Landoltia punctata*). Sci. Total Environ. 710, 136318. https://doi.org/10.1016/j.scitotenv.2019.136318

Lekamge, S., Miranda, A.F., Abraham, A., Ball, A.S., Shukla, R., Nugegoda, D., 2020. The toxicity of coated silver nanoparticles to the alga *Raphidocelis subcapitata*. SN Appl. Sci. https://doi.org/10.1007/s42452-020-2430-z

Lin, C.A.O., Jiexin, C.A.O., Cong, W., Ping, C.H.E., An, P.A.N.D.E., Volinsky, A.A., 2012. Anti-tumor activity of self-charged (Eu, Ca): WO_3 and Eu : $CaWO_4$ nanoparticles 35, 767–772.

Lodeiro, P., Browning, T.J., Achterberg, E.P., Guillou, A., El-Shahawi, M.S., 2017. Mechanisms of silver nanoparticle toxicity to the coastal marine diatom *Chaetoceros curvisetus*. Sci. Rep. 7, 1–10. https://doi.org/10.1038/s41598-017-11402-x

Lopes, S., Ribeiro, F., Wojnarowicz, J., Lojkowski, W., Jurkschat, K., Crossley, A., Soares, A.M.V.M., Loureiro, S., 2014. Zinc oxide nanoparticles toxicity to *Daphnia magna*: Size-dependent effects and dissolution. Environ. Toxicol. Chem. 33, 190–198. https://doi.org/10.1002/etc.2413

Macedo, N.G., Gouveia, A.F., Roca, R.A., Assis, M., Gracia, L., Andre, J., Leite, E.R., Longo, E., Box, P.O., 2018. Surfactant-Mediated Morphology and Photocatalytic Activity of α-Ag_2WO_4 Material . https://doi.org/10.1021/acs.jpcc.8b01898

Macedo, N.G., Machado, T.R., Roca, R.A., Assis, M., Foggi, C.C., Puerto-Belda, V., Mínguez-Vega, G., Rodrigues, A., San-Miguel, M.A., Cordoncillo, E., Beltrán-Mir, H., Andrés, J., Longo, E., 2019. Tailoring the Bactericidal Activity of Ag Nanoparticles/α-Ag_2WO_4 Composite Induced by Electron Beam and Femtosecond Laser Irradiation: Integration of Experiment and Computational Modeling. ACS Appl. Bio Mater. 2, 824–837. https://doi.org/10.1021/acsabm.8b00673

Mansano, A.S., Vieira, E.M., Sarmento, H., Rocha, O., Seleghim, M.H.R., 2017. Effects of diuron and carbofuran and their mixtures on the microalgae *Raphidocelis subcapitata*. Ecotoxicol. Environ. Saf. 142, 312–321. https://doi.org/10.1016/j. ecoenv.2017.04.024.

Moos, N. Von, Slaveykova, V.I., 2013. Oxidative stress induced by inorganic nanoparticles in bacteria and aquatic microalgae – state of the art and knowledge gaps sation . At acidic pH, it is in equilibrium with its protonated 1–26. https://doi.org/10.3109/17435390.2013.809810

Munawar, M., Munawar, I.F., Mayfield, C.I., McCarthy, L.H., 1990. Probing ecosystem health: a multi-disciplinary and multi-trophic assay strategy. Environ. bioassay Tech. their Appl. Proc. Conf. Lancaster, 1988 93–116. https://doi.org/10.1007/978-94-009-1896-2_8

Muthamizh, S., Suresh, R., Giribabu, K., Manigandan, R., Praveen Kumar, S., Munusamy, S., Narayanan, V., 2015. $MnWO_4$nanocapsules: Synthesis, characterization and its electrochemical sensing property. J. Alloys Compd. 619, 601–609. https://doi.org/10.1016/j.jallcom.2014.09.049

Navarro, E., Baun, Æ.A., Behra, Æ.R., Hartmann, Æ.N.B., Filser, J., Antonietta, Æ.A.M.Æ., Peter, Q.Æ., 2008. Environmental behavior and ecotoxicity of engineered nanoparticles

to algae, plantsb, and fungi 372–386. https://doi.org/10.1007/s10646-008-0214-0

Nobre, F.X., Bastos, I.S., dos Santos Fontenelle, R.O., Júnior, E.A.A., Takeno, M.L., Manzato, L., de Matos, J.M.E., Orlandi, P.P., de Fátima Souza Mendes, J., Brito, W.R., da Costa Couceiro, P.R., 2019. Antimicrobial properties of α-Ag_2WO_4 rod-like microcrystals synthesized by sonochemistry and sonochemistry followed by hydrothermal conventional method. Ultrason. Sonochem. 58, 104620. https://doi.org/10.1016/j.ultsonch.2019.104620

Odzak, N., Kistler, D., Sigg, L., 2017. Influence of daylight on the fate of silver and zinc oxide nanoparticles in natural aquatic environments *. Environ. Pollut. 226, 1–11. https://doi.org/10.1016/j.envpol.2017.04.006

OECD, O. Guidelines For The Testing Of Chemicals No. 201 Freshwater Alga and Cyanobacteria. **Growth Inhibition Test**, v. 201, 2011.

Okamoto, O.K., Quı, I. De, Morse, D., 2003. Review heavy metal – induced oxidative stress in Algae 1 Ernani Pinto Teresa C . S . Sigaud-Kutner , Maria A . S . Leita 1018, 1008–1018.

Penha, M.D., Gouveia, A.F., Teixeira, M.M., De Oliveira, R.C., Assis, M., Sambrano, J.R., Yokaichya, F., Santos, C.C., Goncalves, R.F., Li, M.S., 2020. Structure, optical properties, and photocatalytic activity of α-$Ag_2W_{0.75}Mo_{0.25}O_4$. Mater. Res. Bull. 132, 111011.

Qian, H., Zhu, K., Lu, H., Lavoie, M., Chen, S., Zhou, Z., Deng, Z., Chen, J., Fu, Z., 2016. Contrasting silver nanoparticle toxicity and detoxification strategies in *Microcystis aeruginosa* and *Chlorella vulgaris*: New insights from proteomic and physiological analyses. Sci. Total Environ. 572, 1213–1221. https://doi.org/10.1016/j.scitotenv.2016.08.039

Reis, L.L., Alho, L.O.G., Abreu, C.B., Melão, M.G.G., 2021. Using Multiple Endpoints to Assess the Toxicity of Cadmium and Cobalt for Chlorophycean *Raphidocelis subcapitata*. Ecotoxicol. Environ. Saf 208, 111628. https://doi.org/10.1016/j. ecoenv.2020.111628.

Ribeiro, F., Gallego-Urrea, J.A., Goodhead, R.M., Van Gestel, C.A.M., Moger, J., Soares, A.M.V.M., Loureiro, S., 2015. Uptake and elimination kinetics of silver nanoparticles and silver nitrate by *Raphidocelis subcapitata*: The influence of silver behaviour in solution. Nanotoxicology 9. https://doi.org/10.3109/ 17435390.2014.963724.

Rogers, K.R., Navratilova, J., Stefaniak, A., Bowers, L., Knepp, A.K., Al-Abed, S.R., Potter, P., Gitipour, A., Radwan, I., Nelson, C., Bradham, K.D., 2018. Characterization of engineered nanoparticles in commercially available spray disinfectant products advertised to contain colloidal silver. Sci. Total Environ. 619–620, 1375–1384. https://doi.org/10.1016/j.scitotenv.2017.11.195

Sarmento, H., Unrein, F., Isumbisho, M., Stenuite, S., Gasol, J.M., Descy, J.P., 2008. Abundance and distribution of picoplankton in tropical, oligotrophic Lake Kivu, eastern Africa. Freshw. Biol. 756–771. https://doi.org/10.1111/j.1365- 2427.2007.01939.x.

Sekine, R., Khurana, K., Vasilev, K., Lombi, E., Donner, E., 2015. Quantifying the adsorption of ionic silver and functionalized nanoparticles during ecotoxicity testing : Test container effects and recommendations 5390, 1–8. https://doi.org/10.3109/17435390.2014.994570

Sendra, M., Yeste, M.P., Gatica, J.M., Blasco, J., 2017. Direct and indirect effects of silver nanoparticles on freshwater and marine microalgae (*Chlamydomonas reinhardtii* and *Phaeodactylum tricornutum*). Chemosphere. https://doi.org/10.1016/j.chemosphere.2017.03.123.

Silva, L.F., Catto, A.C., Avansi, W., Cavalcante, L.S., Andrés, J., Aguir, K., Mastelaro, V.R., Longo, E., 2014. A novel ozone gas sensor based on one-dimensional (1D) α-Ag_2WO_4 nanostructures. Nanoscale 6, 4058–4062. https://doi.org/10.1039/c3nr05837a.

Silva, L.F., Catto, A.C., Avansi, W., Cavalcante, L.S., Mastelaro, V.R., Andrés, J., Aguir, K., Longo, E., 2016. Acetone gas sensor based on α-Ag_2WO_4 nanorods obtained via a microwave-assisted hydrothermal route. J. Alloys Compd. 683, 186–190. https://doi.org/10.1016/j.jallcom.2016.05.078.

Sohn, E.K., Johari, S.A., Kim, T.G., Kim, J.K., Kim, E., Lee, J.H., Chung, Y.S., Yu, I.J., 2015. Aquatic Toxicity Comparison of Silver Nanoparticles and Silver Nanowires. Biomed Res Int. https://doi.org/10.1155/2015/893049.

Sørensen, S.N., Lützhøft, H.H., Rasmussen, R., Baun, A., 2016. Acute and chronic effects from pulse exposure of *D. magna* to silver and copper oxide nanoparticles. Aquat. Toxicol. https://doi.org/10.1016/j.aquatox.2016.10.004

Stensberg, M.C., Wei, Q., Mclamore, E.S., Marshall, D., 2011. Toxicological studies on silver nanoparticles: challenges and oopportunities in assessment, monitoring and imaging. Nanomedicine 6, 879–898. https://doi.org/10.2217/nnm.11.78.

Statsoft Inc, 2004. STATISTICA, Version 07. www.statsoft.com. Systat, 2008.

Systat Software, Incorporation SigmaPlot for Windows version 11.0.

Taylor, P., Street, M., Wt, L., 2015. sp .), Toxicity , bioaccumulation and biomagnification of silver nanoparticles in green algae (*Chlorella* sp .), water flea (*Moina macrocopa*), blood worm (*Chironomus* spp .) and silver barb (*Barbonymus goniono* 37–41. https://doi.org/10.3184/095422914X14144332205573

Vale, Gonçalo, Mehennaouic, K., Cambierc, S., Libralatod, G., Jominie, S., Domingosa, R. F., 2015. Manufactured nanoparticles in the aquatic environment – biochemical responses on freshwater organisms: a critical overview. Aquat. Toxicol. 170, 162–174. https://doi.org/10.1016/j.aquatox.2015.11.019.

Varga, A.M., Horvati, J., 2018. Physiological and biochemical effect of silver on the aquatic plant Lemna gibba L.: evaluation of commercially available product containing colloidal silver. Aquat. Toxicol. https://doi.org/10.1016/j.aquatox.2018.11.018

Wang, S., Lv, J., Ma, J., Zhang, S., 2016. Cellular internalization and intracellular biotransformation of silver nanoparticles in *Chlamydomonas reinhardtii.* Nanotoxicology 10, 1129–1135. https://doi.org/10.1080/17435390.2016.1179809

Zhao, C., Wang, W., 2012. Importance of surface coatings and soluble silver in silver nanoparticles toxicity to *Daphnia magna* 6, 361–370. https://doi.org/10.3109/17435390.2011.579632

Supplementary material

Tables

Table S1: Measured concentrations (ICP-MS) of α-Ag_2WO_4 – C, concentration of silver and amount of free silver (in relation to silver) used in experiments with *Raphidocelis subcapitata.*

Concentration of α-Ag_2WO_4 - C (µg L^{-1})	**[Ag] (µg L^{-1})**	**[Ag] free ion (µg L^{-1})**
8.81	4.1 ± 0.08	2.95 ± 0.03 (71.22%)
19.32	8.99 ± 0.16	3.37 ± 0.06 (37.48%)
27.78	12.93 ± 0.19	7.28 ± 0.16 (56.22%)
32.87	15.3 ± 0.27	5.24 ± 0.08 (34.24%)
36.25	16.87 ± 0.21	10.97 ± 0.07 (65.02%)

Table S2: Measured concentrations (ICP-MS) of α-Ag_2WO_4 – R, concentration of silver and amount of free silver (in relation to silver) used in experiments with *Raphidocelis subcapitata.*

Concentration of α-Ag_2WO_4 - R (µg L^{-1})	**[Ag] (µg L^{-1})**	**[Ag] free ion (µg L^{-1})**
4.11	1,91 ± 0.02	1.45 ± 0.0 (75.9%)
5.84	2.72 ± 0.03	1.2 ± 0.02 (44.11%)
10.55	4.91 ± 0.07	3.41 ± 0.02 (69.03%)
10.67	4.94 ± 0.04	4.55 ± 0.14 (96.66%)
31.76	14.78 ± 0.23	5.25 ± 0.06 (35.52%)

Table S3: Composition of the culture medium CHU-12.

Chemical	Concentration (mM)
$Ca(NO_3)_2.4H_2O$	18.20
K_2HPO_4	2.87
$MgSO_4.7H_2O$	30.4
KCl	6.70
Na_2CO_3	18.86
$FeCl_3.6H_2O$	0.18

Table S4: Silver Tungstate α-Ag_2WO_4 - C characterization in the CHU-12 culture medium and ultrapure water.

α-Ag_2WO_4 (μg L^{-1})	**Time (h)**	**Zeta-Potential (mV)**	**Hydrodynamic size (nm)**	**PdI**	**Zeta-Potential (mV)**	**Hydrodynamic size (nm)**	**PdI**
		CHU-12 (test solutions)			Ultrapure Water		
8.81	0	-6.34 ± 0.91	1474.7 ± 745.66	0.696 ± 0.40	-6.83 ± 0.91	2196.0 ± 0.00	0.705 ± 0.51
	96	-7.33 ± 0.23	588.65 ± 113.77	0.773 ± 0.22	-2.80 ± 0.07	916.43 ± 0.00	0.565 ± 0.29
27.78	0	-6.07 ± 0.08	1012.9 ± 434.84	0.724 ± 0.23	-0.95 ± 0.91	771.33 ± 547.63	0.870 ± 0.18
	96	-6.97 ± 0.25	1011.4 ± 66.31	0.510 ± 0.22	-3.55 ± 1.23	ND	ND
36.25	0	-7.09 ± 1.06	1127.6 ± 596.66	0.675 ± 0.16	-1.10 ± 2.86	1930.0 ± 0.00	0.517 ± 0.42
	96	-7.96 ± 0.95	893.36 ± 70.40	0.583 ± 0.93	-4.47 ± 1.45	1991.8 ± 0.00	0.497 ± 0.06

ND - not determined.

Table S5: Silver Tungstate α-Ag_2WO_4 - R characterization in the CHU-12 culture medium and ultrapure water.

α-Ag_2WO_4 (µg L^{-1})	**Time (h)**	**Zeta-Potential (mV)**	**Hydrodynamic size (nm)**	**PdI**	**Zeta-Potential (mV)**	**Hydrodynamic size (nm)**	**PdI**
		CHU-12 (test solutions)			Ultrapure Water		
4.11	0	-13.00 ± 1.41	670.26 ± 267.44	0.705 ± 0.34	-6.56 ± 1.43	380.23 ± 424.82	0.932 ± 0.12
	96	-9.06 ± 0.94	728.90 ± 190.15	0.626 ± 0.07	-5.88 ± 4.53	345.30 ± 55.32	0.701 ± 0.18
10.55	0	-12.87 ± 0.06	341.27 ± 114.42	0.907 ± 0.08	-17.60 ± 1.06	959.80 ± 448.6	0.787 ± 0.30
	96	-12.77 ± 1.36	735.47 ± 185.04	0.421 ± 0.07	-9.50 ± 3.10	232.85 ± 135.67	0.689 ± 0.44
31.76	0	-14.93 ± 0.30	202.10 ± 59.40	0.989 ± 0.02	-8.35 ± 3.45	371.90 ± 391.63	0.425 ± 0.29
	96	-10.57 ± 0.74	731.53 ± 139.72	0.708 ± 0.38	-2.55 ± 1.23	204.30 ± 29.52	0.457 ± 0.05

Table S6: Yield inhibition (%) of *Raphidocelis subcapitata* during 96 h exposure to α-Ag_2WO_4 – C. Asterisks represent a significant difference (Dunnett's test, $p < 0.05$) of treatments compared to the control group.

Concentration (μg L^{-1})	Yield inhibition (%)
Control	0
8.81	22.74*
19.32	22.46*
27.78	87.19*
32.87	90.29*
36.25	101.93*

Table S7: Yield inhibition (%) of *Raphidocelis subcapitata* during 96 h exposure to α-Ag_2WO_4 – R. Asterisks represent a significant difference (Dunnett's test, $p < 0.05$) of treatments compared to the control group.

Concentration (μg L^{-1})	Yield inhibition (%)
Control	0
4.11	-7.96*
5.84	7.29*
10.55	15.57*
10.67	30.13*
31.76	109.41*

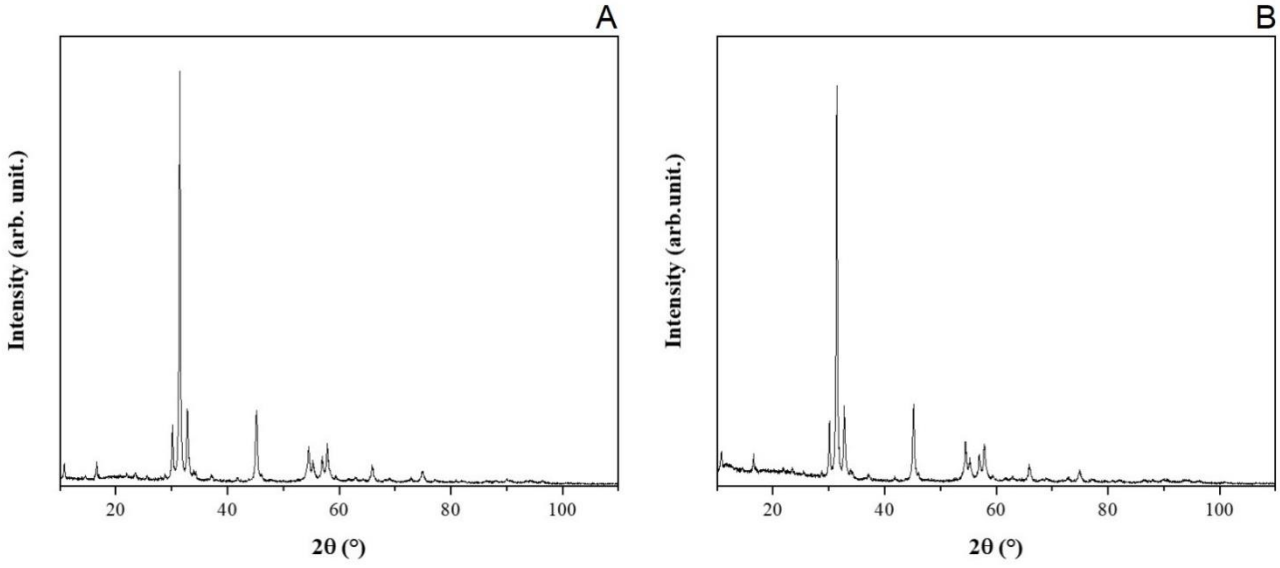

Fig. S1. X-ray diffraction patterns of α-Ag_2WO_4 – C (A) and α-Ag_2WO_4 – R (B).

Reference

Chu, S.P., 1942. The Influence of the Mineral Composition of the Medium on the Growth of Planktonic Algae: Part I. Methods and Culture Media. J. Ecol. 30, 284. https://doi.org/10.2307/2256574

Capítulo 2 - Effects of α-Ag_2WO_4 crystals on photosynthetic efficiency and biomolecule composition of the algae *Raphidocelis subcapitata*

Publicado em: Water, Air & Soil Pollution, **233,** 121 (2022). https://doi.org/10.1007/s11270-022-05604-x., pela Springer Nature.

Highlights

- High concentrations of α-Ag_2WO_4 inhibited *R. subcapitata* growth.
- Φ_M and F_0/F_V results indicated that α-Ag_2WO_4 damaged the photosynthetic processes.
- α-Ag_2WO_4 reduced the content of Chl *a* and carbohydrate, except for 31.76 μg L^{-1}.
- Increases in Chl *a* and carbohydrate levels at 31.76 μg L^{-1} were an algal protection mechanism.

ABSTRACT

The α-Ag_2WO_4 (hexagonal rod-shaped) is a multifunctional material with interesting physical and chemical properties, such as good electronic, photocatalytic, anticancer and microbicidal performance. Considering this, its use can contribute to the presence and accumulation of this compound in freshwater ecosystems. Therefore, the present study investigated the effects of α-Ag_2WO_4 on the freshwater Chlorophyceae *Raphidocelis subcapitata*, at the level of cell density, chlorophyll *a* (Chl *a*), total carbohydrate contents, and photosynthetic activity (maximum quantum yield and oxygen-evolving complex - OEC). The α-Ag_2WO_4 reduced cell density by ~ 48% already in the first 24 h of exposure at 31.76 μg L^{-1} (highest concentration). Moreover, at 31.76 μg L^{-1}, we observed a drastic reduction in the maximum quantum yield, and impact in the oxygen evolving complex at 24 h and 48 h. However, our results indicated a

possible recovery of the photosynthetic activity in the surviving algal cells at 72 and 96 h. The contents of chlorophyll *a* (Chl *a*) and total carbohydrates decreased significantly (Dunnett's test, $p<0.05$) at 4.11, 5.84, 10.55, and 10.67 μg L^{-1} treatments and increased significantly (Dunnett's test, $p<0.05$) at the highest concentration (31.76 μg L^{-1}), which is possibly a mechanism for the algal cells to optimize the amount of energy to be used in the photosynthetic process and maintaining the integrity of the cell wall. This study contributes to clarifying how α-Ag_2WO_4 interacts with *R. subcapitata*¸ showing the toxicity mechanism of photosynthetic activity. This can help predict the fate and effect of these composites by providing a basis for their ecological risk assessment.

Keywords: silver tungstate; toxicity; Chlorophyceae; Phyto-PAM; photosynthetic efficiency.

1. Introduction

Given the great applicability of alpha-silver tungstate (α-Ag_2WO_4) crystals (Nobre et al., 2019; Macedo et al., 2019; Penha et al., 2020; Cruz et al., 2020; Assis et al., 2020), mainly in photocatalysis (Macedo et al., 2018) and microbicidal activity (Longo et al., 2014; Foggi et al., 2017; Assis et al., 2018; Assis et al., 2019; Laier et al., 2020), its increase in natural ecosystems is expected. Increased concentrations of α-Ag_2WO_4 in the environment may occur due to the recovery of the semiconductor from the reaction mixture (consisting of the catalyst and the substance to be degraded) is not always possible, favoring the presence and accumulation in water bodies (Kumari et al., 2019; Matos et al., 2020**)**. In addition, particles can be absorbed into the soil and carried to water bodies (Dewez et al., 2018), and are a source of ionic silver release into aquatic ecosystems, which can pose serious threats to their biota (Navarro et al., 2008).

Among the organisms that make up aquatic environments, phytoplankton contributes significantly to nutrient cycling (fixing carbon), oxygen production and is responsible for a

large part of overall primary productivity (Baracho et al., 2019). As microalgae are at the base of aquatic food webs, any modification of the photosynthesis process through damage to their photosynthetic apparatus can affect higher trophic levels and, consequently, reach the entire ecosystem (Kahru & Dubourguier, 2010**)**. Fast and relatively simple methods, such as the parameters obtained in Phyto-PAM and the chlorophyll *a* (Chl *a*) content, can indicate the physiological health in primary producers, i.e. algae and higher plants (Juneau et al., 2005). It is known that several environmental factors affect the physiological state of autotrophs by impairing photosynthesis or biochemical processes, and therefore the measurement of photosynthetic parameters is important and reliable to identify environmental stress (Juneau & Popovic, 2000; Rocha et al., 2021). Furthermore, macromolecules such as carbohydrates are essential in photosynthetic and respiratory processes (Martinez-Ruiz & Martinez-Jeronimo, 2015**)**, energy storage, and the structural component of the cell wall (Markou et al., 2012). When microalgae are exposed to stressful conditions, changes often occur in the amount of carbohydrates (Rossi et al., 2018). Some studies show that different species of microalgae can alter the amount of carbohydrates when exposed to different types of contaminants (Huang et al., 2016; Silva et al., 2018; Alho et al., 2020). Thus, assessing the content of carbohydrates of *Raphidocelis subcapitata* provided relevant information about α-Ag_2WO_4 toxicity.

In this context, given the great applicability of α-Ag_2WO_4 combined with the lack of studies regarding its effects on the physiology and biochemical composition of microalgae in general; and considering the importance of these autotrophic organisms for aquatic ecosystems, our objective was to evaluate the effects of α-Ag_2WO_4 on photosynthetic activity, biological molecules and cell density of the Chlorophyceae *R. subcapitata*. This study contributes to clarifying and understanding how α-Ag_2WO_4 interacts with *R. subcapitata*¸ showing the toxicity mechanisms on photosynthetic activity, providing information that can

help predict the fate and effects of these compounds. In addition, our study provides a basis for their ecological risk assessment.

2. Material and methods

2.1 Synthesis and characterization of α-Ag_2WO_4

The samples of α-Ag_2WO_4 were synthesized using the coprecipitation (CP) method in aqueous medium, according to Macedo et al. (2018). The hydrodynamic size, polydispersity index (PdI), and zeta potential of the particles were measured in exposure medium and in ultrapure water at 0, 24, 48, 72, and 96 h by dynamic light scattering (DLS) using Zetasizer Nano ZS90, Malvern. The results from 0 and 96 h are described in our previous study (Abreu et al., 2022). The results from 24, 48, and 72 h are presented in Table S1 (Supplementary material). Silver concentrations in α-Ag_2WO_4 test solutions used in the toxicity tests (data not shown) were determined by inductively coupled plasma mass spectrometry (ICP-MS PerkinElmer NexION 2000) (Abreu et al., 2021).

2.2 Algal cultures

The cosmopolitan freshwater microalga *R. subcapitata* (Chlorophyceae), which is recommended in international standards for ecotoxicological testing (OECD, 2011), was cultivated in CHU-12 culture medium (CHU, 1942) (Table S2, Supplementary material) at 25 ± 1 ºC, with a light intensity of ≅130 μmol photon m^{-2} s^{-1} LED light and 12h/12h of light/ dark photoperiod. The pH values were around 7 – 8.5 and did not vary by more than 1.5 units. The toxicity tests followed the same culture conditions. We used a bath sonicator (Ultra cleaner 1400 Unique, Brazil) for 30 min to disperse the α-Ag_2WO_4 in ultrapure water and immediately afterwards we prepared the test solutions. Exponentially growing *R. subcapitata* cells were inoculated (initial concentration of 1 x 10^5 cells ml^{-1}) and exposed to the concentrations of 0.00, 4.11, 5.84, 10.55, 10.67, and 31.76 μg L^{-1} of α-Ag_2WO_4 for 96 h in

500 mL polycarbonate Erlenmeyers containing 250 mL of culture medium. These concentrations were chosen based on preliminary tests results. The toxicity tests followed the OECD (201) guidelines (OECD 2011), with 3 tests performed, each one with triplicates for the control and treatments.

Every day, 1.8 mL samples were fixed with formaldehyde buffered with borax (1% final concentration) and the cells were counted in a FACS Calibur cytometer (Becton Dickinson, San Jose, CA, USA) with a 15mW argon-ion laser (488 nm excitation), using 6 µm fluorescent beads as an internal standard (Fluoresbrite carboxylate microspheres; Polysciences, Warrington, Pennsylvania, USA). To identify the cells, we followed exactly the protocol described in Sarmento et al. (2008).

2.3 PAM fluorescence measurements

We utilized an amplitude modulated fluorometer (PHYTO-PAM, Heinz Walz GmbH, Germany), equipped with an optical drive ED- 101US/MP, to perform chlorophyll *a* fluorescence measurements. Daily, 3 mL of each sample were left in the dark for 15 minutes before measurements. The parameters F_0 (minimum fluorescence), F_M (maximum fluorescence) and Φ_M (maximum quantum yield) are provided by Phyto-PAM **(**Schreiber et al., 1986; Schreiber & Bilger, 1993). The efficiency of the oxygen evolving complex of PSII (F_0 / F_V, where $F_V = F_M - F_0$) was also determined by the fluorescence emission from algal cells acclimated to the dark (Kriedemann et al., 1985).

2.4 Determination of chlorophyll *a* and total carbohydrates

We determined the amount of chlorophyll *a* with dimethylsulfoxide (DMSO) according to the methodology described by Shoaf and Lium (1976). After extraction, we used equation (1) established by Jeffrey and Humphrey (1975) to quantify the content of chlorophyll *a* where E_{664} and E_{647} are the absorbance at 664 and 647 nm λ, respectively.

$$\text{Chl } a = 11.93\ E_{664} - 1.93\ E_{647} \text{ (Eq 1)}$$

Total carbohydrate quantification was determined based on the phenol-sulfuric reaction and anhydrous dextrose (Mallinckrodt Chemicals, USA) as a standard for the calibration curve, according to Liu et al. (1973). A spectrophotometer (HACH Company, Loveland, CO, USA) was used for the reading at 485 nm.

2.5 Statistical analysis

The IC_{50} (inhibitory concentrations) based on cell density rates were calculated by non-linear regression logistic curves using Statistica 7.0 software (Statsoft Inc, 2004). Data were tested for normality and homogeneity of variance. Statistical analyses were performed using the SigmaPlot software version 11.0 (Systat, 2008). Statistically significant differences among treatments and controls were determined using one-way ANOVA, followed by Dunnett's post-hoc multiple comparison test. For non-normal data, the Kruskal-Wallis test and multiple comparisons with Dunn's test were performed. The statistical significance level was defined as $p < 0.05$. The data were obtained from three experimental replicate cultures and are presented as the mean ± SD of the replicates. Uniquely for the total carbohydrate data, we normalized these data using log transformation.

3. Results and Discussion

The results of the microparticle characterization are available in Fig.S1 and Table S1 (Supplementary Material). The α-Ag_2WO_4 particles were obtained with a hexagonal rod shape and orthorhombic structure (Fig. 1), and average transversal and longitudinal sizes of 0.23 and 1.22 µm, respectively. Overall, the zeta potential values averaged between -5.39 and -12.8 mV, indicating electrostatic instability **(**Lodeiro et al., 2017; Kleiven et al., 2018; Kleiven et al., 2019), because the aqueous solutions considered stable have values around ±30 mV

(Stensberg et al., 2011). The PdI values were higher than 0.22 ± 0.07, which indicated that the α-Ag_2WO_4 particles formed aggregates/agglomerates.

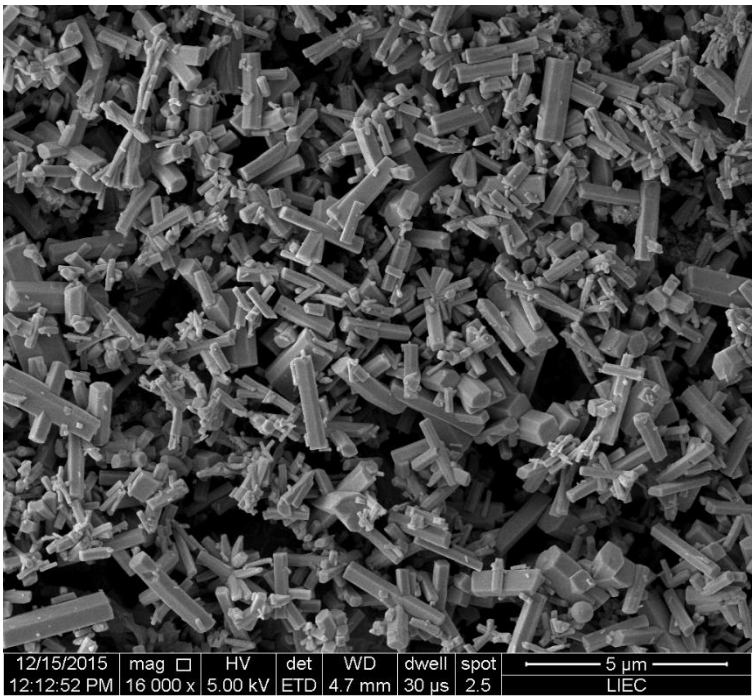

Fig. 1 Field emission scanning electron microscopy (FE-SEM) of the α-Ag_2WO_4 sample obtained by a Supra 35 VP, Carl Zeiss operated at 10 kV

We observed significant changes in algae growth when in contact with α-Ag_2WO_4 particles (Fig. 2). At 24 h there was a difference (Dunn's test, $p < 0.05$) only between the control and the highest concentration (31.76 µg L^{-1}), with a ~ 48 % reduction. On the other hand, at 48 h, all treatments entailed significant reductions (Dunnett's test, $p < 0.05$) in the cell density. Finally, at 72 h the 3 highest concentrations (10.55, 10.67 and 31.76 µg L^{-1}) caused significant reductions (Dunnett's test, $p < 0.05$) in cell density and at 96 h the 2 highest concentrations (10.67 and 31.76 µg L^{-1}) reduced (Dunnett's test, $p < 0.05$) the cell number when compared with the control. The IC_{50} based on relative growth rates (RGR),

calculated according to Bao et al., (2011), in a previous work (Abreu et al., 2022) was 13.72 ± 1.48 µg L^{-1} and the IC_{50} based on the cell density was 14.9 ± 1.05 µg L^{-1}.

According to previous studies, materials with silver in their composition are highly toxic to aquatic biota, especially for microalgae, inhibiting growth, forming reactive oxygen species, DNA damage, among others (He et al., 2012; Huang et al., 2016; Sorensen et al., 2016; Odzak et al., 2017; Lekamge et al., 2020; Abreu et al., 2022). Even at very low concentrations, dissolved silver can compromise photosynthesis and growth in phytoplankton (Navarro et al., 2008). This can help to explain the growth inhibition of *R. subcapitata* at the highest concentrations of α-Ag_2WO_4, which was probably due to the effects of the released silver ions into the medium and ROS production, as we observed in a previous study with α-Ag_2WO_4 (Abreu et al., 2022).

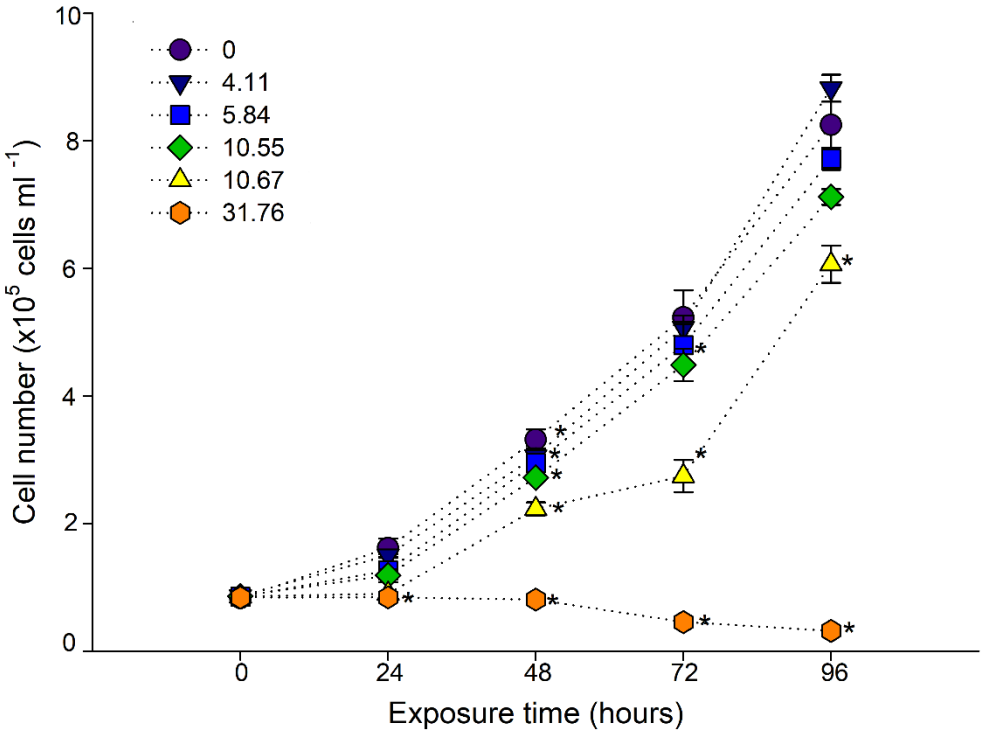

Fig. 2 Cell density (mean ± SD) of *Raphidocelis subcapitata* under α-Ag_2WO_4 -R exposure during 96 h. The concentrations are expressed in µg L^{-1}. Asterisks * represent a significant

difference (Dunn's test, $p < 0.05$; Dunnett's test, $p < 0.05$) of treatments compared to the control group.

Regarding the photosynthetic activity, the maximum quantum yield, obtained via Phyto-PAM, indicates the amount of light used in photosynthesis, providing information about the physiology of the microalgae (Herlory et al., 2013). According to Dewez and Oukarroum (2012), the decrease in maximum quantum yield values indicates a reduction in the ability of PSII to perform primary photochemical reactions. The results of the maximum quantum yield (ΦM) are shown in Fig. 3. After 24 h and 48 h of exposure, there was a drastic reduction (Dunn's test, $p < 0.05$) of ~72% and ~78%, respectively, of this parameter at the highest concentration tested (31.76 µg L^{-1}). At 72 h, the concentrations of 10.67 µg L^{-1} and 31.76 µg L^{-1} of α-Ag_2WO_4 caused a significant reduction (Dunnett's test, $p<0.05$) of ~ 4.5% and 35%, respectively, in the Φ_M, when compared to the control. Finally, at 96 h there was a ~6% and 9% decrease (Dunnett's test, $p<0.05$) in 10.67 and 31.76 µg L^{-1} concentrations, respectively. In light of this, our results indicate that the photosynthetic apparatus was affected, especially at the highest concentration of α-Ag_2WO_4 (31.76 µg L^{-1}), but this impairment was gradually reduced throughout the days of the experiment at this concentration, since the percentage of reduction of Φ_M diminished from the first to the last day of treatment.

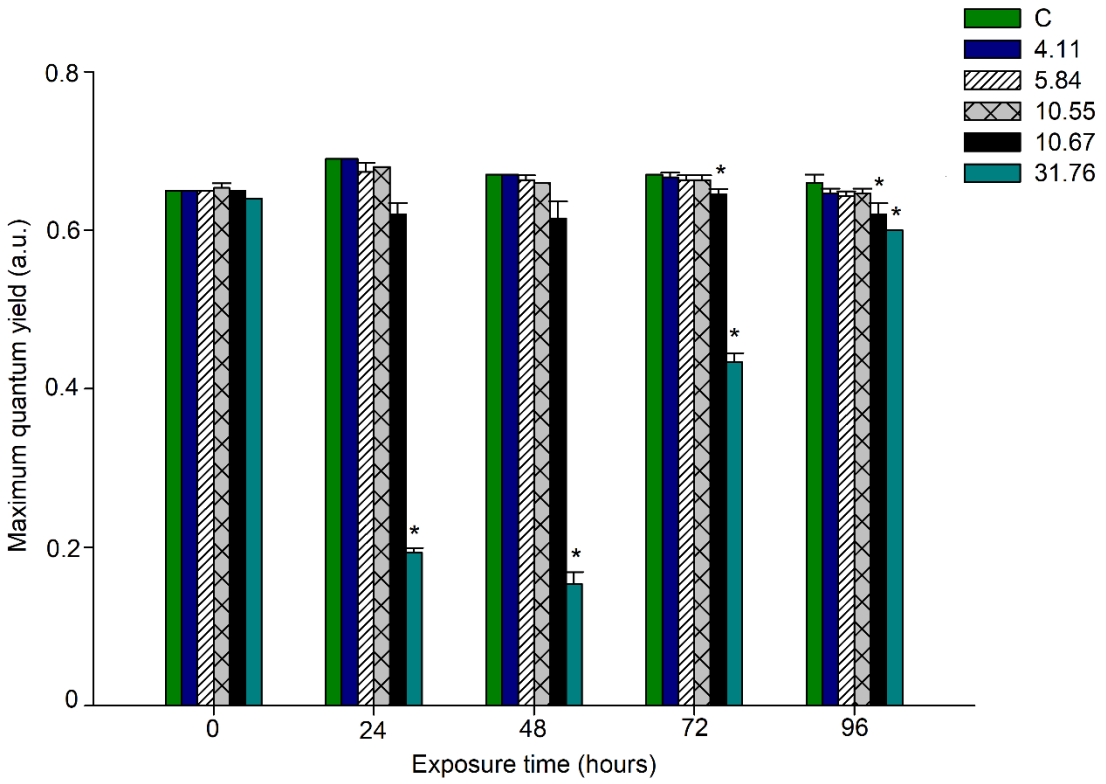

Fig. 3 Maximum quantum yield (mean ± SD) of *Raphidocelis subcapitata* after 24, 48, 72, and 96 h under α-Ag_2WO_4 exposure. Concentrations are expressed in µg L^{-1}, where: C = control group and asterisks * represent a significant difference (Dunn's test, $p< 0.05$; Dunnett's test, $p < 0.05$) of treatments compared to the control group

We observed that the efficiency of the oxygen-evolving complex (F_0/F_v) was significantly affected at the highest concentration tested of α-Ag_2WO_4. In general, at 31.76 µg L^{-1}, F_0/F_v it increased 9.3 times (Dunn's test, $p<0.05$) at 24 h and 11 times (Dunn's test, $p<0.05$) at 48 h, when compared to the control (Fig. 4). At 72 h, the increase was around 2.7 times (Dunn's test, $p<0.05$) and at 96 h it was about 1.3 times higher than in control cells. High values of $F_0/F_{v,}$ especially on the first two days of exposure to α-Ag_2WO_4 indicate that possibly water-splitting apparatus was damaged **(**Alho et al., 2019; Reis et al., 2021), which was already expected, due to the excellent photocatalytic property of α-Ag_2WO_4 (Macedo et

al., 2018). The OEC constitutes the water splitting system, where the water molecule is broken down in the presence of light and this process is responsible for the production of oxygen **(**Mattoo et al., 1999**)**. The composition of the OEC is basically formed by manganese atoms and proteins, which require the presence of chloride and calcium. Here, probably the silver ions released by the microcrystal have bound to chloride ions and this may have compromised the water-splitting apparatus mainly in 24 and 48 h. Therefore, we can assume that the water splitting apparatus was the main target of α-Ag_2WO_4, and the reduced maximum quantum yield was probably a consequence of the impacted OEC. Already in the last days of exposure, even with F_0/F_v values significantly different from the control, the not so high values indicate a recovery of the physiology of the algal cells that survived at the end of the ecotoxicity test.

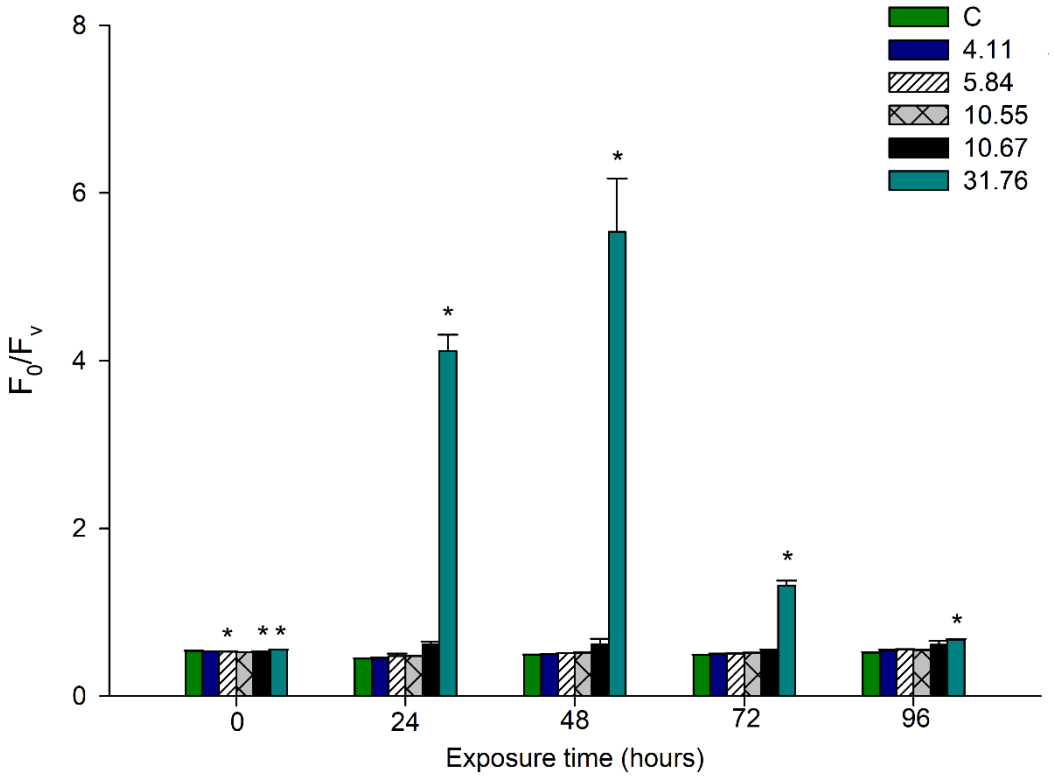

Fig. 4 Efficiency of the Oxygen Evolving Complex (F_0/F_V) (mean ± SD) of *Raphidocelis subcapitata* after 24, 48, 72, and 96 h under α-Ag_2WO_4 exposure. Concentrations are expressed in µg L^{-1}, where: C = control group and asterisks * represent a significant difference (Dunn's test, $p< 0.05$; Dunnett's test, $p < 0.05$) of treatments compared to the control group

Regarding Chl *a* content, we observed a decrease of ~ 41, 47, 52, and 43% (Dunnett's test, $p<0.05$) at concentrations of 4.11, 5.84, 10.55, and 10.67µg L^{-1} of α-Ag_2WO_4, respectively (Fig. 5A). This is probably a result of reactive oxygen species production, because the chloroplast is a site that favors ROS generation (Li et al., 2015), as recently observed in a study by our research group **(**Abreu et al., 2022**).** On the other hand, at the highest concentration of α-Ag_2WO_4 (31.76 µg L^{-1}), the amount of Chl *a* increased ~ 47%

(Dunnett's test, $p<0.05$), which is possibly a mechanism for the algal cells to optimize the amount of energy to be used in the photosynthetic process (Wacker et al., 2015, Silva et al., 2018; Alho et al., 2020; Rocha et al., 2021), in order to compensate for the stress caused by α-Ag_2WO_4 and maintain photosynthesis at high rates**.**

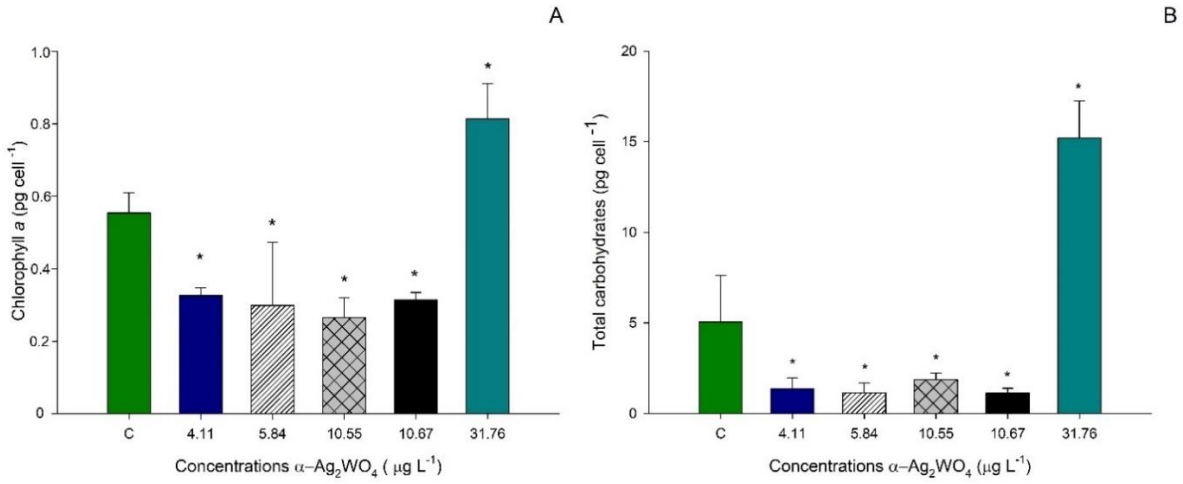

Fig. 5 Chlorophyll *a* content (mean ± SD) (A) and total carbohydrates (mean ± SD) of *Raphidocelis subcapitata* after 96 h exposed to α-Ag_2WO_4 (B). C = control group and asterisks * represent a significant difference (Dunnett's test, $p< 0.05$) of treatments compared to the control group.

Following the same pattern as the Chl *a* content, the amount of total carbohydrates (Fig. 5B) decreased significantly ~ 3.6, 4.4, 2.7, and 4.5 times (Dunnett's test, $p<0.05$) at concentrations of 4.11, 5.84, 10.55, and 10.67 µg L^{-1} and increased ~ 3 times (Dunnett's test, $p<0.05$) at 31.76 µg L^{-1} of α-Ag_2WO_4. This is closely related to the higher production of Chl *a*, because the increased production of this pigment can enable greater amounts of CO_2 to be fixed and then converted into carbohydrates (Chia et al., 2015). Furthermore, under stress

conditions, it is common that carbohydrate content in microalgae to increase (Rossi et al., 2018), which may be related to a protective mechanism of the algal cells, thus maintaining the integrity of the cell wall. This biomolecule has structural and storage functions, supplying the energy demand necessary for the maintenance of metabolism and cell wall structure (Markou et al., 2012), which explains why we observed higher carbohydrate content at the highest concentration (31.76 μg L^{-1}) of α-Ag_2WO_4.

Considering that the percentage of reduction of Φ_M values gradually diminished from 24 to 96 h at the highest concentration of α-Ag_2WO_4, and the F_0/F_V values indicated a gradually less severe impact at this same concentration between the beginning and the end of the experiment. This pattern can be a consequence of the increase in the Chl *a* and carbohydrate content that occurred at this concentration (31.76 μg L^{-1}) in the surviving cells. Probably an algal attempt to reduce the negative impacts of α-Ag_2WO_4, combined with the possible chelation of metals to dead cells, decreasing the metal available to the remaining cells.

4. Conclusion

Our results showed evidence of toxic effects of α-Ag_2WO_4 crystals on the photosynthetic activity of the microalga *R. subcapitata*, through a drastic reduction of the maximum quantum yield and loss of efficiency in OEC (increased values of F_0/F_v), mainly in the first hours of exposure. Besides the physiological aspects, we observed a reduction in the cell density and an increase in the biomolecules, such as Chl *a* and total carbohydrates contents at the highest experimental concentration of α-Ag_2WO_4, probably in an attempt to decrease the impacts of the α-Ag_2WO_4. At the end of the exposure, even with reduced cell number, the increased Chl *a* content possibly enabled the remaining cells to compensate for

the stress caused by α-Ag_2WO_4 and maintain photosynthesis, which is also corroborated by the maximum yield and OEC values, indicating the tendency to recover the physiological health. The parameters evaluated in this study were efficient and sensitive, with significant variations compared to the control group, which reinforces the importance of evaluating physiological, populational (cell density) aspects, as well as biomolecules contents (as Chl *a* and carbohydrate) in ecotoxicity studies. Therefore, identifying the targets of α-Ag_2WO_4 contributes to the elucidation of the mechanisms of action of this semiconductor on the microalga *R. subcapitata*. The changes observed in the microalgae in this study may be harmful in the long term, because as these are autotrophic organisms, impacts at the base of the food chain may pose threats to higher trophic levels. Thus, these data are useful for predicting and assessing risks caused by microcrystals.

Acknowledgements

This study was funded in part by the São Paulo Research Foundation - FAPESP (FAPESP CEPID-finance code 2013/07296-2; finance code 2018/07988-5), Financier of Studies and Projects FINEP, the National Council for Scientific and Technological Development - CNPq (finance code 141255/2018-8; ; CNPq 316064/2021-1), and the Coordination for the Improvement of Higher Education Personnel - CAPES (finance code 001 and 88887.364036/2019-00). We would also like to thank Dr. Ana Teresa Lombardi and Dr. Hugo Miguel Preto de Morais Sarmento for the permission to use their laboratories, as well as the equipment.

Author contributions This manuscript describes original work and is not under consideration by any other journal. All authors assume that they have read the final version of the manuscript and agreed with it. The contribution of each author of this work is described below:

CBA: co-developed the experimental design, carried out experimental tests and collected the data; performed statistical analysis; analyzed and interpreted the data and wrote the paper.

RCG: co-developed the experimental design, carried out experimental tests and collected the data; performed statistical analysis; analyzed and interpreted the data and reviewed the paper.

LLR: carried out experimental tests, collected the data and reviewed the paper.

GSR: carried out experimental tests and collected the data; performed statistical analysis; analyzed and interpreted the data and reviewed the paper.

LOGA: analyzed and interpreted the data and reviewed the paper.

LMA: performed the characterization of α-Ag2WO4 and reviewed the paper.

LSV: performed the characterization of α-Ag2WO4 and reviewed the paper.

MA: co-developed the experimental design; analyzed and interpreted the data and reviewed the paper.

ASM: co-developed the experimental design; performed statistical analysis, analyzed and interpreted the data and reviewed the paper.

EL: co-developed the experimental design; analyzed and interpreted the data and reviewed the paper. This author is also one of the sponsors, responsible for obtaining financial grant that supported this study (FAPESP CEPID-finance code 2013/07296-2).

MGGM: co-developed the experimental design; analyzed and interpreted the data and reviewed the paper. This author is also one of the sponsors, responsible for obtaining financial grant that supported this study (FAPESP 2018/07988–5; CNPq 316,064/2021–1).

Data availability The datasets generated during and/or analyzed during the current study are available from the corresponding author on reasonable request.

Declarations

Conflict of interest The authors declare that there is no conflict of interest. No conflicts, informed consent, human or animal rights are applicable for this work.

References

Alho, L. O. G., Gebara, R. C., Paina, K. A., Sarmento, H., Melao, M. G. G. (2019). Responses of *Raphidocelis subcapitata* exposed to Cd and Pb: Mechanisms of toxicity assessed by multiple endpoints. Ecotoxicology and Environmental Safety, *169*, 950–959. https:// doi. org/ 10. 1016/j. ecoenv. 2018. 11. 087.

Abreu, C.B., Gebara, R.C., Reis, L.L., Rocha, G.S., Alho, L O.G., Alvarenga, L.M., Virtuoso, L.S., Assis, M., Mansano, A.S, Longo, E., Melão, M.G.G., (2022). Toxicity of α - Ag_2WO_4 microcrystals to freshwater microalga *Raphidocelis subcapitata* at cellular and population levels. Chemosphere. 288, 9–16. https://doi.org/10.1016/j.chemosphere.2021.132536

Alho, L.O.G., Souza, J.P., Rocha, G.S., Mansano, A.S., Lombardi, A. T., Sarmento, H. M.P.M., Melão, M.G.G., (2020). Photosynthetic, morphological and biochemical biomarkers as tools to investigate copper oxide nanoparticle toxicity to a freshwater chlorophyceae. Environ Pollut. 265, 114856. https://doi.org/10.1016/j.envpol.2020.114856

Assis, M., Cordoncillo, E., Torres-Mendieta, R., Beltrán-Mir, H., Mínguez-Vega, G., Oliveira, R., Leite, E.R., Foggi, C.C., Vergani, C.E., Longo, E., Andrés, J., (2018). Towards the scale-up of the formation of nanoparticles on α-Ag_2WO_4 with bactericidal properties by femtosecond laser irradiation. Sci. Rep. 8, 1–11. https://doi.org/10.1038/s41598-018-19270-9

Assis, M., Pontes Ribeiro, R.A., Carvalho, M.H., Teixeira, M.M., Gobato, Y.G., Prando, G.A., Mendonça, C.R., De Boni, L., Aparecido De Oliveira, A.J., Bettini, J., Andrés, J., Longo, E., (2020). Unconventional Magnetization Generated from Electron Beam and Femtosecond Irradiation on α-Ag_2WO_4: A Quantum Chemical Investigation. ACS Omega 5, 10052–10067. https://doi.org/10.1021/acsomega.0c00542

Assis, M., Robeldo, T., Foggi, C.C., Kubo, A.M., Condoncillo, E., (2019). Composite Formed by Electron Beam and Femtosecond Irradiation as Potent Antifungal and Antitumor Agents. Sci. Rep. 9 (1),1–15. https://doi.org/10.1038/s41598-019-46159-y

Bao, V.W.W., Leung, K.M.Y., Qiu, J.W., Lam, M.H.W., (2011). Acute toxicities of five commonly used antifouling booster biocides to selected subtropical and cosmopolitan marine species. Mar. Pollut. Bull. 62, 1147–1151. https://doi.org/10.1016/j.marpolbul.2011.02.041.

Baracho, D.H., Silva, J.C., Lombardi, A.T., (2019). The effects of copper on photosynthesis and biomolecules yield in *Chlorolobion braunii*. J. Phycol. 55, 1335–1347. https://doi.org/10.1111/jpy.12914

Chia, M.A., Lombardi, A.T., da Graça Gama Melão, M., Parrish, C.C., (2015). Combined nitrogen limitation and cadmium stress stimulate total carbohydrates, lipids, protein and amino acid accumulation in *Chlorella vulgaris* (Trebouxiophyceae). Aquat. Toxicol. 160, 87–95. https://doi.org/10.1016/j.aquatox.2015.01.002

Chu, S.P., (1942). The Influence of the Mineral Composition of the Medium on the Growth of Planktonic Algae: Part I. Methods and Culture Media. J. Ecol. 30, 284. https://doi.org/10.2307/2256574

Cruz, L., Teixeira, M.M., Teodoro, V., Jacomaci, N., Laier, L.O., Assis, M., Macedo, N.G.,

Tello, A.C.M., Da Silva, L.F., Marques, G.E., Zaghete, M.A., Teodoro, M.D., Longo, E., (2020). Multi-dimensional architecture of Ag/α-Ag_2WO_4 crystals: insights into microstructural, morphological, and photoluminescence properties. CrystEngComm 22, 7903–7917. https://doi.org/10.1039/d0ce00876a

Dewez, D., Goltsev, V., Kalaji, H.M., Oukarroum, A., (2018). Inhibitory effects of silver nanoparticles on photosystem II performance in *Lemna gibba* probed by chlorophyll fluorescence. Curr. Plant Biol. https://doi.org/10.1016/j.cpb.2018.11.006

Dewez, D., Oukarroum, A., (2012). Silver nanoparticles toxicity effect on photosystem II photochemistry of the green alga *Chlamydomonas reinhardtii* treated in light and dark conditions. Toxicol. Environ. Chem. 94, 1536–1546. https://doi.org/10.1080/02772248.2012.712124

Foggi, C.C., Fabbro, M.T., Santos, L.P.S., de Santana, Y.V.B., Vergani, C.E., Machado, A.L., Cordoncillo, E., Andrés, J., Longo, E., (2017). Synthesis and evaluation of A-Ag_2WO_4 as novel antifungal agent. Chem. Phys. Lett. 674, 125–129. https://doi.org/10.1016/j.cplett.2017.02.067

He, D., Dorantes-Aranda, J.J., Waite, T.D., (2012). Silver nanoparticle-algae interactions: Oxidative dissolution, reactive oxygen species generation and synergistic toxic effects. Environ. Sci. Technol. 46, 8731–8738. https://doi.org/10.1021/es300588a

Herlory, O., Bonzom, J., Gilbin, R., (2013). Sensitivity evaluation of the green alga *Chlamydomonas reinhardtii* to uranium by pulse amplitude modulated (PAM) fluorometry. Aquat. Toxicol. 140–141, 288–294. https://doi.org/10.1016/j.aquatox.2013.06.007

Huang, J., Cheng, J., Yi, J., (2016). Impact of silver nanoparticles on marine diatom

Skeletonema costatum. J. Appl. Toxicol *36*(10), 1343-1354. https://doi.org/10.1002/jat.3325

Jeffrey, S.W., Humphrey, G.F., (1975). New spectrophotometric equations for determining chlorophylls a, b, c1 and c2 in higher plants, algae and natural phytoplankton. Biochem. und Physiol. der Pflanz. 167, 191–194. https://doi.org/10.1016/s0015-3796(17)30778-3

Juneau, P., Green, B.R., Harrison, P.J., (2005). Simulation of Pulse-Amplitude-Modulated (PAM) fluorescence : Limitations of some PAM-parameters in studying environmental stress effects. Photosynthetica 43, 75–83.

Juneau, P., Popovic, R., (2000). Evidence for the Rapid Phytotoxicity and Environmental Stress Evaluation Using the PAM Fluorometric Method : Importance and Future Application. Ecotoxicology, 8(6), 449-455. https://doi.org/10.1023/A:1008955819527

Kahru, A., Dubourguier, H.-C., (2010). From ecotoxicology to nanoecotoxicology. Toxicology 269, 105–119.

Kleiven, M., Macken, A., Oughton, D.H., (2019). Growth inhibition in *Raphidocelis subcapita* e Evidence of nanospecific toxicity of silver nanoparticles. Chemosphere 221, 785–792. https://doi.org/10.1016/j.chemosphere.2019.01.055

Kleiven, M., Rossbach, L.M., Gallego-Urrea, J.A., Brede, D.A., Oughton, D.H., Coutris, C., (2018). Characterizing the behavior, uptake, and toxicity of NM300K silver nanoparticles in *Caenorhabditis elegans*. Environ. Toxicol. Chem. 37, 1799–1810. https://doi.org/10.1002/etc.4144

Kriedemann, P.E., Graham, R.D., Wiskich, J.T., (1985). Photosynthetic dysfunction and in vivo changes in chlorophyll a fluorescence from manganese-deficient wheat leaves. Aust. J. Agric. Res. 36, 157–169. https://doi.org/10.1071/AR9850157

Kumari, K., Singh, P., Bauddh, K., Mallick, S., Chandra, R., (2019). Implications of metal nanoparticles on aquatic fauna: A review. Nanosci. Nanotechnology-Asia 9, 30–43.

Laier, L.O., Assis, M., Foggi, C.C., Gouveia, A.F., Vergani, C.E., Santana, L.C.L., Cavalcante, L.S., Andrés, J., Longo, E., (2020). Surface - dependent properties of α - Ag_2WO_4 : a joint experimental and theoretical investigation. Theor. Chem. Acc. 1–11. https://doi.org/10.1007/s00214-020-02613-z

Lekamge, S., Miranda, A.F., Abraham, A., Ball, A.S., Shukla, R., Nugegoda, D., (2020). The toxicity of coated silver nanoparticles to the alga *Raphidocelis subcapitata*. SN Appl. Sci. 2, 596. https://doi.org/10.1007/s42452-020-2430-z

Li, F., Liang, Z., Zheng, X., Zhao, W., Wu, M., Wang, Z., (2015). Toxicity of nano-TiO_2 on algae and the site of reactive oxygen species production. Aquat. Toxicol. 158, 1–13. https://doi.org/10.1016/j.aquatox.2014.10.014

Liu, D., Wong, P.T.S., Dutka, B.J., (1973). Determination of carbohydrate in lake sediment by a modified phenol-sulfuric acid method. Water Res. 7, 741–746. https://doi.org/10.1016/0043-1354(73)90090-0

Lodeiro, P., Browning, T.J., Achterberg, E.P., Guillou, A., El-Shahawi, M.S., (2017). Mechanisms of silver nanoparticle toxicity to the coastal marine diatom *Chaetoceros curvisetus*. Sci. Rep. 7, 1–10. https://doi.org/10.1038/s41598-017-11402-x

Longo, V.M., De Foggi, C.C., Ferrer, M.M., Gouveia, A.F., André, R.S., Avansi, W., Vergani, C.E., Machado, A.L., Andrés, J., Cavalcante, L.S., Hernandes, A.C., Longo, E., (2014). Potentiated electron transference in α-Ag_2WO_4 microcrystals with Ag nanofilaments as microbial agent. J. Phys. Chem. A 118, 5769–5778. https://doi.org/10.1021/jp410564p

Macedo, N.G., Gouveia, A.F., Roca, R.A., Assis, M., Gracia, L., Andre, J., Leite, E.R., Longo, E., Box, P.O., (2018). Surfactant-Mediated Morphology and Photocatalytic Activity of α -Ag_2WO_4 Material . J. Phys. Chem C, 122, 8667-8679. https://doi.org/10.1021/acs.jpcc.8b01898

Macedo, N.G., Machado, T.R., Roca, R.A., Assis, M., Gladys, M., Rodrigues, A., Foggi, C.C., Andre, J., San-miguel, M.A., Cordoncillo, E., (2019). Tailoring the Bactericidal Activity of Ag Nanoparticles / α -Ag_2WO_4 Composite Induced by Electron Beam and Femtosecond Laser Irradiation : Integration of Experiment and Computational Modeling. ACS Appl. Bio Mater. *2* (2), 824-837. https://doi.org/10.1021/acsabm.8b00673

Markou, G., Chatzipavlidis, I., Georgakakis, D., (2012). Carbohydrates Production and Bio-flocculation Characteristics in Cultures of *Arthrospira* (*Spirulina*) *platensis*: Improvements Through Phosphorus Limitation Process. Bioenergy Res. 5, 915–925. https://doi.org/10.1007/s12155-012-9205-3

Martínez-Ruiz, E.B., Martínez-Jerónimo, F., (2015). Nickel has biochemical , physiological , and structural effects on the green microalga *Ankistrodesmus falcatus* : An integrative study. Aquat. Toxicol. 169, 27–36. https://doi.org/10.1016/j.aquatox.2015.10.007

Matos, B., Martins, M., Samamed, A.C., Sousa, D., Ferreira, I., Diniz, M.S., (2020). Toxicity evaluation of quantum dots (ZnS and CdS) singly and combined in zebrafish (*Danio rerio*). Int. J. Environ. Res. Public Health 17, 232.

Mattoo, A.K., Giardi, M.T., Raskind, A., Edelman, M., (1999). Dynamic metabolism of photosystem II reaction center proteins and pigments. Physiol. Plant. 107, 454–461. https://doi.org/10.1034/j.1399-3054.1999.100412.x

Navarro, E., Baun, Æ.A., Behra, Æ.R., Hartmann, Æ.N.B., Filser, J., Antonietta, Æ.A.M.Æ.,

Peter, Q.Æ., (2008). Environmental behavior and ecotoxicity of engineered nanoparticles to algae, plants, and fungi. Ecotoxicology, 17(5), 372–386. https://doi.org/10.1007/s10646-008-0214-0

Nobre, F.X., Bastos, I.S., dos Santos Fontenelle, R.O., Júnior, E.A.A., Takeno, M.L., Manzato, L., de Matos, J.M.E., Orlandi, P.P., de Fátima Souza Mendes, J., Brito, W.R., da Costa Couceiro, P.R., (2019). Antimicrobial properties of α-Ag_2WO_4 rod-like microcrystals synthesized by sonochemistry and sonochemistry followed by hydrothermal conventional method. Ultrason. Sonochem. 58, 104620. https://doi.org/10.1016/j.ultsonch.2019.104620

Odzak, N., Kistler, D., Sigg, L., (2017). Influence of daylight on the fate of silver and zinc oxide nanoparticles in natural aquatic environments *. Environ. Pollut. 226, 1–11. https://doi.org/10.1016/j.envpol.2017.04.006

OECD, O., (2011). Guidelines For The Testing Of Chemicals No. 201 Freshwater AlgaAnd Cyanobacteria. Growth Inhib. Test 201.

Penha, M.D., Gouveia, A.F., Teixeira, M.M., De Oliveira, R.C., Assis, M., Sambrano, J.R., Yokaichya, F., Santos, C.C., Goncalves, R.F., Li, M.S., (2020). Structure , optical properties, and photocatalytic activity of α- $Ag_2W_{0.75}Mo_{0.25}O_4$. Mater. Res. Bull. 132, 111011. https://doi.org/10.1016/j.materresbull.2020.111011

Reis, L.L., Alho, L O.G., Abreu, C.B, Melão, M.G.G., (2021). Using multiple endpoints to assess the toxicity of cadmium and cobalt for chlorophycean *Raphidocelis subcapitata*. Ecotoxicol. Environ. Saf.. 208. https://doi.org/10.1016/j.ecoenv.2020.111628

Rocha, G.S., Lombardi, A.T., Espíndola, E.L.G., (2021). Combination of P-limitation and cadmium in photosynthetic responses of the freshwater microalga *Ankistrodesmus*

densus (Chlorophyceae). Environ. Pollut. 275, 116673. https://doi.org/10.1016/j.envpol.2021.116673

Rossi, R.A., Camargo, E.C., Crnkovic, P.C.G.M., Lombardi, A.T., (2018). Physiological and Biochemical Responses of *Chlorella vulgaris* to Real Cement Flue Gas Under Controlled Conditions. Water. Air. Soil Pollut. 229. https://doi.org/10.1007/s11270-018-3914-y

Sarmento, H., Unrein, F., Isumbisho, M., Stenuite, S., Gasol, J.M., Descy, J.P., (2008). Abundance and distribution of picoplankton in tropical , oligotrophic Lake Kivu , eastern Africa. Freshw. Biol. 756–771. https://doi.org/10.1111/j.1365-2427.2007.01939.x

Schreiber, U., (1986). Detection of rapid induction kinetics with a new type of high-frequency modulated chlorophyll fluorometer. Photosynth. Res. 9, 261–272. https://doi.org/10.1007/BF00029749

Schreiber, U., & Bilger, W. (1993). Progress in Chlorophyll Fluorescence Research: Major Developments During the Past Years in Retrospect. In *Progress in Botany / Fortschritte der Botanik* (pp. 151–173). Berlin, Heidelberg: Springer. https:// doi. org/ 10. 1007/ 978-3- 642- 78020-2_8.

Shoaf, W.T., Lium, B.W., (1976.) Improved extraction of chlorophyll a and b from algae using dimethyl sulfoxide. Limnol. Oceanogr. 21, 926–928. https://doi.org/10.4319/lo.1976.21.6.0926

Silva, J.C., Echeveste, P., Lombardi, A.T., (2018). Higher biomolecules yield in phytoplankton under copper exposure. Ecotoxicol. Environ. Saf. 161, 57–63. https://doi.org/10.1016/j.ecoenv.2018.05.059

Sørensen, S.N., Lützhøft, H.H., Rasmussen, R., Baun, A., (2016). Acute and chronic effects

from pulse exposure of *D. magna* to silver and copper oxide nanoparticles. Aquat. Toxicol. https://doi.org/10.1016/j.aquatox.2016.10.004

Statsoft Inc, 2004. STATISTICA, Version 07. www.statsoft.com

Stensberg, M.C., Wei, Q., Mclamore, E.S., Marshall, D., (2011). Toxicological studies on silver nanoparticles: challenges and oopportunities in assessment, monitoring and imaging. Nanomedicine 6, 879–898. https://doi.org/10.2217/nnm.11.78.

Systat, 2008. Systat Software, Incorporation SigmaPlot for Windows version 11.0.

Wacker, A., Piepho, M., Spijkerman, E., (2015). Photosynthetic and fatty acid acclimation of four phytoplankton species in response to light intensity and phosphorus availability. Eur. J. Phycol. 50, 288–300. https://doi.org/10.1080/09670262.2015.1050068

Supplementary material

Figure S1 X-ray diffraction of the α-Ag_2WO_4 sample using a D/Max 2500PC diffractometer (Rigaku)

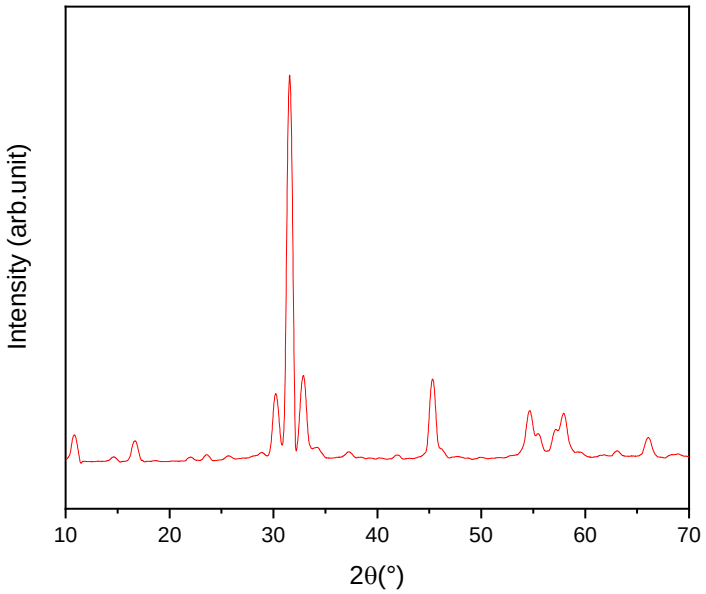

Table S1 Silver Tungstate α-Ag_2WO_4 – R characterization in the CHU-12 culture medium and ultrapure water

α-Ag_2WO_4 (µg L^{-1})	**Time (h)**	**Zeta-Potential (mV)**	**Hydrodynamic size (nm)**	**PdI**	**Zeta-Potential (mV)**	**Hydrodynamic size (nm)**	**PdI**
		CHU-12 (test solutions)			Ultrapure Water		
4.11	0	Abreu et al., 2022	Abreu et al., 2022	Abreu et al., 2022	Abreu et al., 2022	Abreu et al., 2022	Abreu et al., 2022
	24	-9.94 ± 0.5	574.23 ± 113.5	0.75 ± 0.10	-3.39 ± 2	117.16 ± 66.51	0.83 ± 0.15
	48	-10.80 ± 0.75	647.66 ± 130.5	0.37 ± 0.14	1.35 ± 0.56	446.5 ± 0	0.60 ± 0
	72	-10.29 ± 0.72	687.1 ± 24.53	0.21 ± 0.07	-9.99 ± 3.16	309.4 ± 94.33	0.48 ± 0.12
	96	Abreu et al., 2022	Abreu et al., 2022	Abreu et al., 2022	Abreu et al., 2022	Abreu et al., 2022	Abreu et al., 2022
10.55	0	Abreu et al., 2022	Abreu et al., 2022	Abreu et al., 2022	Abreu et al., 2022	Abreu et al., 2022	Abreu et al., 2022
	24	-12 ± 1.00	1129.5 ± 283.5	0.44 ± 0.33	-5.82 ± 0.05	230.65 ± 58.9	0.65 ± 0.47
	48	-11.53 ± 0.30	629.6 ± 169.7	0.7 ± 0.36	-0.27 ± 1.24	594.35 ± 215.21	0.54 ± 017
	72	-11.55 ± 0.55	815.25 ± 285.86	0.80 ± 0.38	-1.57 ± 4.24	221.1 ± 16.24	0.4 ± 0.25

	96	Abreu et al., 2022	Abreu et al., 2022	Abreu et al., 2022	Abreu et al., 2022	Abreu et al., 2022	Abreu et al., 2022
31.76	0	Abreu et al., 2022	Abreu et al., 2022	Abreu et al., 2022	Abreu et al., 2022	Abreu et al., 2022	Abreu et al., 2022
	24	-12.80 ± 1.4	472.5 ± 23.33	0.86 ± 0.09	-5.37 ± 4.23	356.45 ± 100.48	0,36 ± 0.12
	48	-5.39 ± 1.16	704.1 ± 199.25	0.84 ± 0.21	-1.24 ± 1.06	339.7 ± 198.3	0.33 ± 0.10
	72	-11.06 ± 0.72	1496 ± 157.13	0.29 ± 0.14	-2.66 ± 1.92	121.24 ± 69.27	0.55 ± 0.31
	96	Abreu et al., 2022	Abreu et al., 2022	Abreu et al., 2022	Abreu et al., 2022	Abreu et al., 2022	Abreu et al., 2022

Table S2 Composition of the culture medium CHU-12

Reagent	Concentration (mM)
$Ca(NO_3)_2.4H_2O$	18.20
K_2HPO_4	2.87
$MgSO_4.7H_2O$	30.4
KCl	6.70
Na_2CO_3	18.86
$FeCl_3.6H_2O$	0.18

Reference

Chu, S. P. (1942). The Influence of the Mineral Composition of the Medium on the Growth of Planktonic Algae: Part I. Methods and Culture Media. The Journal of Ecology, v. 30, n. 2, p. 284.

Abreu, C.B., Gebara, R.C., Reis, L.L., Rocha, G.S., Alho, L O.G., Alvarenga, L.M., Virtuoso, L.S., Assis, M., Mansano, A.S, Longo, E., Melão, M.G.G. (2022). Toxicity of α- Ag_2WO_4 microcrystals to freshwater microalga *Raphidocelis subcapitata* at cellular and population levels. Chemosphere 132536. https://doi.org/10.1016/j.chemosphere.2021.132536

Capítulo 3 - Effects of different α-Ag_2WO_4 morphologies isolated and mixture for a Neotropical cladoceran – Artigo em revisão no periódico *Chemosphere*

Highlights

- Both microcrystal shapes caused immobility to the cladoceran
- The 48 h EC_{50} was 0.64 μg L^{-1} ± 0.11 for α-Ag_2WO_4 – C
- The 48 h EC_{50} was 0.81 μg L^{-1} ± 0.15 for α-Ag_2WO_4 –R
- In mixture experiments, the data best fitted the IA model and DL deviation
- We found synergic effects in low microcrystals concentrations during mixture tests

ABSTRACT

The high production and consumption of Ag-based materials contributes directly to their availability in the freshwater ecosystems, causing toxicity to organisms. In addition, they are important sources of ions, which also negatively affect the biota. Therefore, this study intended to assess the effects of the silver tungstate (α-Ag_2WO_4), in different morphologies (α-Ag_2WO_4 – C, cube and α-Ag_2WO_4 – R, rod), for *Ceriodaphnia silvestrii*. We investigated the acute effects of microcrystals isolated and mixture from immobility (48 h) and ingestion rates (at 24 h). We also performed chronic toxicity tests for single microcrystals. Considering the high release of silver ions from the microcrystals, ~ 59% for α-Ag_2WO_4 – C and 70% for α-Ag_2WO_4 – R, our results revealed that the immobility of the organisms in the acute tests was mainly induced by the silver ions. The 48 h EC_{50} and EC_{10} for *C. silvestrii* were respectively 0.64 μg L^{-1} ± 0.11 and 0.38 μg L^{-1} ± 0.06 for α-Ag_2WO_4 – C and 0.81 μg L^{-1} ± 0.15 and 0.52 μg L^{-1} ± 0.04 for α-Ag_2WO_4 –R. Regarding the ingestion rate, we also did not observe significant changes. Moreover, we did not observe significant effects in the chronic exposure (up to 0.4 μg L^{-1}). Regarding the mixture, data were best fitted to the independent action model (IA) with dose-level dependent (DL) deviation, showing synergism at low concentrations and antagonism at high concentrations of microcrystals. Our results can support ecological risk assessment and public policy making about safe thresholds of α-Ag_2WO_4 and silver ions in aquatic ecosystems, mainly because we have identified synergistic effects at low doses of microcrystal mixtures.

Keywords: *Ceriodaphnia silvestrii*, acute toxicity, ingestion rates, chronic toxicity, silver tungstate.

1. INTRODUCTION

Currently, much has been discussed about risks associated with Ag-based materials as their interactions with biological systems may cause toxicity (Navarro et al., 2008; Zhu et al., 2019). The increase in production and frequent use increases their availability in the environment, because commonly all compounds that are used in daily life can be carried by surface runoff, reaching water bodies (Dewez et al., 2018). In particular alpha silver tungstate (α-Ag_2WO_4), a metal oxide and component of an important class of functional materials that has interesting physical and chemical properties (Assis et al., 2018; Laier et al., 2020), has drawn attention as a multifunctional composite (Silva et al., 2014). The main aspects of the material involved with its reactivity are the morphology (α-Ag_2WO_4 – C (cube) and α-Ag_2WO_4 – R (rod)), which is directly related to the surface and active sites of the composite; size; composition; among others (Macedo et al., 2018; Laier et al., 2020; Assis et al., 2021).

Given the wide range of applications of α-Ag_2WO_4, such as use in sensors (Silva et al., 2014; Muthamizh et al., 2015; Silva et al., 2016), magnetic materials (Assis et al., 2020), antimicrobial materials (Foggi et al., 2017a, 2017b**;** Nobre et al., 2019; Macedo et al., 2019; Laier et al., 2020; Alvarez-Roca et al., 2021), antitumor agent (Lin et al., 2012; Assis et al., 2019) and photocatalytic (Macedo et al., 2018; Arumugam et al., 2020; Ayappan et al., 2020; Cruz et al., 2020; Dai et al., 2010; Macedo et al., 2019), the increased production and use of this compound may increase its availability in the environment, especially in freshwater ecosystems. In addition, the compound may be a source of silver ions, which poses a hazard to aquatic organisms (Stoiber et al., 2015; Abreu et al., 2022).

Some studies show that particles with silver cause toxicity in aquatic organisms, as reported for different taxa (Navarro et al., 2008; Oukarroum et al., 2012; He et al., 2012; Angel et al., 2013; Ribeiro et al., 2014; Sohn et al., 2015; Koser et al., 2017, Martins et al., 2007), in particular Cladocera, such as *Simocephalus* (Hook and Fisher, 2001) and *Ceriodaphnia dubia* (Hook and Fisher, 2001; Angel et al., 2013), *Chydorus sphaericus* (Wang et al., 2012), *Daphnia galeata* and *Bosmina longirostris* (Sakamoto et al., 2014), *Daphnia magna* (Kim et

al., 2011; Gaiser et al., 2011; Seitz et al., 2015; Sohn et al., 2015; Shen et al., 2015) and *Daphnia similis* (Becaro et al., 2015).

The deleterious effects of Ag-based materials on microcrustaceans include changes at organism and cellular levels, such as growth inhibition (Zhao and Wang, 2010), reproduction (Bielmyer et al., 2002), feeding inhibition (Ribeiro et al., 2014) and oxidative stress, with ROS formation (Poynton et al., 2012; Levard et al., 2012; Newton et al., 2013; Fu et al., 2014). According to Bianchini and Wood (2003), the silver toxicity mechanism for these organisms is similar to the toxicity seen for freshwater fish, which consists of inhibiting the active absorption of sodium by blocking Na^+, K^+ and ATPase.

Thus, the effects caused to microcrustaceans can result in changes in the upper trophic levels, which compromises the balance of ecosystems. Therefore, verifying the toxicity of silver to aquatic organisms helps to assess the impact on the ecosystem (Newton, et al., 2013). The Neotropical species *Ceriodaphnia silvestrii* (Cladocera), used a test organism in this study, has been shown to be very sensitive to environmental contaminants (Mansano et al., 2016), including metallic nanoparticles, such as copper oxide (Mansano et al., 2018), iron oxide (Gebara et al., 2019), titanium dioxide (de Lucca et al., 2018), agrochemicals (Moreira et al., 2014; Mansano et al., 2016), metals (Gebara et al., 2021) and pharmaceutical drugs (Damasceno et al., 2018). However, to date, the α-Ag_2WO_4 toxicity to tropical cladoceran *C. silvestrii* has never been evaluated. Moreover, most ecotoxicity studies are on other species (Hook and Fisher, 2001; Zhao and Wang, 2010; Kim et al., 2011; Poynton et al., 2012; Ribeiro et al., 2014; Sakamoto et al., 2014; Seitz et al., 2015).

In addition, ecotoxicity tests with compounds in mixtures are still scarce for various pollutants, but essential (Uwizeyimana et al., 2017), because in the environment, contaminants are rarely present alone. Especially for α-Ag_2WO_4 – C and α-Ag_2WO_4 – R, to the best of our knowledge, there are no toxicity evaluation studies of these compounds alone or in mixture for microcrustaceans. Therefore, an important aspect in the environmental risk assessment is to predict the possible results caused by the contaminant combination.

Here, we aimed to investigate the toxicity of α-Ag_2WO_4, in the α-Ag_2WO_4-C (cube) and α-Ag_2WO_4-R (rod) morphology, to the Neotropical cladoceran *Ceriodaphnia silvestrii.* In the acute toxicity tests (48h), we evaluated the effects of α-Ag_2WO_4-C and α-Ag_2WO_4-R, on the mobility of *C. silvestrii* in both single and mixture exposures. In the chronic toxicity tests (8 days), we evaluated the effects of isolated α-Ag_2WO_4 on the reproduction and growth of *C. silvestrii.* In addition, we evaluated the ingestion rate of the organisms over 24h and at the

same concentrations used in the chronic tests. Our hypothesis was to test whether the α-Ag_2WO_4, in different morphologies, causes different effects on the test organism, and at higher concentrations, the damage caused to the species *C. silvestrii* is concentration-dependent. Furthermore, when these substances are in a mixture, the toxicity effects of the studied compounds cause more serious damage than when analyzed in isolation.

2. MATERIAL AND METHODS

2.1 Synthesis, Characterization of α-Ag_2WO_4, Silver concentrations and ion release

To synthesize α-Ag_2WO_4 microparticles, the coprecipitation method was used (Macedo et al., 2018). After that, the samples were characterized by X-ray diffraction (XRD) using a D/Max-2500 PC diffractometer (Rigaku) with Cu Kα radiation (λ = 1.5406 Å) and the cube and rod morphologies of the samples were observed by field emission scanning electronic microscopy (FE-SEM) operated at 10 kV (Supra 35-VP, Carl Zeiss) (see Abreu et al., 2022). Furthermore, we measured the hydrodynamic size, polydispersity index (PdI) and zeta potential of the particles in soft synthetic water and in ultrapure water at 0 h and 48 h by dynamic light scattering (DLS) using Zetasizer Nano ZS90, Malvern.

We determined the silver concentrations in the α-Ag_2WO_4 stock solutions used to prepare the test solutions. Quantification was done via inductively coupled plasma mass spectrometry (ICP-MS PerkinElmer NexION, 2000), with respective limits of quantification and detection of 0.0084 and 0.0028 μg L^{-1}. On the other hand, to determine free silver ions, the stock solutions were centrifuged (Eppendorf 5702 R, Germany) at 4400 rpm for 60 min using a 3 kDa Amicon centrifugal filter (Merck Millipore, Darmstadt, Germany) to remove particles or agglomerates of α-Ag_2WO_4. Then, the filtered volumes were quantified by ICP-MS and thus the fraction < 3kDa was considered dissolved Ag.

2.2 Test organism

Ceriodaphnia silvestrii was obtained from laboratory cultures of the NEEA/CRHEA (São Carlos School of Engineering, University of São Paulo, USP, Brazil) and the stock cultures were maintained in the Laboratory of Plankton (Department of Hydrobiology, Federal University of São Carlos, UFSCar, Brazil) in reconstituted water (pH 7.0 - 7.6, conductivity 160 μS cm^1 and hardness 40 - 48mg $CaCO_3$ L^{-1}) at 25 ±1 °C and 12:12 h light/dark

photoperiod, as recommended by the Brazilian Association of Technical Standards (ABNT NBR 13373, 2017). The organisms were fed 3 times a week with the algae *Raphidocelis subcapitata* ($2x10^5$ cells ml^{-1}) and a food supplement containing yeast and fish food was added (ABNT NBR 13373, 2017).

2.3 Toxicity tests

For the exposures, the stock solution (1 mg L^{-1}) was dispersed using a bath sonicator (Ultra cleaner 1400 Unique), during 30 min. The toxicity tests followed ABNT guidelines (2016, 2017). For the acute toxicity test, the following concentrations of 0.0, 0.29, 0.40, 0.52, 0.63 and 0.92 μg L^{-1} for α-Ag_2WO_4 – C and 0.0, 0.39, 0.59, 0.98, 1.97 and 2.95 μg L^{-1} for α-Ag_2WO_4 – R were tested. The acute assay was performed in four replicates per treatment and five neonates (<24 h-old) per replicate, with a total of 20 organisms per concentration. The tests were kept in the dark, at 25 ± 1 °C, without addition food. The number of immobile individuals was counted after 48 h of exposure and they were used to calculate the median effective concentration (EC_{50}).

Regarding mixture experiments (48 h of exposure), the tests were carried out adopting the same protocols used for the tests with the isolated compounds. For the trials, an experimental design that simultaneously includes a test for each individual compound and a set of combinations was selected. A full factorial design was used for the acute mixture test (Freitas et al., 2014).

Based on the acute toxicity tests, the chronic tests were made at the following sublethal concentrations 0.1; 0.15; 0.25; 0.30 and 0.4 μg L^{-1} for both α-Ag_2WO_4 – C and α-Ag_2WO_4 – R. The duration of the chronic test was 8 days. Chronic assays were conducted using 10 replicates, with one animal each (< 24 h), in 20 ml of test solution, replaced every other day. The organisms were maintained under the same conditions of the culture maintenance. The number of neonates/females were observed under a stereomicroscope daily, and at the end of the test the size of the females (mothers) was measured. The variables temperature, dissolved oxygen and pH variables were measured at the start and at the end of every test solution change.

2.4 Ingestion rates

The feeding inhibition assays were based on the method described by McWilliam and Baird (2002). The individuals of *C. silvestrii* (48h-old) were exposed to the same sublethal

concentrations of microcrystals from the chronic toxicity tests, and they were fed with 2 x 10^5 cells ml^{-1} of *R. subcapitata* during 24h in the dark. The test had 4 replicates per treatment and 5 animals per replicate (n=20). One additional replicate was run with algae and without animals, to measure possible algal growth during the experiments. At the end of the experiment (after 24h), the samples with algal cells were fixed with 1% formaldehyde and analyzed in a flow cytometer (FACSCalibur, Becton Dickinson, San Jose, CA, USA) equipped with a 15 mW blue-argon ion laser (488 nm of excitation), using an internal standard (6 µm fluorescent beads, Fluoresbrite carboxylate microspheres; Polysciences, Warrington, Pennsylvania, USA), according to Sarmento et al. (2008). These data were analyzed in the FlowJo software, version 10 (Treestar.com, USA). The ingestion rates were calculated according to Villarroel et al. (1999) and the equations used are described below (1, 2 and 3). Where F is the filtration rate (mL ind^{-1-1}), I is the ingestion rate (cells ind^{-1} h^{-1}), C_0 is the algae density (cells mL^{-1}) at 0 h, Ct is the algae density (cells mL^{-1}) at 24 h, n is the number of organisms per replicate, V is the volume of test solution (mL), and A is the correction factor for changes in algal concentrations at 24 h (C't) in treatments without animals.

$$F = \frac{V}{n} \text{ x } \frac{\ln C_0 - \ln C_t}{t} - A \quad (1)$$

$$A = \frac{\ln C_0 - \ln C't}{t} \quad (2)$$

$$I = F \text{ x } \sqrt{C_0 \text{ x } C_t} \quad (3)$$

2.5 Data analysis

The EC_{50} and EC_{10} values for acute exposure were calculated by nonlinear regression using logistic curves. Data from acute and chronic tests were analyzed for normality and homogeneity of variances, and then the normal data were analyzed by one-way ANOVA. This was followed by Dunnett's post-hoc test and data with non-normal distribution using the with Kruskal-Wallis test, followed by Dunn's post-hoc test. These data analyses were made using the SigmaPlot software, version 11.0 (Systat, 2008) and Statistica version 7.0 (Statsoft Inc, 2004).

Data from the mixture tests were analyzed using the conceptual models of concentration addition (CA) and independent action (IA). Initially, the observed data were compared with the expected combined effect calculated from the individual exposures using the MIXTOX tool (Jonker et al., 2005). Then, the analyses were extended as described by Jonker et al. (2005) and the three deviations from the reference models, such as synergistic/antagonistic interactions (S/A), dose ratio-dependent (DR) and dose level-dependent (DL) deviations were modeled. The next step was to choose the best fit using the maximum likelihood method and the best descriptive deviation was statistically identified.

3. RESULTS AND DISCUSSION

3.1 Characterization of α-Ag_2WO_4, chemical analysis and abiotic variables

The data of α-Ag_2WO_4 characterization are available in Tables S1 and S2 (Supplementary material). On average, the zeta potential at 0 h and 48 h was respectively -23.97 ± 2.03 and -11.21 ± 4.88 mV for α-Ag_2WO_4 - C and -9.80 ± 3.28 and -10.65 ± 5.6 mV for α-Ag_2WO_4 - R. Because these values are above -30mV and below +30mV, our results indicated electrostatic instability **(**Lodeiro et al., 2017; Kleiven et al., 2018; Kleiven et al., 2019; Abreu et al., 2022a, Abreu et al., 2022b). Overall, the PdI values found were, on average, 0.49 ± 0.07 in 0 h and 0.6 ± 0.1 in 48 h for α-Ag_2WO_4–C and 0.77 ± 0.1 in 0h and 0.59 ± 0.22 in 48h for α-Ag_2WO_4–R, indicating that the microparticles formed agglomerates/ aggregates.

Regarding the amount of Ag ions released by the microcrystals, we observed that in the stock solution of α-Ag_2WO_4-C there was approximately 59% dissolved silver ions and in the α-Ag_2WO_4-R there was about 70% free Ag (Table 1), which was responsible for the toxicity to microcrustaceans, especially on acute exposure, as discussed below.

Table 1: Measured concentrations (ICP-MS) of α-Ag_2WO_4, concentration of silver and amount of free silver (in relation to silver) used in experiments with *Ceriodaphnia silvestrii.*

[α-Ag_2WO_4] (µg L^{-1})	[Ag] free ion (µg L^{-1})	% [Ag] free ion (µg L^{-1})
Cube 1154.52	677.90 ± 22.51	58.7

Rod 985.79	690.52 ± 11.75	70

3.2 Single acute and chronic effects

The toxicity tests (acute and chronic) were validated according to ABNT criteria (2016, 2017) i.e. mortality in control group lower than 10 and 20%, respectively, to acute and chronic exposures. Especially in the chronic test the mean number of live neonates was ≥15, after 8 d. In an acute toxicity test, we observed that α-Ag_2WO_4 caused immobility of *C. silvestrii* (Fig. 1A and Fig. 1B). The α-Ag_2WO_4 – C caused significant (Dunnett's test $p < 0.05$) effects when compared to the control from 0.4 μg L^{-1}. On the other hand, α-Ag_2WO_4 – R caused significant (Dunn's test $p < 0.05$) effects on immobility at the highest concentrations tested (1.97 and 2.95 μg L^{-1}), when compared to the control.

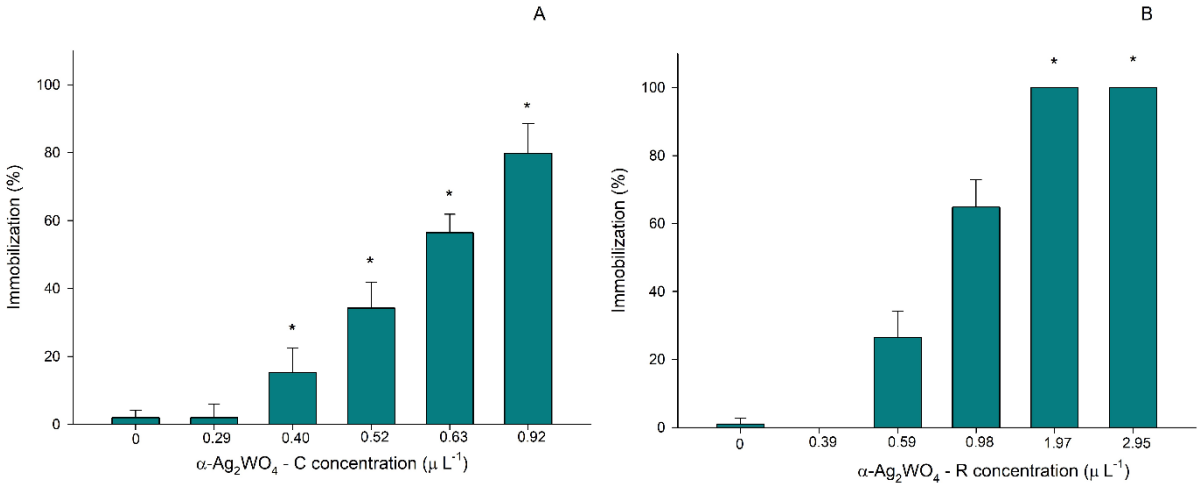

Fig. 1: Immobility (%) of *Ceriodaphnia silvestrii* (mean ± SD) after 48 h of exposure to single α-Ag_2WO_4 – C (A) and α-Ag_2WO_4 - C (B). Asterisks (*) represent significant differences from the control group (one-way ANOVA, Dunnett's test, $p < 0.05$ for cube and Dunn's test, $p < 0.05$ for rod). Control group is the number "0".

Regarding EC_{50} and EC_{10}, our results showed the average 48 h EC_{50} and EC_{10} values of 0.64 μg L^{-1} ± 0.11 and 0.38 μg L^{-1} ± 0.06 for α-Ag_2WO_4 – C, while the 48 h EC_{50} and EC_{10} for α-Ag_2WO_4 – R were 0.81 μg L^{-1} ± 0.15 and 0.52 μg L^{-1} ± 0.04. Comparing only the 48h EC_{50} values, we found that α-Ag_2WO_4 - C was 1.3 times more toxic to *C. silvestrii* than α-Ag_2WO_4 - R, although the EC_{50} of the compounds were not statistically significant (t-test, $p = 0.07$), contradicting our expectations. The absence of significant difference in toxicity between the

EC_{50} values obtained for different morphologies of α-Ag_2WO_4 contradicted our expectations. Hypothetically, we would expect α-Ag_2WO_4 - R to cause greater toxicity to the organisms than α-Ag_2WO_4 - C, because it is known that α-Ag_2WO_4 – R and α-Ag_2WO_4 – C have distinct surface energies, which is directly related to its reactivity (Macedo et al., 2018; Abreu et al., 2022).

When comparing the toxicity of α-Ag_2WO_4 with other species, the *C. silvestrii* was more sensitive to α-Ag_2WO_4 than the microalgae *R. subcapitata* (IC_{50} for α-Ag_2WO_4 – R (rod) was 13.72 ± 1.48 μg L^{-1} and for α-Ag_2WO_4 – C was 18.60 ± 1.61 μg L^{-1}) (Abreu et al., 2022). Here, the concentrations causing an effect on microcrustaceans were almost 30 times lower for α-Ag_2WO_4 – C and almost 17 times lower for α-Ag_2WO_4 – R. We highlight that the medium in which the cladocerans were exposed was different from that of the microalgae, which may influence the toxicity of the sample (Sakamoto et al., 2014). Possibly the high toxicity of α-Ag_2WO_4 for *C. silvestrii* is related to the release of silver ions from microcrystals, as silver is highly toxic to different species of aquatic organisms (Hook and Fisher, 2001; Wang et al., 2012; Sakamoto et al., 2014; Kim et al., 2011; Gaiser et al., 2011; Seitz et al., 2015; Sohn et al., 2015; Shen et al., 2015; Becaro et al., 2015), causing growth inhibition, formation of reactive oxygen species and immobility. Considering the different responses of organisms to the same material, we reinforce the importance of ecotoxicological studies using different species in toxicity assessment, as pointed out by Zhang et al. (2019), Metreveli et al. (2016) and Ivask et al. (2013).

According to Bianchini and Wood (2003), the mechanism of silver toxicity to aquatic organisms is related to problems in ion regulation. These authors explain that silver affects the activity of Na^+, K^+ and ATPase. Moreover, although our study did not evaluate the production of reactive oxygen species for *C. silvestrii*, it is well established in the literature that silver and silver -based materials produce ROS in freshwater species (Poynton et al., 2012; Levard et al., 2012; Newton et al., 2013; Fu et al., 2014). Thus, it is possible that microcrustaceans exposed to α-Ag_2WO_4 – R and α-Ag_2WO_4 – C may have suffered oxidative stress as a result of ROS production, which combined with ion regulation problems compromised the mobility of the organisms in acute exposure.

Comparing our data with the literature, we found that α-Ag_2WO_4 had higher toxicity compared to EC_{50} values previously described for other cladoceran species and using Ag-based compounds such as silver nanoparticles and silver nitrate. For example, in acute tests, Ribeiro et al. (2014) and Park et al. (2019) described LC_{50} values for *D. magna* of 11.02 μg L^{-}

[1] for silver nanoparticles and 1.06 µg L^{-1} and 10.4 µg L^{-1} for $AgNO_3$, Seitz et al. (2015) found EC_{50}-48h values of 1.7 to 3 µg Ag L^{-1} for *D. magna* exposed to $AgNO_3$. All of these studies report higher toxicity values than our data. On the other hand, Poynton et al. (2012) found an 24h-LC_{50} of 0.4 µg L^{-1} for *D. magna* for $AgNO_3$, similar to the values determined in our study.

Regarding the toxicity of tungsten (W) to aquatic organisms, based on data reported by Khangarot and Ray (1989), with 48 h EC_{50} for Na_2WO_4 of 89.39 mg L^{-1} and Strigul et al. (2009) with LD_{50} of 0.344 g L^{-1}, both for microcrustaceans, we assume that Na_2WO_4 exert low toxicity to these organisms. Furthermore, Strigul et al. (2009) found that sodium tungstate (used in the synthesis of α-Ag_2WO_4) inhibits the growth of *Selenastrum capricornutum* (*R. subcapitata*) by 75% at a concentration of approximately 2.42 g L^{-1}. All of these reported values are higher than the EC_{50} (µg L^{-1}) values reported for the two morphologies of α-Ag_2WO_4 in this study.

In chronic toxicity tests, we did not observe significant changes in the parameters analyzed. There was no reduction in the number of neonates in the tested concentrations (Fig. 2A and Fig.2B). Thus, the fertility of *C. silvestrii* was not significantly altered when compared to the control (p= 0.323 for α-Ag_2WO_4 – C and p= 0.467 for α-Ag_2WO_4 – R). Moreover, the length of females was not affected at 8-d. for both α-Ag_2WO_4- C (p= 0,584) and α-Ag_2WO_4 -R (p = 0.745) exposures (Fig. 3A and B).

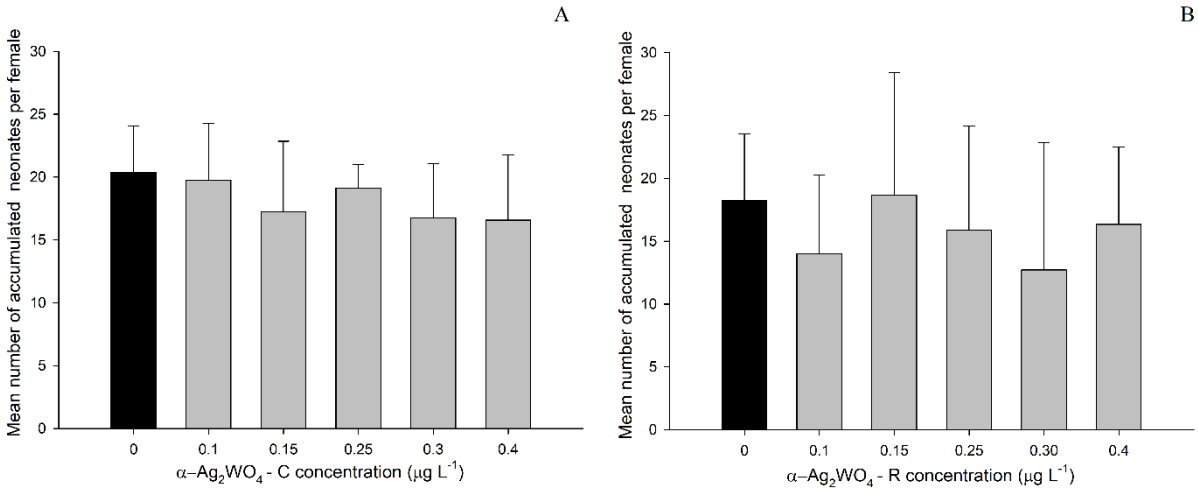

Fig. 2: Mean number of accumulated neonates per female of *Ceriodaphnia silvestrii* (mean ± SD) exposed to α-Ag_2WO_4- C (A) and α-Ag_2WO_4 -R (B) after 8-d, during chronic toxicity tests. Columns and bars represent mean values and standard deviation, respectively. Control group is the number "0".

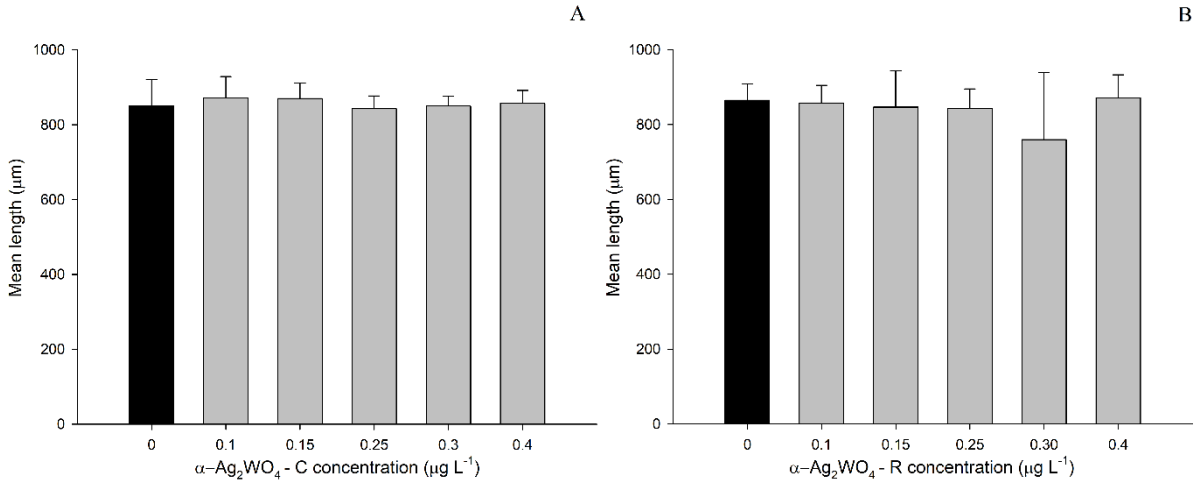

Fig. 3: Body length of adult females of *Ceriodaphnia silvestrii* (mean ± SD) exposed to α-Ag_2WO_4- C (A) and α-Ag_2WO_4 -R (B) in the chronic exhibition (during 8-d). Columns and bars represent mean values and standard deviation, respectively. Control group is the number "0".

Although our results show no significant toxic effects of α-Ag_2WO_4 on the bionomy of the cladocerans during chronic exposure, it is important to point out that this is possibly due to the availability of food for the cladoceran in the test solution. There are studies highlighting the correlation between reduced toxicity of Ag-based particles and food availability. For example, Conine and Frost (2016) concluded that the presence of algae decreased the toxicity of silver nanoparticles on the growth and survival of *Daphnia magna*. Newton et al. (2013) pointed out that the presence of dissolved organic carbon can influence ion release by coating and blocking the sites responsible for ion release. Liu and Hurt (2010) also point out that the existence of organic matter in the medium can shield the ion release sites. Therefore, our data are consistent with results previously described in the literature.

Regarding the ingestion rate, we also did not observe significant changes in the treatments when compared to the control (Fig. 4).

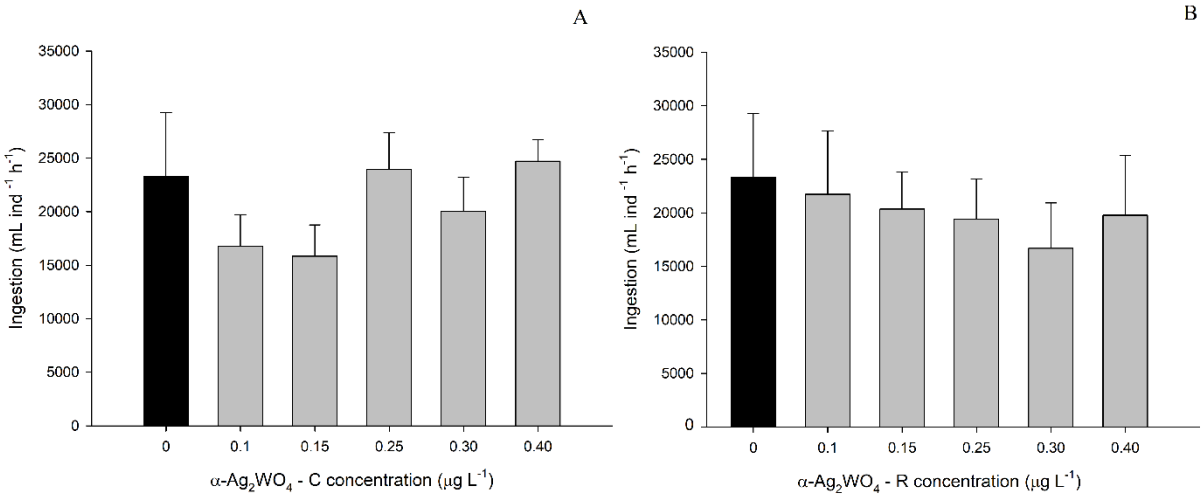

Fig. 4: Ingestion rates (mL ind^{-1} h^{-1}) of *Ceriodaphnia. silvestrii* (mean ± SD) exposed to α-Ag_2WO_4- C (A) and α-Ag_2WO_4 -R (B) for 24 h. Control group is the number "0".

3.3 Mixture effects

In this study, the independent action (IA) and concentration addition (CA) theoretical models were tested to assess the *C. silvestrii* response when exposed to mixtures of the α-Ag_2WO_4 – C and α-Ag_2WO_4 – R. Results modeled from MIXTOX tool are available in Table 2 and both the CA and IA models fitted our mixture data.

Table 2: Summary of the MIXTOX analysis of acute toxicity tests of mixtures of α-Ag_2WO_4C and α-Ag_2WO_4 -R to *Ceriodaphnia silvestrii*

	Concentration addition				Independent action			
	CA	S/A	DR	DL	IA	S/A	DR	**DL**
Max	0.95	0.94	0.94	0.93	0.93	0.94	0.95	**0.91**
$\beta_{\alpha\text{-}Ag2WO4-R}$	4.78	7.50	7.62	13.98	129.53	530.89	129.44	**16.27**
$\beta_{\alpha\text{-}Ag2WO4-C}$	5.32	7.17	7.07	9.79	4.78	6.22	5.46	**16.61**
EC_{50} to α-Ag_2WO_4 – R	0.66	0.57	0.57	0.57	0.59	0.59	0.59	**0.57**
EC_{50} to α-Ag_2WO_4 – C	0.57	0.53	0.53	0.54	0.44	0.53	0.52	**0.55**

a	-	1.24	1.04	-0.24	-	- 4.91	- 3.60	**- 10.25**
$b_{DR/DL}$	-	-	0.41	4.34	-	-	- 0.97	**1.12**
SS	45.02	29.91	29.86	29.55	48.14	NC	31.99	**23.50**
r^2	0.86	0.91	0.91	0.91	0.85	NC	0.90	**0.93**
X^2 or test F	285.16	15.11	0.05	0.36	282.04	NC	16.15	**24.64**
df	-	1.00	1.00	1.00	-	1.00	2.00	**2.00**
p (X^2/F)	1.72×10^{-60}	0.0001	0.83	0.55	8.10×10^{-60}	NC	0.0003	**4.46×10^{-6}**

NC = not calculated

Bold represents results from the best deviation. Data are interpreted according to the methodology proposed by Jonker et al. (2005). For more details, see the Supplemental Data, Table S3. Max= maximum value of the response; β = slope of the individual response–dose curve; EC_{50} = median effect concentration; a, b_{DR} and b_{DL} = s function parameters; SS =sum of the squares of the residuals; r^2 = regression coefficient; test χ^2 or F= statistical test; df= degree of freedom; p (χ^2/F) = level of significance for the statistical test; IA = independent action model; S/A= deviation synergism/antagonism; DR= dose ratio-dependent deviation; and DL = dose level-dependent deviation.

The fitting of the mixture data to the CA model (Fig. S1) yielded a sum of squared residuals (SS) of 45.02 ($p=1.72 \times 10^{-60}$; $r^2=0.86$). After adding parameter "a" to the model to describe the S/A deviation, the SS value decreased to 29.91 and was statistically significant ($p<0.05$; $r^2=0.91$). For dose-ratio dependent (DR) deviation, when the parameters "a" and "bDR" were added, there was a small decrease of the SS value to 29.86, which was not statistically significant (p=0.83). Moreover, the dose-level dependent (DL) deviation was not significant (p=0.55) (Table 2).

On the other hand, the fitting of the mixture data to the IA model yielded a SS of 48.14 ($p=8.10 \times 10^{-60}$; $r^2=0.85$). After adding parameter "a" to the model to describe the S/A deviation, the SS, r^2 and p value were not calculated. For dose-ratio dependent (DR) deviation, when the parameters "a" and "bDR" were added, SS decreased to 31.99, which was statistically significant (p=0.0003; $r^2=0.90$). Finally, the dose-level dependent (DL) deviation was significant ($p=4.46 \times 10^{-6}$; $r^2= 0.93$), with SS of 23.50 (Table 2). Therefore, the IA model

best fitted the (DL) deviation (Fig. 5**)**, because it presented a significant p value, the smallest SS and largest r^2 value compared with other deviations. Thus, the combination of microcrystals showed synergism at low doses and antagonism at high doses (a= -10.25), with a change in dose level greater than EC_{50} (b_{DL} = 1.12). The occurrence of synergism at low doses is of concern, because generally the environmental concentrations are low, and it is precisely at these concentrations that the organisms will be most affected.

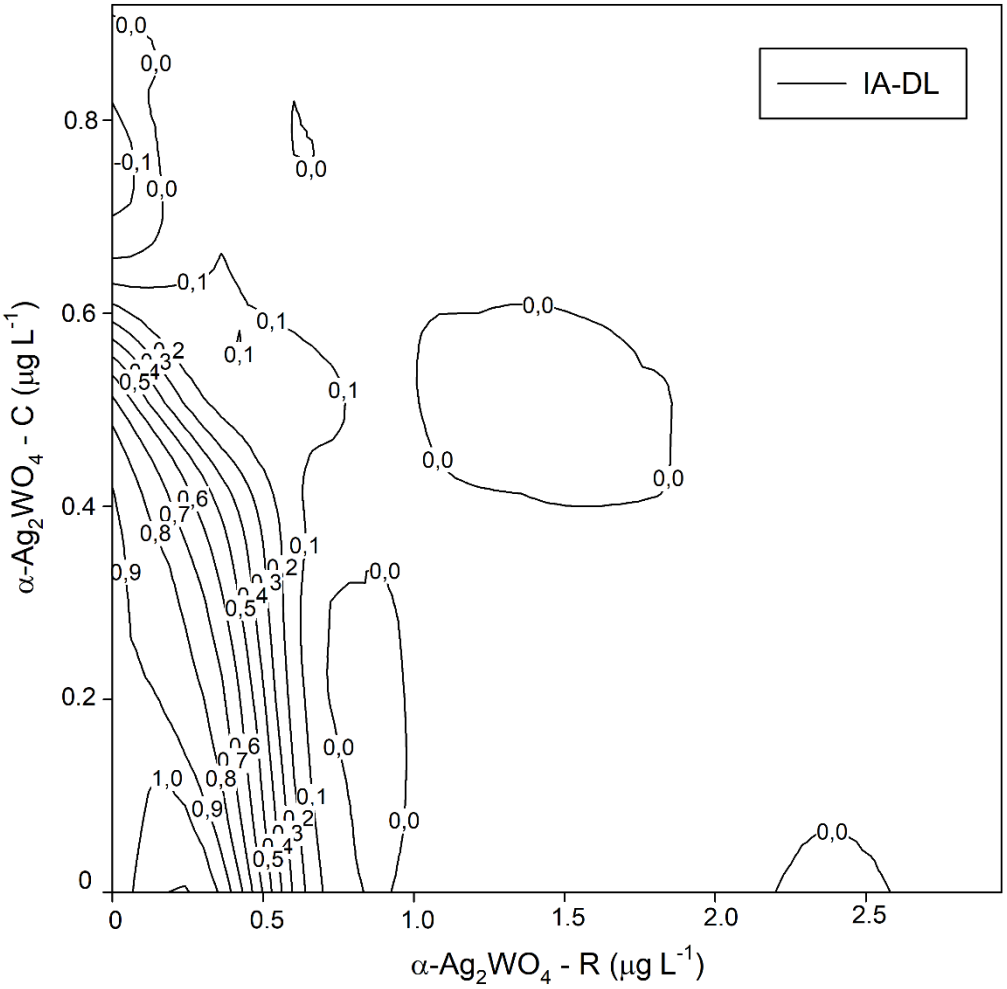

Fig. 5: Isobologram representing mixtures of α-Ag_2WO_4 – C and α-Ag_2WO_4 - R on immobility of *Ceriodaphnia silvestrii* after 48 h. Data followed the independent action model (IA) and dose level-dependence (DL) deviation.

As discussed above, silver ions are highly toxic to aquatic organisms (Navarro et al., 2008; Oukarroum et al., 2012), especially to microcrustaceans by causing problems in ion regulation (Bianchini and Wood, 2003) and induction of ROS generation (Poynton et al., 2012, Levard et al., 2012; Newton et al., 2013; Fu et al., 2014).

The occurrence of synergism at low doses of α-Ag_2WO_4 – C and α-Ag_2WO_4 - R mixture can be explained by the availability of silver ions in the test solution, which were possibly absorbed by the organisms. According to Cedergreen (2014), the toxic effects of mixtures on organisms depend on how interactions among the mixture components affect the processes of adsorption, bioavailability, distribution and biotransformation (metabolism), processes binding to the target site, and excretion, with synergistic interactions likely arising from interactions related to one or more of these processes.

On the other hand, at high doses the amount of dissolved ions from microparticles may be lower. That is, the antagonistic effect at high concentrations is possible as higher particle concentrations compromise dissolution and aggregation factors. These factors can modify the toxic effects of particles with silver in their composition, as pointed out by Zhang et al. (2019). Moreover, Xiao et al. (2015) evaluated the toxicity of metallic particles to *Daphnia magna* and reported that at small concentrations, the proportion of dissolved particles tends to be higher. However, at high particle concentration the dissolved proportion tends to be lower. Thus, when compared, a higher proportion of ions released from particles can be absorbed by organisms at low doses than at high doses of combined particles. Based on that, our results show that this occurred and are consistent with what we had hypothesized, in that the mixture effects of microcrystals of different morphologies would be more severe for *C. silvestrii* organisms. Therefore, environmental risk assessments should consider the toxicity of microcrystals at low concentrations, since there was a synergistic effect at the lowest concentrations.

4. CONCLUSION

To the best of our knowledge, this is the first study on the toxic effects of α-Ag_2WO_4 using microcrustaceans. The Neotropical species *Ceriodaphnia silvestrii* was sensitive, which shows the relevance of its use in toxicity studies. Our study showed that α-Ag_2WO_4, in both morphologies caused immobility to the cladoceran in acute exposure. The 48 h EC_{50} and EC_{10} for *C. silvestrii* were 0.64 μg L^{-1} ± 0.11 and 0.38 μg L^{-1} ± 0.06 for α-Ag_2WO_4 – C and 0.81 μg L^{-1} ± 0.15 and 0.52 μg L^{-1} ± 0.04 for α-Ag_2WO_4 –R, indicating that the toxicity of the

microcrystals was similar. We did not observe chronic effects on reproduction, probably because in this type of exposure food was available to the microcrustaceans, reducing particle and ion toxicity. Moreover, we did not observe significant changes in ingestion rates at low concentrations. Furthermore, in the mixture test (acute exposure) we found that the best fit was the independent action (IA) dose level-dependence (DL) deviation, indicating that there was synergism at low concentrations and antagonism at high concentrations. This is a matter of concern because microcrustacean populations can be severely affected when exposed to low concentrations (environmentally relevant) of silver. Therefore, our results reinforce the importance of verifying the effects at low concentrations, both acute and chronic exposures in isolated and mixture on zooplanktonic organisms. This knowledge can be useful in future studies of risk assessment to microcrustaceans and by agencies to establish safe limits for both alpha-silver tungstate and ionic silver for aquatic biota. Thus, imbalance in aquatic ecosystems caused by these compounds could be mitigated as cladocerans occupy a transition zone of the food web between the autotrophs and higher trophic levels.

Acknowledgements

This work was funded by the São Paulo Research Foundation - FAPESP (FAPESP CEPID-finance code 2013/07296-2; finance code 2018/07988-5), Financier of Studies and Projects FINEP, National Council for Scientific and Technological Development - CNPq (finance code 141255/2018-8; 316064/2021-1). This study was financed in part by the Coordenação de Aperfeiçoamento de Pessoal de Nível Superior - Brasil (CAPES) - Finance Code 001 and 88887.364036/2019-00. M.A. was supported by the Margarita Salas postdoctoral contract MGS/2021/21 (UP2021-021) financed by the European Union-NextGenerationEU. We would also like to thank Dr. Hugo Miguel Preto de Morais Sarmento for the permission to use laboratories, as well as the equipment.

References

Abreu, Cínthia B, Gebara, R.C., Dos Reis, L.L., Rocha, G.S., Alho, L. de O.G., Alvarenga, L.M., Virtuoso, L.S., Assis, M., da Silva Mansano, A., Longo, E., 2022. Toxicity of α-Ag_2WO_4 microcrystals to freshwater microalga *Raphidocelis subcapitata* at cellular and population levels. Chemosphere 132536.

Abreu, Cínthia Bruno, Gebara, R.C., dos Reis, L.L., Rocha, G.S., Alho, L.O.G., Alvarenga, L.M.,

Virtuoso, L.S., Assis, M., Mansano, A. da S., Longo, E., Melão, M. da G.G., 2022. Effects of α-Ag_2WO_4 crystals on photosynthetic efficiency and biomolecule composition of the algae *Raphidocelis subcapitata*. Water, Air, Soil Pollut. 233, 121. https://doi.org/10.1007/s11270-022-05604-x

Alvarez-Roca, R., Gouveia, A.F., De Foggi, C.C., Lemos, P.S., Gracia, L., Da Silva, L.F., Vergani, C.E., San-Miguel, M., Longo, E., Andrés, J., 2021. Selective Synthesis of α-, β-, and γ-Ag_2WO_4 Polymorphs: Promising Platforms for Photocatalytic and Antibacterial Materials. Inorg. Chem. 60, 1062–1079. https://doi.org/10.1021/acs.inorgchem.0c03186

Angel, B.M., Batley, G.E., Jarolimek, C. V., Rogers, N.J., 2013. The impact of size on the fate and toxicity of nanoparticulate silver in aquatic systems. Chemosphere 93, 359–365. https://doi.org/10.1016/j.chemosphere.2013.04.096

Arumugam, R., Osman, S., Pan, J., Khan, A., Yang, V., 2020. One-pot preparation of AgBr / α-Ag_2WO_4 composite with superior photocatalytic activity under visible-light irradiation. Colloids Surfaces A 586, 124079. https://doi.org/10.1016/j.colsurfa.2019.124079

Assis, M., Cordoncillo, E., Torres-Mendieta, R., Beltrán-Mir, H., Mínguez-Vega, G., Oliveira, R., Leite, E.R., Foggi, C.C., Vergani, C.E., Longo, E., Andrés, J., 2018. Towards the scale-up of the formation of nanoparticles on α-Ag_2WO_4 with bactericidal properties by femtosecond laser irradiation. Sci. Rep. 8, 1–11. https://doi.org/10.1038/s41598-018-19270-9

Assis, M., Ponce, M.A., Gouveia, A.F., Souza, D., de Campos da Costa, J.P., Teodoro, V., Gobato, Y.G., Andres, J., Macchi, C., Somoza, A., Longo, E., 2021. Revealing the nature of defects in α-Ag_2WO_4 by positron annihilation lifetime spectroscopy: A joint experimental and theoretical study. Cryst. Growth Des. 21, 1093–1102. https://doi.org/10.1021/acs.cgd.0c01417

Assis, M., Pontes Ribeiro, R.A., Carvalho, M.H., Teixeira, M.M., Gobato, Y.G., Prando, G.A., Mendonça, C.R., De Boni, L., Aparecido De Oliveira, A.J., Bettini, J., Andrés, J., Longo, E., 2020. Unconventional Magnetization Generated from Electron Beam and Femtosecond Irradiation on α-Ag2WO4: A Quantum Chemical Investigation. ACS Omega 5, 10052–10067. https://doi.org/10.1021/acsomega.0c00542

Assis, M., Robeldo, T., Foggi, C.C., Kubo, A.M., Condoncillo, E., 2019. Composite Formed by Electron Beam and Femtosecond Irradiation as Potent Antifungal and Antitumor Agents 1–15. https://doi.org/10.1038/s41598-019-46159-y

Ayappan, C., Jayaraman, V., Palanivel, B., Pandikumar, A., 2020. Separation and Puri fi cation Technology Facile preparation of novel Sb 2 S 3 nanoparticles / rod-like α -Ag_2WO_4 heterojunction photocatalysts : Continuous modulation of band structure towards the e ffi cient

removal of organic contaminants. Sep. Purif. Technol. 236, 116302. https://doi.org/10.1016/j.seppur.2019.116302

Becaro, A.A., Jonsson, C.M., Puti, F.C., Siqueira, M.C., Mattoso, L.H.C., Correa, D.S., Ferreira, M.D., 2015. Toxicity of PVA-stabilized silver nanoparticles to algae and microcrustaceans. Environ. Nanotechnology, Monit. Manag. 3, 22–29. https://doi.org/10.1016/j.enmm.2014.11.002

Bianchini, A., Wood, C.M., 2003. Mechanism of acute silver toxicity in *Daphnia magna*. Environ. Toxicol. Chem. 22, 1361–1367. https://doi.org/10.1897/1551-5028(2003)022<1361:MOASTI>2.0.CO;2

Bielmyer, G.R.K.B., Ell, R.U.A.B., Laine, S.T.J.K., 2002. Effects of ligand-bound silver on *Ceriodaphnia dubia* 21, 2204–2208.

Brazilian National Standards Organization - ABNT. (2016). Aquatic ecotoxicology-Acute toxicity-Test with *Daphnia* spp (Cladocera, Crustacea). NBR 12713. Rio de Janeiro, RJ, Brazil.

Brazilian National Standards Organization - ABNT. (2017). Aquatic ecotoxicology-Chronic toxicity-Test method with *Ceriodaphnia* spp (Crustacea, Cladocera). NBR 13373. Rio de Janeiro, RJ, Brazil.

Cedergreen, N., 2014. Quantifying synergy: A systematic review of mixture toxicity studies within environmental toxicology. PLoS One 9. https://doi.org/10.1371/journal.pone.0096580

Conine, A.L., Frost, P.C., 2016. Variable toxicity of silver nanoparticles to *Daphnia magna* : effects of algal particles and animal nutrition. Ecotoxicology 0–1. https://doi.org/10.1007/s10646-016-1747-2

Cruz, L., Teixeira, M.M., Teodoro, V., Jacomaci, N., Laier, L.O., Assis, M., Macedo, N.G., Tello, A.C.M., Da Silva, L.F., Marques, G.E., Zaghete, M.A., Teodoro, M.D., Longo, E., 2020. Multi-dimensional architecture of Ag/α-Ag_2WO_4 crystals: insights into microstructural, morphological, and photoluminescence properties. CrystEngComm 22, 7903–7917. https://doi.org/10.1039/d0ce00876a

Dai, X., Luo, Y., Zhang, W., Fu, S., 2010. Facile hydrothermal synthesis and photocatalytic activity of bismuth tungstate hierarchical hollow spheres with an ultrahigh surface area † 3426–3432. https://doi.org/10.1039/b923443h

Dewez, D., Goltsev, V., Kalaji, H.M., Oukarroum, A., 2018. Current Plant Biology Inhibitory e ff ects of silver nanoparticles on photosystem II performance in *Lemna gibba* probed by chlorophyll fl uorescence. Curr. Plant Biol. 16, 15–21. https://doi.org/10.1016/j.cpb.2018.11.006

Foggi, C.C., Fabbro, M.T., Santos, L.P.S., de Santana, Y.V.B., Vergani, C.E., Machado, A.L.,

Cordoncillo, E., Andrés, J., Longo, E., 2017. Synthesis and evaluation of A-Ag_2WO_4 as novel antifungal agent. Chem. Phys. Lett. 674, 125–129. https://doi.org/10.1016/j.cplett.2017.02.067

Foggi, C.C., de Oliveira, R.C., Fabbro, M.T., Vergani, C.E., Andres, J., Longo, E., Machado, A.L., 2017. Tuning the Morphological, Optical, and Antimicrobial Properties of α-Ag_2WO_4 Microcrystals Using Different Solvents. Cryst. Growth Des. 17, 6239–6246. https://doi.org/10.1021/acs.cgd.7b00786

Fu, P.P., Xia, Q., Hwang, H.M., Ray, P.C., Yu, H., 2014. Mechanisms of nanotoxicity: Generation of reactive oxygen species. J. Food Drug Anal. 22, 64–75. https://doi.org/10.1016/j.jfda.2014.01.005

Gaiser, B.K., Biswas, A., Rosenkranz, P., Jepson, M.A., Lead, J.R., Stone, V., Tyler, C.R., Fernandes, T.F., 2011. Effects of silver and cerium dioxide micro- and nano-sized particles on *Daphnia magna* † 1227–1235. https://doi.org/10.1039/c1em10060b

Gebara, R.C., Pérola, J., Mansano, S., Sarmento, H., Gama, G., 2019. Ecotoxicology and Environmental Safety Effects of iron oxide nanoparticles (Fe_3O_4) on life history and metabolism of the Neotropical cladoceran *Ceriodaphnia silvestrii*. Ecotoxicol. Environ. Saf. 186, 109743. https://doi.org/10.1016/j.ecoenv.2019.109743

Gebara, R., de Oliveira Gonçalves Alho, L., Bruno de Abreu, C., da Silva Mansano, A., Moreira, R.A., Swerts Rocha, G., Gama Melão, M. da G., 2021. Toxicity and Risk Assessment of Zinc and Aluminum Mixtures to *Ceriodaphnia silvestrii* (Crustacea: Cladocera). Environ. Toxicol. Chem. 40, 2912–2922. https://doi.org/10.1002/etc.5162

He, D., Dorantes-Aranda, J.J., Waite, T.D., 2012. Silver nanoparticle-algae interactions: Oxidative dissolution, reactive oxygen species generation and synergistic toxic effects. Environ. Sci. Technol. 46, 8731–8738. https://doi.org/10.1021/es300588a

Hook, S.E., Fisher, N.S., 2001. Sublethal effects of silver in zooplankton: Importance of exposure pathways and implications for toxicity testing. Environ. Toxicol. Chem. 20, 568–574. https://doi.org/10.1002/etc.5620200316

Ivask, A., Kasemets, K., Mortimer, M., Kahru, A., 2013. Toxicity of Ag , CuO and ZnO nanoparticles to selected environmentally relevant test organisms and mammalian cells in vitro : a critical review 1181–1200. https://doi.org/10.1007/s00204-013-1079-4

Jonker, M.J., Svendsen, C., Bedaux, J.J.M., Bongers, M., Kammenga, J.E., 2005. Significance testing of synergistic/antagonistic, dose level-dependent, or dose ratio-dependent effects in mixture dose-response analysis. Environ. Toxicol. Chem. An Int. J. 24, 2701–2713.

Khangarot, B.S., Ray, P.K., 1989. Investigation of correlation between physicochemical properties of metals and their toxicity to the water flea *Daphnia magna* Straus. Ecotoxicol. Environ. Saf. 18, 109–120. https://doi.org/10.1016/0147-6513(89)90071-7

Kim, J., Kim, S., Lee, S., 2011. Differentiation of the toxicities of silver nanoparticles and silver ions to the Japanese medaka (Oryzias latipes) and the cladoceran *Daphnia magna*. Nanotoxicology 5, 208–214. https://doi.org/10.3109/17435390.2010.508137

Kleiven, M., Macken, A., Oughton, D.H., 2019. Chemosphere Growth inhibition in *Raphidocelis subcapita* e Evidence of nanospeci fi c toxicity of silver nanoparticles. Chemosphere 221, 785–792. https://doi.org/10.1016/j.chemosphere.2019.01.055

Kleiven, M., Rossbach, L.M., Gallego-Urrea, J.A., Brede, D.A., Oughton, D.H., Coutris, C., 2018. Characterizing the behavior, uptake, and toxicity of NM300K silver nanoparticles in *Caenorhabditis elegans*. Environ. Toxicol. Chem. 37, 1799–1810. https://doi.org/10.1002/etc.4144

Köser, J., Engelke, M., Hoppe, M., 2017. Environmental Science Nanotoxicity in ecotoxicological media † 1470–1483. https://doi.org/10.1039/c7en00026j

Laier, L.O., Assis, M., Foggi, C.C., Gouveia, A.F., Vergani, C.E., Santana, L.C.L., Cavalcante, L.S., Andrés, J., Longo, E., 2020. Surface - dependent properties of α - Ag 2 WO 4 : a joint experimental and theoretical investigation. Theor. Chem. Acc. 1–11. https://doi.org/10.1007/s00214-020-02613-z

Levard, C., Hotze, E.M., Lowry, G. V., Brown, G.E., 2012. Environmental transformations of silver nanoparticles: Impact on stability and toxicity. Environ. Sci. Technol. 46, 6900–6914. https://doi.org/10.1021/es2037405

Lin, C.A.O., Jiexin, C.A.O., Cong, W., Ping, C.H.E., An, P.A.N.D.E., Volinsky, A.A., 2012. Anti-tumor activity of self-charged (Eu , Ca): WO_3 and Eu : $CaWO_4$ nanoparticles 35, 767–772.

Liu, J., Hurt, R.H., 2010. Ion release kinetics and particle persistence in aqueous nano-silver colloids. Environ. Sci. Technol. 44, 2169–2175. https://doi.org/10.1021/es9035557

Lodeiro, P., Browning, T.J., Achterberg, E.P., Guillou, A., El-Shahawi, M.S., 2017. Mechanisms of silver nanoparticle toxicity to the coastal marine diatom Chaetoceros curvisetus. Sci. Rep. 7, 1–10. https://doi.org/10.1038/s41598-017-11402-x

Lucca, G.M. De, Freitas, E.C., 2018. Effects of TiO 2 Nanoparticles on the Neotropical Cladoceran *Ceriodaphnia silvestrii* by Waterborne and Dietary Routes.

Macedo, N.G., Gouveia, A.F., Roca, R.A., Assis, M., Gracia, L., Andre, J., Leite, E.R., Longo, E.,

Box, P.O., 2018. Surfactant-Mediated Morphology and Photocatalytic Activity of. https://doi.org/10.1021/acs.jpcc.8b01898

Macedo, N.G., Machado, T.R., Roca, R.A., Assis, M., Foggi, C.C., Puerto-Belda, V., Mínguez-Vega, G., Rodrigues, A., San-Miguel, M.A., Cordoncillo, E., Beltrán-Mir, H., Andrés, J., Longo, E., 2019. Tailoring the Bactericidal Activity of Ag Nanoparticles/α-Ag_2WO_4 Composite Induced by Electron Beam and Femtosecond Laser Irradiation: Integration of Experiment and Computational Modeling. ACS Appl. Bio Mater. 2, 824–837. https://doi.org/10.1021/acsabm.8b00673

Mansano, A.S., Moreira, R.A., Pierozzi, M., Oliveira, T.M.A., Vieira, E.M., Rocha, O., Regali-seleghim, M.H., 2016. Effects of diuron and carbofuran pesticides in their pure and commercial forms on *Paramecium caudatum*: The use of protozoan in. Environ. Pollut. 213, 160–172. https://doi.org/10.1016/j.envpol.2015.11.054

Mansano, A.S., Souza, J.P., Cancino-Bernardi, J., Venturini, F.P., Marangoni, V.S., Zucolotto, V., 2018. Toxicity of copper oxide nanoparticles to Neotropical species *Ceriodaphnia silvestrii* and *Hyphessobrycon eques*. Environ. Pollut. 243, 723–733. https://doi.org/10.1016/j.envpol.2018.09.020

Martins, J., Oliva Teles, L., Vasconcelos, V., 2007. Assays with *Daphnia magna* and *Danio rerio* as alert systems in aquatic toxicology. Environ. Int. 33, 414–25. https://doi.org/10.1016/j.envint.2006.12.006

McWilliam, R.A., Baird, D.J., 2002. Postexposure feeding depression: a new toxicity endpoint for use in laboratory studies with *Daphnia magna*. Environ. Toxicol. Chem. An Int. J. 21, 1198–1205.

Metreveli, G., Frombold, B., Seitz, F., Grün, A., Philippe, A., Rosenfeldt, R.R., Bundschuh, M., Schulz, R., Manz, W., Schaumann, G.E., 2016. Impact of chemical composition of ecotoxicological test media on the stability and aggregation status of silver nanoparticles. Environ. Sci. Nano 3, 418–433. https://doi.org/10.1039/C5EN00152H

Moreira, R.A., Mansano, A. da S., Silva, L.C. da, Rocha, O., 2014. A comparative study of the acute toxicity of the herbicide atrazine to cladocerans *Daphnia magna*, *Ceriodaphnia silvestrii* and *Macrothrix flabelligera*. Acta Limnol. Bras. 26, 1–8. https://doi.org/10.1590/S2179-975X2014000100002

Muthamizh, S., Suresh, R., Giribabu, K., Manigandan, R., Praveen Kumar, S., Munusamy, S., Narayanan, V., 2015. $MnWO_4$ nanocapsules: Synthesis, characterization and its electrochemical sensing property. J. Alloys Compd. 619, 601–609. https://doi.org/10.1016/j.jallcom.2014.09.049

Navarro, E., Baun, Æ.A., Behra, Æ.R., Hartmann, Æ.N.B., Filser, J., Antonietta, Æ.A.M.Æ., Peter, Q.Æ., 2008. Environmental behavior and ecotoxicity of engineered nanoparticles to algae , plants

, and fungi 372–386. https://doi.org/10.1007/s10646-008-0214-0

Newton, K.M., Puppala, H.L., Kitchens, C.L., Colvin, V.L., Klaine, S.J., 2013. Silver nanoparticle toxicity to *Daphnia magna* is a function of dissolved silver concentration. Environ. Toxicol. Chem. 32, 2356–2364. https://doi.org/10.1002/etc.2300

Oukarroum, A., Bras, S., Perreault, F., Popovic, R., 2012. Inhibitory effects of silver nanoparticles in two green algae, *Chlorella vulgaris* and *Dunaliella tertiolecta*. Ecotoxicol. Environ. Saf. 78, 80–85. https://doi.org/10.1016/j.ecoenv.2011.11.012

Park, C., Jung, J., Baek, M., Sung, B., 2019. Mixture toxicity of metal oxide nanoparticles and silver ions on *Daphnia magna* 1–13.

Poynton, H.C., Lazorchak, J.M., Impellitteri, C.A., Blalock, B.J., Rogers, K., Allen, H.J., Loguinov, A., Heckman, J.L., Govindasmawy, S., 2012. Toxicogenomic responses of nanotoxicity in Daphnia magna exposed to silver nitrate and coated silver nanoparticles. Environ. Sci. Technol. 46, 6288–6296. https://doi.org/10.1021/es3001618

Ribeiro, F., Gallego-Urrea, J.A., Jurkschat, K., Crossley, A., Hassellöv, M., Taylor, C., Soares, A.M.V.M., Loureiro, S., 2014. Silver nanoparticles and silver nitrate induce high toxicity to *Pseudokirchneriella subcapitata*, *Daphnia magna* and *Danio rerio*. Sci. Total Environ. 466, 232–241

Ro, I., Tejamaya, M., Lead, J.R., Luoma, S.N., Stoiber, T., 2015. Influence of hardness on the bioavailability of silver to a freshwater snail after waterborne exposure to silver nitrate and silver nanoparticles 5390, 1–10. https://doi.org/10.3109/17435390.2014.991772

Sakamoto, M., Ha, J.-Y., Yoneshima, S., Kataoka, C., Tatsuta, H., Kashiwada, S., 2014. Free Silver Ion as the Main Cause of Acute and Chronic Toxicity of Silver Nanoparticles to Cladocerans. Arch. Environ. Contam. Toxicol. 68, 500–509. https://doi.org/10.1007/s00244-014-0091-x

Sarmento, H., Unrein, F., Isumbisho, M., Stenuite, S., Gasol, J.M., DESCY, J., 2008. Abundance and distribution of picoplankton in tropical, oligotrophic Lake Kivu, eastern Africa. Freshw. Biol. 53, 756–771.

Seitz, F., Rosenfeldt, R.R., Storm, K., Metreveli, G., Schaumann, G.E., Schulz, R., Bundschuh, M., 2015. Effects of silver nanoparticle properties, media pH and dissolved organic matter on toxicity to *Daphnia magna*. Ecotoxicol. Environ. Saf. 111, 263–270. https://doi.org/10.1016/j.ecoenv.2014.09.031

Shen, M.H., Zhou, X.X., Yang, X.Y., Chao, J.B., Liu, R., Liu, J.F., 2015. Exposure Medium: Key in Identifying Free Ag^{+} as the Exclusive Species of Silver Nanoparticles with Acute Toxicity to

Daphnia magna. Sci. Rep. 5, 4–11. https://doi.org/10.1038/srep09674

Silva, L.F., Catto, A.C., Avansi, W., Cavalcante, L.S., Andrés, J., Aguir, K., Mastelaro, V.R., Longo, E., 2014. A novel ozone gas sensor based on one-dimensional (1D) α-Ag_2WO_4 nanostructures. Nanoscale 6, 4058–4062. https://doi.org/10.1039/c3nr05837a

Silva, L.F., Catto, A.C., Avansi, W., Cavalcante, L.S., Mastelaro, V.R., Andrés, J., Aguir, K., Longo, E., 2016. Acetone gas sensor based on α-Ag_2WO_4 nanorods obtained via a microwave-assisted hydrothermal route. J. Alloys Compd. 683, 186–190. https://doi.org/10.1016/j.jallcom.2016.05.078

Sohn, E.K., Johari, S.A., Kim, T.G., Kim, J.K., Kim, E., Lee, J.H., Chung, Y.S., Yu, I.J., 2015. Aquatic Toxicity Comparison of Silver Nanoparticles and Silver Nanowires 2015.

Strigul, N., Galdun, C., Vaccari, L., Ryan, T., Braida, W., Christodoulatos, C., 2009. Influence of speciation on tungsten toxicity. Desalination 248, 869–879. https://doi.org/10.1016/j.desal.2009.01.016

Uwizeyimana, H., Wang, M., Chen, W., Khan, K., 2017. The eco-toxic effects of pesticide and heavy metal mixtures towards earthworms in soil. Environ. Toxicol. Pharmacol. 55, 20–29.

Villarroel, M.J., Ferrando, M.D., Sancho, E., Andreu, E., 1999. *Daphnia magna* feeding behavior after exposure to tetradifon and recovery from intoxication. Ecotoxicol. Environ. Saf. 44, 40–46.

Wang, Z., Chen, J., Li, X., Shao, J., Peijnenburg, W.J.G.M., 2012. Aquatic toxicity of nanosilver colloids to different trophic organisms: Contributions of particles and free silver ion. Environ. Toxicol. Chem. 31, 2408–2413. https://doi.org/10.1002/etc.1964

Xiao, Y., Vijver, M.G., Chen, G., Peijnenburg, W.J.G.M., 2015. Toxicity and accumulation of Cu and ZnO nanoparticles in *Daphnia magna*. Environ. Sci. Technol. 49, 4657–4664. https://doi.org/10.1021/acs.est.5b00538

Zhang, W., Ke, S., Sun, C., Xu, X., Chen, J., Yao, L., 2019. Fate and toxicity of silver nanoparticles in freshwater from laboratory to realistic environments : a review.

Zhao, C.M., Wang, W.X., 2010. Biokinetic uptake and efflux of silver nanoparticles in *Daphnia magna*. Environ. Sci. Technol. 44, 7699–7704. https://doi.org/10.1021/es101484s

Zhu, Y., Wu, J., Chen, M., Liu, X., Xiong, Y., Wang, Y., Feng, T., Kang, S., Wang, X., 2019. Chemosphere Recent advances in the biotoxicity of metal oxide nanoparticles : Impacts on plants , animals and microorganisms. Chemosphere 237, 124403. https://doi.org/10.1016/j.chemosphere.2019.124403

Supplementary material

Tables

Table S1: α-Ag_2WO_4 - C characterization in the test solutions and ultrapure water.

α-Ag_2WO_4 ($\mu g\ L^{-1}$)	**Time (h)**	**Zeta-Potential (mV)**	**Hydrodynamic size (nm)**	**PdI**	**Zeta-Potential (mV)**	**Hydrodynamic size (nm)**	**PdI**
		Test solutions			Ultrapure Water		
0.29	0	-23.23 ± 0.42	402.73 ± 163.83	0.544 ± 0.05	-7.61 ± 0.62	470.80 ± 31.68	0.550 ± 0.12
	48	-6.98 ± 2.63	955.87 ± 301.86	0.706 ± 0.22	-27.33 ± 10	1206.63 ± 179.84	0.56 ± 0.27
0.4	0	-23.80 ± 1.15	456.37 ± 161.44	0.507 ± 0.20	-14.13 ± 3.38	340 ± 17.78	0.526 ± 0.18
	48	-14.33 ± 2.80	383.13 ± 17.01	0.436 ± 0.02	-16.32 ± 7.66	882.63 ±393.95	0.568 ± 0.28
0.52	0	-21.17 ± 2.34	532.27 ± 91.87	0.532 ± 0.08	-15.17 ± 6.16	221.37 ± 17.09	0.32 ± 0.04
	48	-10.34 ± 1.09	734 ± 165.53	0.658 ± 0.17	-24.80 ± 3.54	820.53 ± 103.26	0.716 ± 010
0.63	0	-25.03 ± 0.86	526.50 ± 14.14	0.511 ± 0.05	-27.87 ± 1.80	113.97 ± 1.42	0.312 ± 0.03
	48	-6.5 ± 4.49	961.45 ± 340.19	0.631 ± 0.28	-4.89 ± 4.28	817.27 ± 93.98	0.220 ± 0.16
0.92	0	-26.60 ± 2.25	240.60 ± 31.57	0.359 ± 0.09	-28.70 ± 2.97	201.57 ± 7.05	0.389 ± 0.06
	48	-17.9 ± 5.48	1104.67 ± 58.77	0.613 ± 0.02	-17.37 ± 8.66	1569.33 ±438.75	0.753 ± 0.22

Table S2: α-Ag_2WO_4 - R characterization in the test solutions and ultrapure water.

α-Ag_2WO_4 ($\mu g\ L^{-1}$)	**Time (h)**	**Zeta-Potential (mV)**	**Hydrodynamic size (nm)**	**PdI**	**Zeta-Potential (mV)**	**Hydrodynamic size (nm)**	**PdI**
		Test solutions			Ultrapure Water		
0.39	0	-15.03 ± 5.53	1489.50 ± 183.14	0.900 ± 0.11	-9.15 ± 3.61	1280 ± 2.83	0.872 ± 0.18
	48	-6.49 ± 1.20	1361 ± 383.25	0.249 ± 0.06	-11.38 ± 2.72	1713.67 ± 135.30	0.653 ± 0.27
0.59	0	-10.37 ± 7.83	1315.07 ± 589.71	0.747 ± 0.37	-1.33 ± 0.73	2314 ± 196.58	1 ± 0
	48	-14 ± 1.86	1115.83 ± 312.06	0.734 ± 0.20	-15.25 ± 5.16	1855 ± 0	0.873 ± 0.12
0.98	0	-6.43 ± 0.30	1677 ± 97.58	0.812 ± 0.16	-14.95 ± 2.90	3000 ± 0	1 ± 0
	48	-10.78 ± 2.29	948.60 ± 0	0.68 ± 0	-5.30 ± 1.15	1783 ± 87.68	0.606 ± 0.38
1.97	0	-7.79 ± 0.82	915.37 ± 56.84	0.606 ± 0.15	-7.79 ± 0.82	937.23 ± 443.37	0.518 ± 0.29
	48	-17.95 ± 2.75	1346.50 ± 6.36	0.492 ± 0.22	-3.60 ± 1.91	1310.33 ± 83.68	0.696 ± 043
2.95	0	-9.36 ± 1.21	1548.50 ± 54.45	0.785 ± 0.37	-5.53 ± 3.13	924.27 ± 121.18	0.626 ± 0.07
	48	-4.04 ± 0.77	1301.63 ± 640.58	0.816 ± 0.16	-10.63 ± 3.63	1899 ± 0	1 ± 0

Table S3: Interpretation of parameters referring to the addition of concentration (CA) and independent action (IA) models by Jonker et al. (2005).

Parameter	Value		Meaning
	CA	IA	
		Antagonism/Synergism	
a	>0	<0	Antagonism
	<0	>0	Synergism
		Dose ratio dependence	
a	>0	>0	Antagonism, except for those mixture ratios where significant negative b_{DR} indicate synergism
	<0	<0	Synergism, except for those mixture ratios where significant positive b_{DR} indicate antagonism
b_{DR}	>0	>0	Antagonism where the toxicity of the mixture is caused mainly by toxicant i
	<0	<0	Synergism where the toxicity of the mixture is caused mainly by toxicant i
		Dose level dependence	
a	>0	>0	Antagonism low dose level and synergism high dose level
	<0	<0	Synergism low dose level and antagonism high dose level
b_{DL}	>1	>2	Change at lower dose level than the EC50
	=1	=2	Change at the EC50 level
	$0 < b_{DL} < 1$	$1 < b_{DL} < 2$	Change at higher dose level than the EC50
	<0	<1	No change, but the magnitude of synergism/antagonism is dose level (CA) or effect level (IA) dependent

Fig. S1 Isobologram representing mixtures of α-Ag_2WO_4 – C and α-Ag_2WO_4 - R on immobility of *Ceriodaphnia silvestrii* after 48 h. Data followed concentration addition (CA) model and S/A deviation.

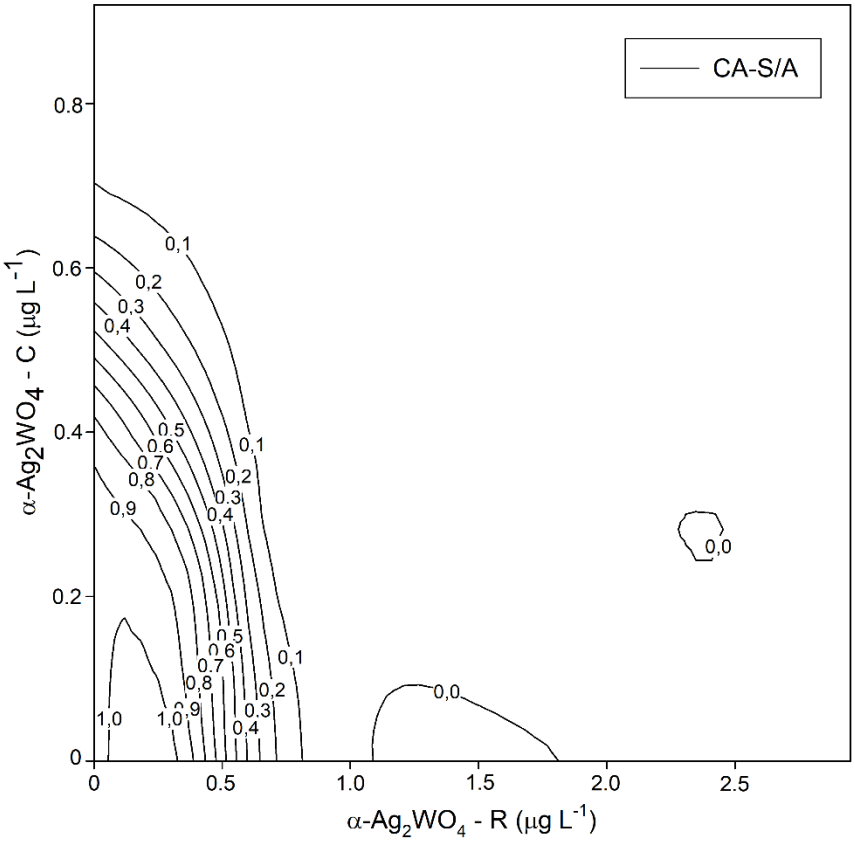

Conclusões gerais

Com essa pesquisa, as seguintes conclusões gerais puderam ser obtidas:

• As diferentes morfologias de α-Ag_2WO_4 inibiram o totalmente o crescimento das células algais nas mais altas concentrações testadas (36,25 μg L^{-1} para α-Ag_2WO_4-C e 31,76 μg L^{-1} para α-Ag_2WO_4-R), em 96 h de exposição;

• α-Ag_2WO_4 -R foi mais tóxica para *R. subcapitata* em comparação com α-Ag_2WO_4 – C;

• α-Ag_2WO_4 -R e α-Ag_2WO_4 – C alteraram a complexidade celular e reduziram a fluorescência da clorofila *a* de *R. subcapitata*;

• α-Ag_2WO_4 -R induziu a produção de espécies reativas de oxigênio (EROs);

• Foram observados danos nos processos fotossintéticos das microalgas, evidenciados pelos parâmetros obtidos via Phyto-PAM;

• α-Ag_2WO_4 -R causou aumento do conteúdo de clorofila *a* e de carboidratos totais nas microalgas;

• Os testes de toxicidade aguda evidenciaram que as morfologias α-Ag_2WO_4 -R e α-Ag_2WO_4 – C causaram imobilidade do cladócero Neotropical *C. silvestrii*, sendo que não foi observado diferenças significativas na toxicidade de diferentes morfologias;

• Os testes de toxicidade aguda indicaram que as misturas das duas morfologias de α-Ag_2WO_4 causaram imobilidade dos microcrustáceos, sendo que o modelo de referência de ação independente (IA) com desvio dependente da dose (DL) foi o que melhor se ajustou aos dados, com sinergismo em baixas concentrações e antagonismo em concentrações elevadas;

• Os testes de toxicidade crônica com os microcristais isolados α-Ag_2WO_4 -R e α-Ag_2WO_4 – C e com as concentrações variando de 0,1 a 0,4 μg L^{-1}, não causaram efeitos significativos na reprodução de *C. silvestrii*;

• α-Ag_2WO_4 -R e α-Ag_2WO_4 – C apresentaram maior toxicidade ao cladócero do que para a microalga.

Considerações Finais

Com relação à primeira hipótese testada neste estudo, a partir dos resultados foi possível concluir que as diferentes morfologias de α-Ag_2WO_4 causam efeitos deletérios aos organismos testados, a microalga *Raphidocelis subcapitata* e o cladócero *C. silvestrii*. Especificamente em *R. subcapitata* houve inibição do crescimento populacional, alterações na morfologia celular (complexidade celular) e, em nível intracelular, induziu a produção de espécies reativas de oxigênio (EROs) e reduziu a fluorescência da clorofila *a*. Ainda, α-Ag_2WO_4 – R ocasionou a redução da atividade fotossintética, diminuiu o conteúdo de clorofila *a* e carboidratos totais nas menores concentrações testadas e aumentou drasticamente a composição dessas biomoléculas na maior concentração.

A segunda hipótese foi comprovada. Os efeitos das micropartículas isoladas são diferentes dos efeitos observados para os compostos em mistura.

Nossos dados evidenciaram que as micropartículas foram altamente tóxicas aos cladóceros quando expostos por um período menor (exposição aguda, 48h), causando imobilidade dos organismos. No entanto, na exposição crônica, não foram observados efeitos adversos dos microcristais na reprodução dos microcrustáceos, o que possivelmente ocorreu pelo fato de haver alimento disponível aos organismos.

A hipótese que diferentes morfologias causam toxicidades diferentes também foi confirmada para a microalga *R. subcapitata*. Foi observado que α-Ag_2WO_4 – R foi mais tóxico do que α-Ag_2WO_4 – C, o que é explicado pela diferença na energia superficial de cada microcristal.

Por outro lado, as diferentes espécies testadas nesse estudo mostraram sensibilidades distintas ao microcristal. A espécie *C. silvestrii* foi mais sensível do que a espécie *R. subcapitata*. As concentrações que causaram efeitos deletérios aos cladóceros foram cerca de 30 vezes menores para α-Ag_2WO_4 – C e 17 vezes menores para α-Ag_2WO_4 – R.

Finalmente, a hipótese que os efeitos tóxicos dos compostos selecionados são mais graves em mistura foi confirmada. Os testes de toxicidade de misturas para *C. silvestrii* comprovaram que quando as diferentes morfologias de α-Ag_2WO_4 são combinadas, há ocorrência de sinergismo em baixas doses e antagonismo em doses elevadas, dependendo do nível da dose. A alta toxicidade ocorre devido a liberação de íons prata do α-Ag_2WO_4. Por sua vez, esses íons atuam diretamente na regulação iônica, comprometendo a atividade de Na^+, K^+ e ATPase.

Futuramente, outros estudos podem incorporar outras espécies e até mesmo outros níveis tróficos, como peixes, na avaliação da toxicidade do microcristal α-Ag_2WO_4. Além disso, seria recomendável aferir os efeitos tóxicos do tungstato de prata sob diferentes meios de exposição, como a via alimentar, com a finalidade de identificar possível bioacumulação do microcristal e dos íons de prata ao longo da cadeia trófica.